diversity

MDPI

Article

Issi saaneq gen. et sp. nov.—A New Sauropodomorph Dinosaur from the Late Triassic (Norian) of Jameson Land, Central East Greenland †

Victor Beccari [1,2,3,*,‡], Octávio Mateus [1,2,‡], Oliver Wings [4,‡], Jesper Milàn [5,‡] and Lars B. Clemmensen [6,‡]

1 GeoBioTec, Department of Earth Sciences, Faculdade de Ciência e Tecnologia, Universidade Nova de Lisboa, 2829-516 Lisbon, Portugal; omateus@fct.unl.pt
2 Museu da Lourinhã, 2530-158 Lourinhã, Portugal
3 SNSB—Bayerische Staatssammlung für Paläontologie und Geologie, 80333 Munich, Germany
4 Natural Sciences Collections (ZNS), Martin Luther University Halle-Wittenberg, 06108 Halle, Germany; oliver.wings@zns.uni-halle.de
5 Geomuseum Faxe, Østsjællands Museum, 4640 Faxe, Denmark; jesperm@oesm.dk
6 Department of Geosciences and Natural Resource Management, University of Copenhagen, 1165 Copenhagen, Denmark; larsc@ign.ku.dk
* Correspondence: victor.beccari@gmail.com
† urn:lsid:zoobank.org:act:76F3ECA8-8B98-4735-8354-398B53A455EA; urn:lsid:zoobank.org:act:8DF8A871-C8D7-4944-A8A9-338BF82AB5CA; urn:lsid:zoobank.org:pub:8AB4D333-BD8E-40B3-B978-37AD481C20E3.
‡ urn:lsid:zoobank.org:author:CF510830-CFDF-4955-8874-2C09C24A123C (V.B.); urn:lsid:zoobank.org:author:9310955D-ACA9-4090-8699-3BB795F7B067 (O.M.); urn:lsid:zoobank.org:author:00B8FDE4-3E97-47B6-9D60-9BBD260615A6 (O.W.); urn:lsid:zoobank.org:author:76740A35-5E64-413B-A561-EAEEB024F79E (J.M.); urn:lsid:zoobank.org:author:04906BD1-B206-448B-94F1-ABBC6388EB10 (L.B.C.).

Citation: Beccari, V.; Mateus, O.; Wings, O.; Milàn, J.; Clemmensen, L.B. *Issi saaneq* gen. et sp. nov.—A New Sauropodomorph Dinosaur from the Late Triassic (Norian) of Jameson Land, Central East Greenland. *Diversity* **2021**, *13*, 561. https://doi.org/10.3390/d13110561

Academic Editor: Eric Buffetaut

Received: 29 September 2021
Accepted: 29 October 2021
Published: 3 November 2021

Abstract: The Late Triassic (Norian) outcrops of the Malmros Klint Formation, Jameson Land (Greenland) have yielded numerous specimens of non-sauropod sauropodomorphs. Relevant fossils were briefly reported in 1994 and were assigned to *Plateosaurus trossingensis*. However, continuous new findings of early non-sauropod sauropodomorphs around the globe facilitate comparisons and allow us to now revise this material. Here, the non-sauropod sauropodomorph *Issi saaneq* gen. et sp. nov. is described based on two almost complete and articulated skulls. The two skulls represent a middle-stage juvenile and a late-stage juvenile or subadult. *Issi saaneq* differs from all other sauropodomorphs by several unique traits: (1) a small foramen at the medial surface of the premaxilla; (2) an anteroposteriorly elongated dorsoposterior process of the squamosal; (3) a relatively high quadrate relative to rostrum height; (4) a well-developed posterodorsal process of the articular. These features cannot be explained by taphonomy, ontogeny, or intraspecific variation. *Issi saaneq* shows affinities to Brazilian plateosaurids and the European *Plateosaurus*, being recovered as the sister clade of the latter in our phylogenetic analysis. It is the northernmost record of a Late Triassic sauropodomorph, and a new dinosaur species erected for Greenland. *Issi saaneq* broadens our knowledge about the evolution of plateosaurid sauropodomorphs.

Keywords: sauropodomorph; Triassic; plateosaurid; dinosaur; Greenland

1. Introduction

The non-sauropod sauropodomorph *Plateosaurus engelhardti* [1], was the first dinosaur to be named outside the UK [2]. Numerous specimens were since assigned to the genus *Plateosaurus*, and new species proposed. Such is the case of *Plateosaurus ingens* [3], formerly *Gresslyosaurus ingens* [4], *Plateosaurus erlenbergiensis* [5], *Plateosaurus gracilis* [2], formerly *Sellosaurus gracilis* [6], and *Plateosaurus trossingensis* [7]. The validity of these specimens has

been debated over the last few decades, with one main alternative of *Plateosaurus* classification being the most accepted. Most authors recognize three valid species, *Pl. gracilis* as a sister taxon of *Pl. engelhardti* and *Pl. ingens* [8–11]. However, the material assigned to *Pl. ingens* is under preparation for a redescription, as it possibly represents a new genus [12]. The main issue with *Plateosaurus* taxonomy arises due to the fragmentary nature of the holotype. Therefore, Galton, [13] proposed that the specimen SMNS 13200, a complete skeleton including cranial and post-cranial material, assigned to *Pl. trossingensis*, should be the neotype of *Plateosaurus*, which was accepted by the decision of the International Commission on Zoological Nomenclature [14].

The interrelationships of early sauropodomorphs and the phylogenetic relationship of *Plateosaurus* are receiving increasing attention with novel taxa described for the Late Triassic of South America, Africa and Europe in the past few decades but it is still plagued by issues that are not yet resolved [12,15–19]. McPhee et al. [18] listed the major issues with early sauropodomorph taxonomy, such as disagreeing and poorly understood character conceptions; fragmentary material and missing data for key specimens; lack of complete descriptions and restricted access to several Chinese taxa; and the inclusion of chimeric specimens as operational taxonomic units (OTUs). Among the first attempts to assess *Plateosaurus* interrelationships was the phylogenetic analysis done by Yates [15], where *Plateosaurus* was recovered at the base of Plateosauria, defined as the least inclusive clade containing *Plateosaurus* and Sauropoda (*sensu* [15]). The clade that includes species closer to *Plateosaurus trossingensis* than to Sauropoda was referred to as Plateosauridae in the same work [15] and is recovered in most cladistic analyses with *Unaysaurus tolentinoi* [20] as the sister taxon to *Plateosaurus* [11,12,15,18,21]. However, this comes as no surprise as the dataset used to assess non-sauropod sauropodomorphs usually derives from the work of Yates [15].

McPhee et al. [18] tested the position of *U. tolentinoi* as the sister taxon to *Plateosaurus* and, although relatively constant in his analysis, the clade Plateosauridae is only supported by two unambiguous synapomorphies of the humerus: a non-convex humeral head (character 220, state 1 in the dataset of [18]) and the length of humerus being three times that of the transverse width of its distal condyles (226 (0) in the dataset of [18]). The latter, however, is shared with several other non-sauropod taxa. The introduction of *Macrocollum itaquii* [22] in recent phylogenetic analyses placed *U. tolentinoi* as a sister taxon to *Mac. itaquii*, both forming with the Indian sauropodomorph *Jaklapallisaurus asymmetrica* [23] the clade Unaysauridae [19,22]. Unaysauridae was first recovered as a sister clade to Plateosauridae and then shifted to a more derived position inside of Massopoda (*sensu* [15]) [19,22]. Although close relationship to the contemporaneous sauropodomorphs from Brazil is expected, the validity of Unaysauridae suffers from the missing data and fragmentary nature of specimens. For example, one synapomorphy of unaysaurids is related to the astragalus medial end length ratio to the anteroposterior length of the lateral end, a which has not been confirmed in *U. tolentinoi*, whereas a second synapomorphy, the presence of a promaxillary fenestra, cannot be observed in *J. asymmetrica* which lacks the required cranial remains [23].

Jenkins et al. [24] reported for the first time the presence of an early sauropodomorph in Late Triassic strata (Norian) of the Fleming Fjord Group (formerly Fleming Fjord Formation, see [25]), of Jameson Land in central East Greenland. Jenkins and colleagues [24] briefly described a skull (NHMD 164741, formerly MCZ Field no. 61/91G) from the Malmros Klint Formation (formerly Malmros Klint Member, see [25]). This specimen was collected in Summer of 1991 and assigned to *Plateosaurus engelhardti* (=*Pl. trossingensis*) due to its dental structure and number of teeth, a single dorsal process of the premaxilla, and a Y-shaped quadratojugal [24]. Unfortunately, the lack of a thorough description rendered the allocation of this specimen to *Pl. trossingensis* as tentative, at most, and recent studies advise that this classification should be taken with caution [26]. Furthermore, other Norian sauropodomorphs described in the last decades added new relevant information about the taxonomy of the Greenland specimens.

More new specimens were collected from the same locality: at least three additional specimens were recovered and are yet to be formally described. Among them is an almost complete skull of a juvenile sauropodomorph (NHMD 164758, formerly 1/G95 or 1/95/G, collected in 1995) and two unpublished individuals with cranial and postcranial material (NHMD 164734, formerly 4.88.G and GM.V 2013-683, collected in 2012; and NHMD 164775, a yet unprepared specimen collected in 2012).

Here we focus on the reassessment and thorough description of the skull NHMD 164741, regarded as *Pl. engelhardti* (=*Pl. trossingensis*) by Jenkins et al. [24], and the first description of specimen NHMD 164758, another skull from the same locality, using µCT-scan for the evaluation of hard-to-access features. New features shared by both specimens also allow us to provide an updated phylogeny of early Sauropodomorpha.

2. Geological Setting

Late Triassic sediments are well exposed in the Jameson Land Basin, located in central East Greenland at about 71° N at the present-day land areas of Jameson Land and Scoresby Land (Figure 1). The Jameson Land Basin is bounded by the N-S stretching Liverpool Land to the east and the Stauning Alper to the west. To the north and south, the basin was demarcated by a fracture zone in the Kong Oscars Fjord and the Scoresby Sund respectively [25,27]. During the Late Triassic, the basin was located at the northern rim of the Pangaea supercontinent at approximately 43° N [28]. This position placed the basin in a transition zone between the relatively dry interior of Pangaea and the more humid peripheral part of this continent [29,30], or well inside the humid temperate belt [28].

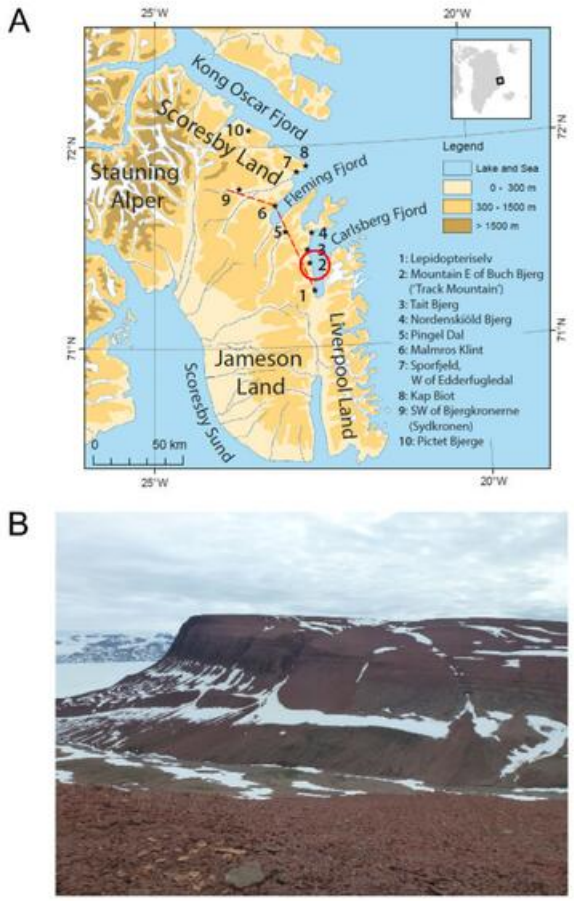

Figure 1. Topographic map of Jameson Land, central East Greenland. (**A**) Topographic map of Jameson Land. The Macknight Bjerg site of the Malmros Klint Formation is marked by the red circle and number 2. Modified from [25]. (**B**) Photograph of the outcrops in Buch Bjerg "Track-site".

The Fleming Group consists of three formations, a lowermost Edderfugledal Formation, a middle Malmros Klint Formation, and an uppermost Ørsted Dal Formations [28]. The Edderfugledal and Malmros Klint formations formed in shallow lacustrine/playa lake environments, whereas a large part of the Ørsted Dal Formation records lake and mudflat deposition [25]. The Malmros Klint Formation is exposed in impressive cliff exposures at Carlsberg Fjord near the eastern margin of the basin, where it has a typical thickness of about 125 m (Figure 2).

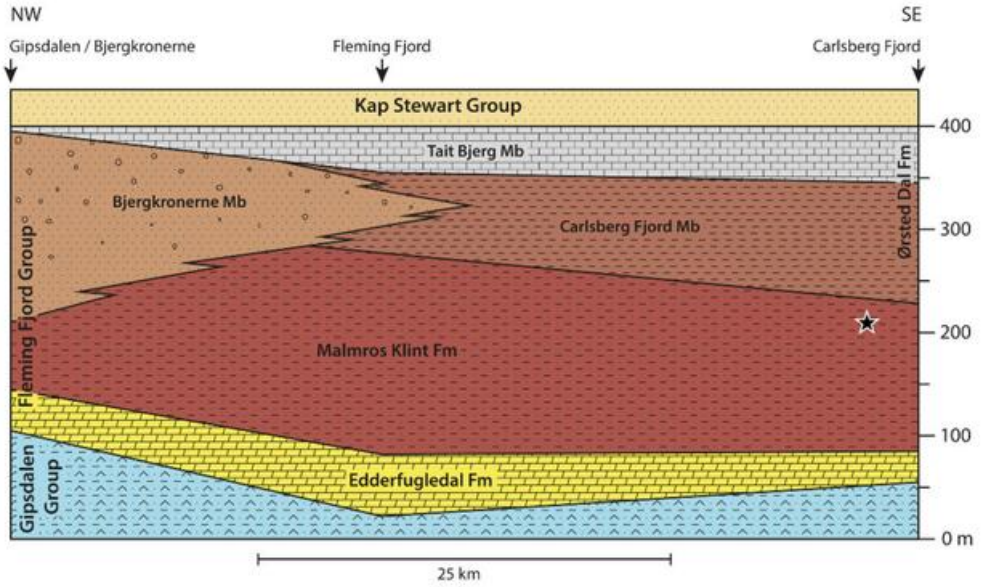

Figure 2. Cross-section of the lithostratigraphic units in the Fleming Fjord Group. Schematic cross-section of the lithostratigraphic units in the Fleming Fjord Group, Jameson Land. The star marks the uppermost Macknight Bjerg site where the sauropodomorph specimens were collected. Modified from [25].

The Malmros Klint and Ørsted Dal Formations comprise a diverse faunal assemblage, containing chondrichthyans and actinopterygian fishes, dipnoans such as *Ceratodus tenuensis* [31], theropod and sauropodomorph dinosaurs, temnospondyls, turtles, aetosaurs, phytosaurs and pterosaurs [24,26,31–36]. Furthermore, the fauna includes teeth and bony elements of early mammaliaforms [24,37,38].

New palaeomagnetic work [28] indicates that the Fleming Fjord Group was deposited between 220 and 209 Ma. Specimens NHMD 164741 and NHMD 164758 were recovered from the same locality, the "Iron Cake" site, in the north side of Macknight Bjerg. This material in the "Iron Cake" site comes from a 1 m thick lake-shore sandstone interval in the uppermost part of the Malmros Klint Formation, 25 m below its boundary to the Ørsted Dal Formation (Figure 2). According to the age model of Kent and Clemmensen [28], this site has an age of 214 Ma (mid Norian), whereas the site in uppermost Carlsberg Fjord Member with other skeletal remains of a sauropodomorph has an age of 211 Ma.

3. Materials and Methods

3.1. Specimens in This Study

NHMD 164741 (Figure 3A) represents a nearly complete, partially articulated, laterally compressed skull with mandible and teeth. NHMD 164758 (Figure 3B) consists of a nearly complete, articulated and laterally compressed skull with mandible and teeth. Postcranial elements of possibly the same individual (NHMD 164758) were collected in 2012 but are yet unprepared and not described in the current work. Both skulls are permanently housed at the Natural History Museum of Denmark (NHMD). Specimen NHMD 164758 was broken into at least two pieces, separating the anterior and posterior regions of the skull, and glued back together using Paraloid® B-72 (Kremer Pigmente, München, Bavaria, Germany)

dissolved in acetone (equal parts/50%). The anatomy of both specimens was compared to other basal sauropodomorph dinosaurs described in the literature (Table 1).

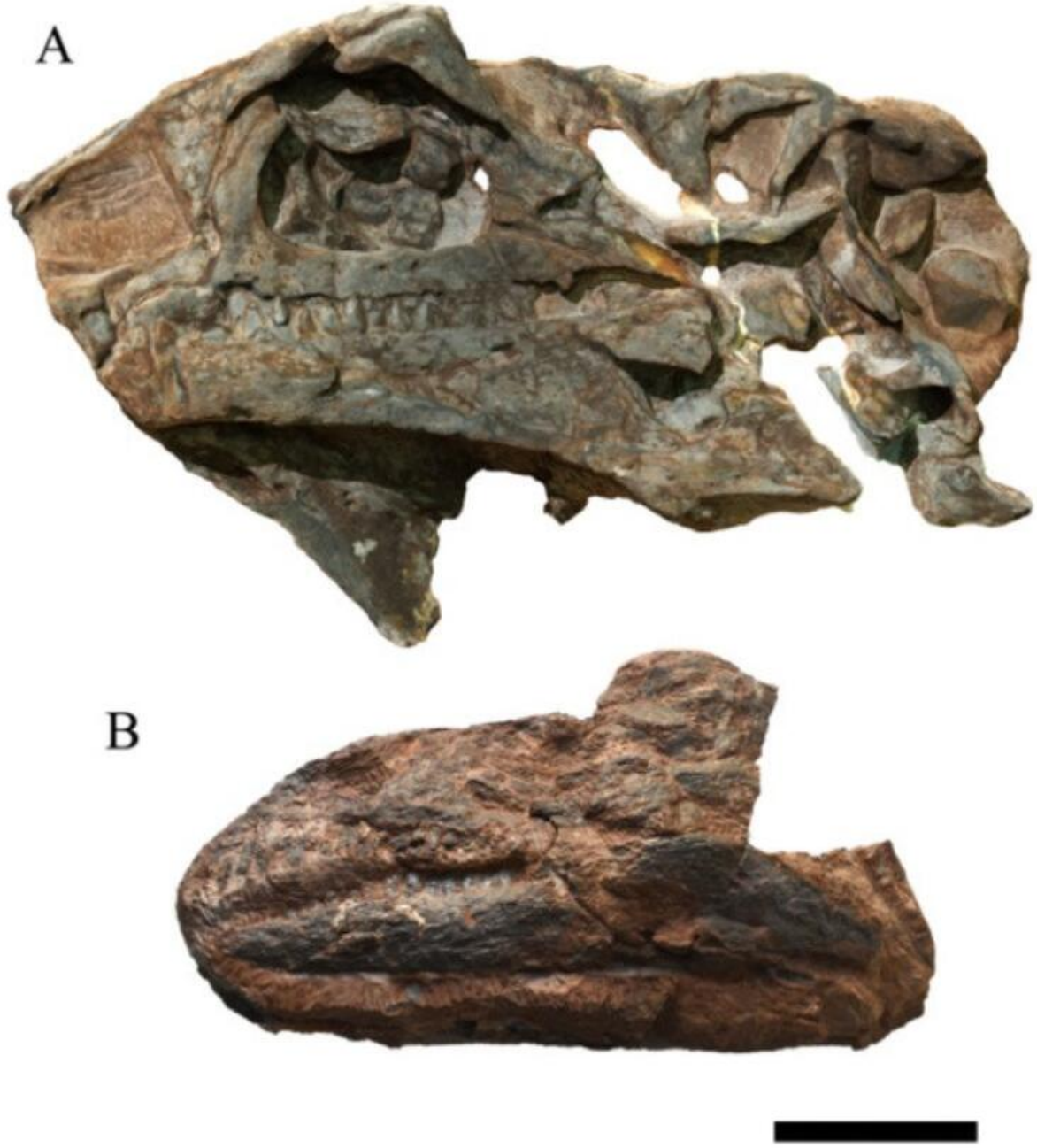

Figure 3. Photograph of the skulls NHMD 164741 and NHMD 164758. (**A**) NHMD 164741 in left lateral view. (**B**) NHMD 164758 in left lateral view.

Table 1. List of specimens used in this study for purposes of comparative anatomy.

Taxon	Specimen(s)	Source(s)
Bagualosaurus agudoensis	UFRGS-PV-1099-T	[39]
Buriolestes schultzi	CAPPA/UFSM 0035; ULBRA-PVT280	[40–42]
Coloradisaurus brevis	PVL 3967	[43,44]

Table 1. *Cont.*

Taxon	Specimen(s)	Source(s)
Efraasia minor	SMNS 12667	[2,45,46]
Leyesaurus marayensis	PVSJ 706	[11]
Lufengosaurus huenei	IVPP V15	[47]
Macrocollum itaquii	CAPPA/UFSM 0001a; CAPPA/UFSM 0001b	[19,22]
Massospondylus carinatus	BP/1/5241; BP/1/4934	[16]
Massospondylus kaalae	SAM-PK-K1325	[48]
Ngwevu intlokoi	BP/1/4779	[17]
Pampadromaeus berberenai	ULBRA-PVT016	[49]
Panphagia protos	PVSJ 874	[50]
Plateosaurus trossingensis	AMNH FARB 6810; GPIT-PV-30704; MB.R.1937; MSF 07.M; MSF 08.M; MSF 08.H; MSF 09.2; MSF 11.4; MSF 12.3; MSF 15.4; MSF 15.8; MSF 16.1; MSF 17.4; MSF 23; MSF 33; NAAG_00011238; NAAG_ 00011239; SMA 09.1; SMNS 12949; SMNS 12950; SMNS 13200; SMNS 52968	[2,3,51–53]
Plateosaurus gracilis	GPIT 18318a	[2]
Saturnalia tupiniquim	MCP 3845-PV	[54]

3.2. Digitization and Image Treatment

The specimens were digitized using both photogrammetry and µCT-scanning, followed by the creation of a texturized 3D model and observations of internal structures. The photogrammetric method used was based on the Walk-Around Method [55] using a D3500 camera (Nikon, Tokyo, Japan). The pictures were taken from the full 360° of each specimen with a 10° interval between each picture. The 3D photogrammetry models were created with the commercial software Metashape v.1.71 (Agisoft, St. Petersburg, Russia). The first alignment was set to High accuracy, then the point cloud was cleaned manually and using gradual selection, then a dense point cloud was generated set to High quality. The meshes were generated using the High Face Count setting and textures were created in 7680/1 Texture Size/Count setting.

Both specimens were CT-scanned at CENIEH (Burgos, Spain), using MicroCT V | Tome | X s 240 by GE Sensing & Inspection Technologies Phoenix X-Ray (Hürth, North Rhine-Westphalia, Germany). The resulting high-resolution stack contains 2848 .tiff images of 0.08999975 mm voxel size and 1922 × 562 × 2636 resolution (NHMD 164741) and a stack of 2821 .tiff images of 0.0679998 mm voxel size and1810 × 756 × 2821 resolution (NHMD 164758). The raw files are available to download at MorphoSource (ark:/87602/m4/393344, accessed on 29 September 2021). Image Segmentation was carried out with the commercial software Avizo v9.1 (Thermo Fisher, Waltham, MA, USA). Due to the low contrast between bones, the process of segmentation was done mainly using the brush selection tool, slice by slice, and applying interpolation when needed. The "Remove Island" feature of Avizo was applied for islands smaller than 30 pixels to remove the excessive noise of the meshes. The image segmentation process resulted in a total of 65 meshes for NHMD 164741 and 73 meshes for NHMD 164758. The meshes were generated using no smooth operator and exported as wavefront (.obj) files.

All meshes were treated and rendered with the free open-source software Blender v2.92. The segmented meshes were smoothed using the Smooth Laplacian modifier with Lambda factor = 1 and 5 repeats and then decimated to 20% of the original face count for rendering purposes. All the meshes (in .obj file format) are available at MorphoSource (ark:/87602/m4/393381, accessed on 29 September 2021). The measurements were taken both on the physical specimens and digitally in Blender. All renders were done using Cycles as a render engine and with an accurate scale bar in the software. All pictures

and renders of the specimens were handled in the commercial imaging softwares Adobe Lightroom 2021 and Adobe Photoshop CC 2021 (Adobe, Mountain View, CA, USA).

3.3. Skull Reconstruction

The digital reconstruction of the specimens was done by retrodeforming, moving, and mirroring the best-preserved elements in the software Blender v2.92. This allowed for tentative volume visualization and natural placement of bones of the laterally crushed specimens. The measurements taken in these skeletal reconstructions are approximated and the digital reconstruction was not used in the description and comparative anatomy section of this manuscript.

3.4. Phylogenetic Analysis

The specimens NHMD 164741 and NHMD 164758 were scored separately in the data matrix of Rauhut et al. [12], containing 67 OTUs and 382 characters (120 cranial and 262 post-cranial) (Supplementary Materials, Data S1). *Mac. itaquii* was scored in this dataset, following the descriptive work of Müller et al. [22] and Müller [19] to assess the validity of the clade Unaysauridae and its relationship to Plateosauridae. The phylogenetic analysis was conducted using the free software TNT v1.5 [56]. The trees were recovered using Traditional Search, with 1000 Wagner trees replicates, holding 20 trees per replicate, with TBR algorithm and 1 random seed, collapsing the trees after the search. Consistency and retention indexes and Bremer Support were obtained using a premade script. Bootstrap was calculated using absolute frequencies and 100 replicates. All characters were treated with the same weight, and characters 8, 13, 19, 23, 40, 57, 62, 69, 92, 102, 117, 121, 122, 129, 132, 148, 150, 151, 158, 168, 170, 171, 178, 210, 211, 213, 232, 237, 254, 263, 268, 282, 295, 316, 322, 330, 352, 365, 368, 370, 375, and 380 were treated as ordered.

3.5. Institutional Abbreviations

AMNH FARB, American Museum of Natural History, Fossil Amphibian, Reptile and Bird Collection, New York, NY, USA; BP, Bernard Price Institute for Palaeontological Research, University of the Witwatersrand, Johannesburg, South Africa; BRSMG, Bristol City Museum and Art Galleries, Bristol, UK; CAPPA/UFSM, Centro de Apoio à Pesquisa Paleontológica da Quarta Colônia da Universidade Federal de Santa Maria, Rio Grande do Sul, Brazil; GPIT, Institut und Museum für Geologie und Paläontologie der Universität Tübingen, Germany; IVPP, Institute of Vertebrate Paleontology and Paleoanthropology, Beijing, People's Republic of China; MB.R., Museum für Naturkunde, collection of fossil Reptilia, Berlin, Germany; MCP, Museu de Ciências e Tecnologia Pontifícia Universidade Católica do Rio Grande do Sul, Porto Alegre, Brazil; MSF, Sauriermuseum Frick, Frick, Switzerland; NHMD, GeoCenter Møns Klint, Møns Klint, Denmark; PVL, Paleontolgía de Vertebrados, Instituto Muíguel Lillo, Tucumán, Argentina; SAM-PK, Iziko South African Museum, Cape Town, South Africa; SMA, Sauriermuseum Aathal, Aathal-Seegräben, Switzerland; SMNS, Staatliches Museum für Naturkunde, Stuttgart, Germany; UFRGS-PV, Paleovertebrate Collection of the Laboratório de Paleovertebrados da Universidade Federal do Rio Grande do Sul, Porto Alegre, Brazil; UFSM, Universidade Federal de Santa Maria, Brazil; ULBRA-PVT, Universidade Luterana do Brasil, Coleção de Paleovertebrados, Canoas, Brazil.

3.6. Nomenclature Acts

The electronic edition of this article conforms to the requirements of the amended International Code of Zoological Nomenclature (ICZN), and hence the new names contained herein are available under that Code from the electronic edition of this article. This published work and the nomenclatural acts it contains have been registered in ZooBank, the online registration system for the ICZN. The ZooBank LSIDs (Life Science Identifiers) can be resolved, and the associated information viewed through any standard web browser by appending the LSID to the prefix http://zoobank.org/. The LSID for this publication

is: (urn:lsid:zoobank.org:pub:8AB4D333-BD8E-40B3-B978-37AD481C20E3). The electronic edition of this work was published in a journal with an ISSN and has been archived and is available from the following digital repositories: PubMed Central, LOCKSS.

4. Results

4.1. Systematic Palaeontology

Dinosauria [57]
Saurischia [58]
Sauropodomorpha [59]
Plateosauridae [60]
Issi saaneq gen. et sp. nov.

4.2. Etymology

From Kalaallisut, "issi" meaning cold and "saaneq" meaning bone. Pronounced 'is-y sa-ah-neq'. In reference to the conditions in which the fossils were recovered. We have selected a name in Inuit language to honor the local culture.

4.3. Holotype

NHMD 164741, (Figures 3A, 4 and 5) a nearly complete and partially articulated skull of a late-stage juvenile to sub-adult specimen, missing the anteriormost region of the premaxillae and dentaries and missing most of the right elements. The skull preserves the left premaxilla, both maxillae, both nasals, the left lacrimal, incomplete jugals, incomplete prefrontals, incomplete left postorbital, left squamosal, left quadratojugal, left quadrate, both frontals, the distal part of the left parietal, parts of the braincase (i.e., fragments of the basisphenoid, a fragment of the left laterosphenoid and the left paroccipital process), both pterygoids, the left ectopterygoid, fragments of the palatines, fragments of the left vomer, both dentaries, the left coronoid process, left splenial, left angular, left surangular, left prearticular, left articular and teeth.

4.4. Paratype

NHMD 164758, (Figures 3B, 6 and 7) a nearly complete and articulated skull of a medium-stage juvenile specimen, with lateral deformation, missing most of the posterodorsal skull elements (i.e., squamosals, most of the parietals, supraoccipital and prootic). The skull preserves both premaxillae, both maxillae, both nasals, both lacrimals, both prefrontals, the left postorbital, both jugals, the condylar area of both quadrates, both frontals, the anterior part of the left parietal, parts of the braincase (i.e., the left orbitosphenoid, the left laterosphenoid, right basipterygoid process and the parasphenoid process of the basisphenoid), the complete palatal region and the complete mandibles.

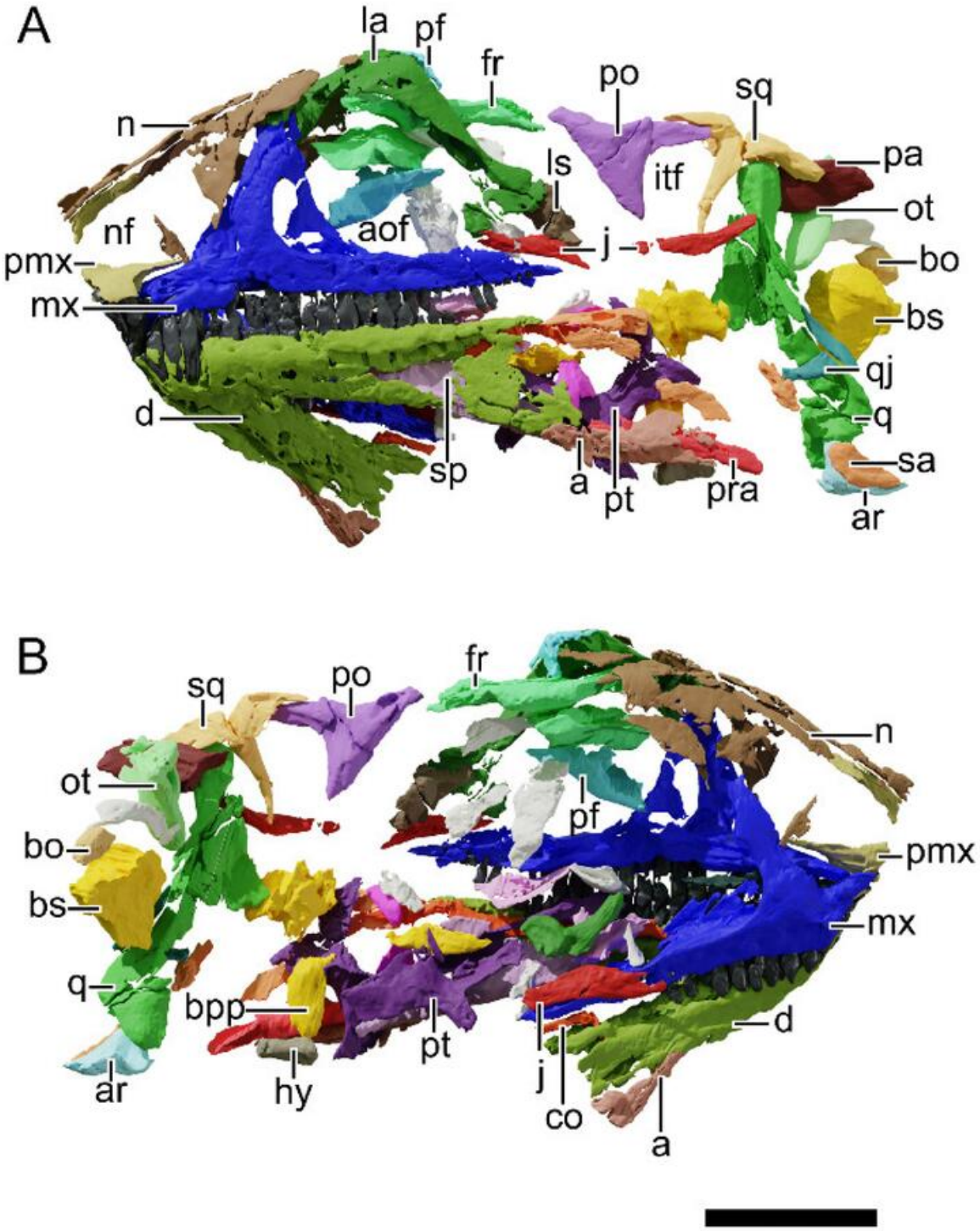

Figure 4. Digital reconstruction of the skull of NHMD 164741. (**A**) Left lateral view. (**B**) Right lateral view. Abbreviations: a, angular; aof, antorbital fenestra; ar, articular; bo, basioccipital; bpp, basipterygoid process; bs, basisphenoid; co, coronoid; d, dentary; fr, frontal; hy, hyoid; itf, infratemporal fenestra; j, jugal; la, lacrimal; ls, laterosphenoid; mx, maxilla; n, nasal; nf, narial fenestra; ot, otoccipital; pa, parietal; pf, prefrontal; pmx, premaxilla; po, postorbital; pra, prearticular; pt, pterygoid; q, quadrate; qj, quadratojugal; sa, surangular; sp, splenial; sq, squamosal. Scale bar = 50 mm.

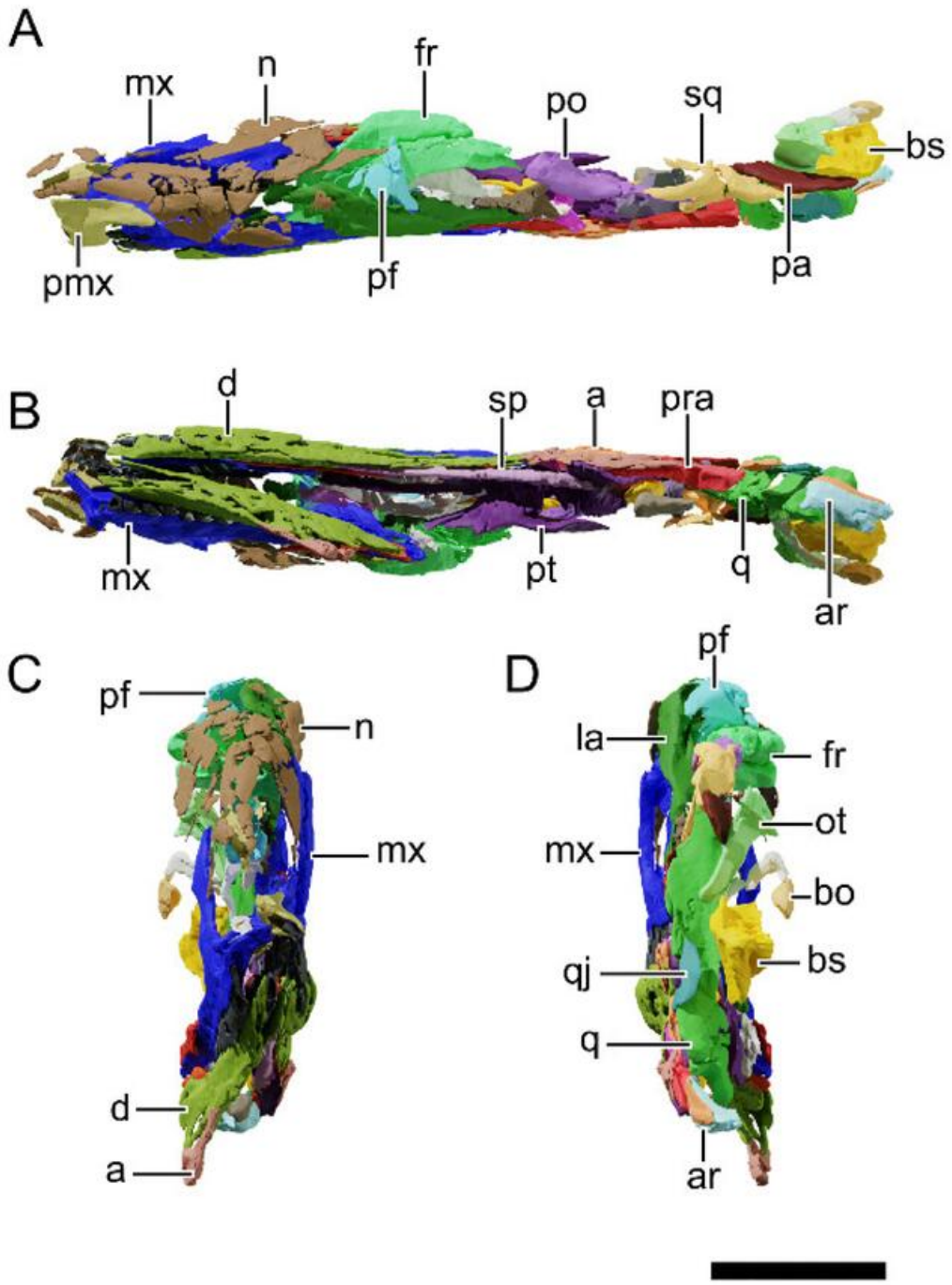

Figure 5. Digital reconstruction of the skull of NHMD 164741. (**A**) Dorsal view. (**B**) Ventral view. (**C**) Anterior view. (**D**) Posterior view. Abbreviations: a, angular; ar, articular; bo, basioccipital; bs, basisphenoid; d, dentary; fr, frontal; la, lacrimal; ls, laterosphenoid; mx, maxilla; n, nasal; ot, otoccipital; pa, parietal; pf, prefrontal; pmx, premaxilla; po, postorbital; pra, prearticular; pt, pterygoid; q, quadrate; qj, quadratojugal; sa, surangular; sp, splenial; sq, squamosal. Scale bar = 50 mm.

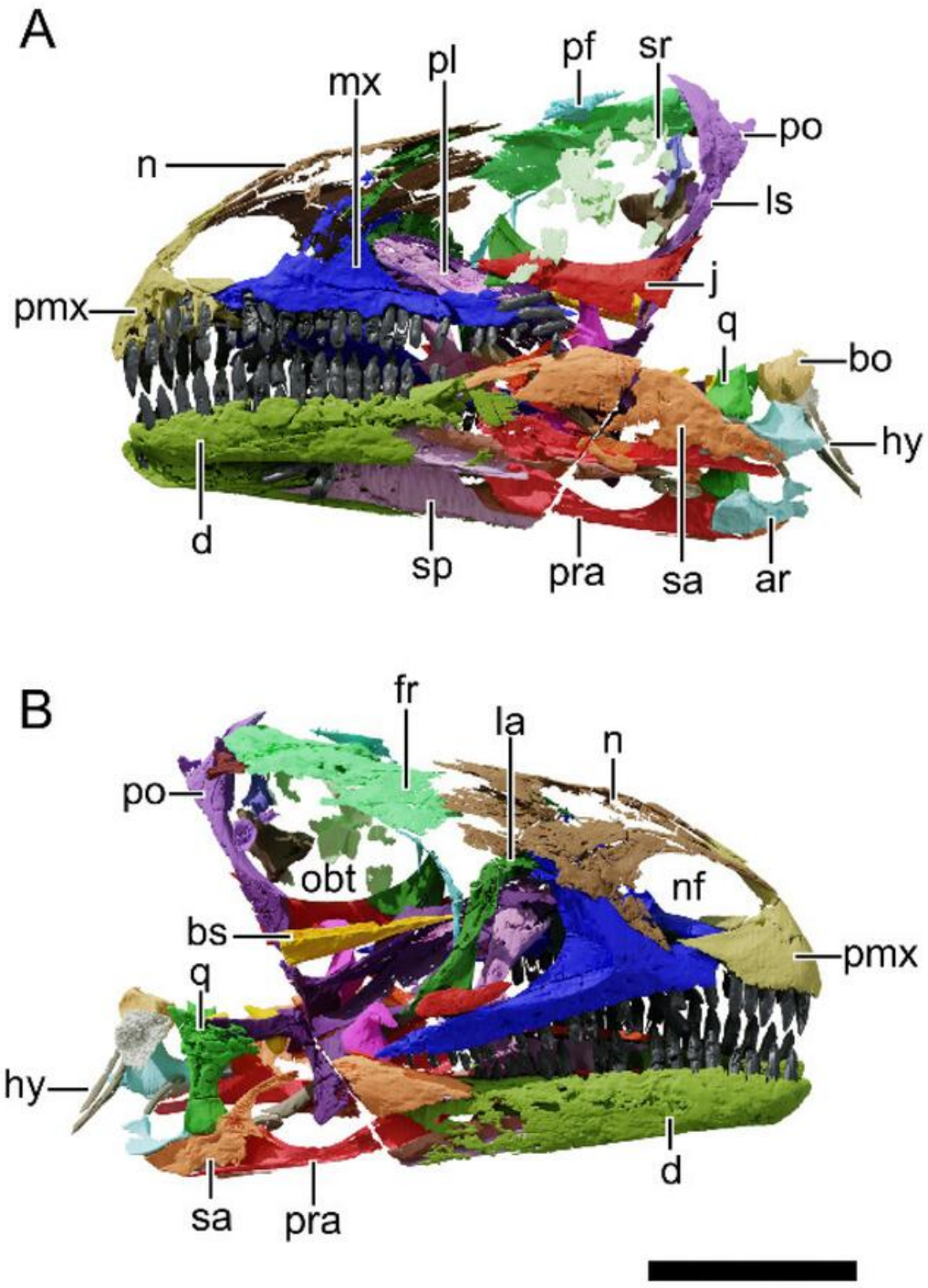

Figure 6. Digital reconstruction of the skull of NHMD 164758. (**A**) Left lateral view. (**B**) Right lateral view. Abbreviations: ar, articular; bo, basioccipital; bs, basisphenoid; d, dentary; fr, frontal; hy, hyoid; j, jugal; la, lacrimal; ls, laterosphenoid; mx, maxilla; n, nasal; nf, narial fenestra; obt, orbit; pf, prefrontal; pl, palatine; pmx, premaxilla; po, postorbital; pra, prearticular; pt, pterygoid; q, quadrate; sa, surangular; sp, splenial; sr, sclerotic ring. Scale bar = 50 mm.

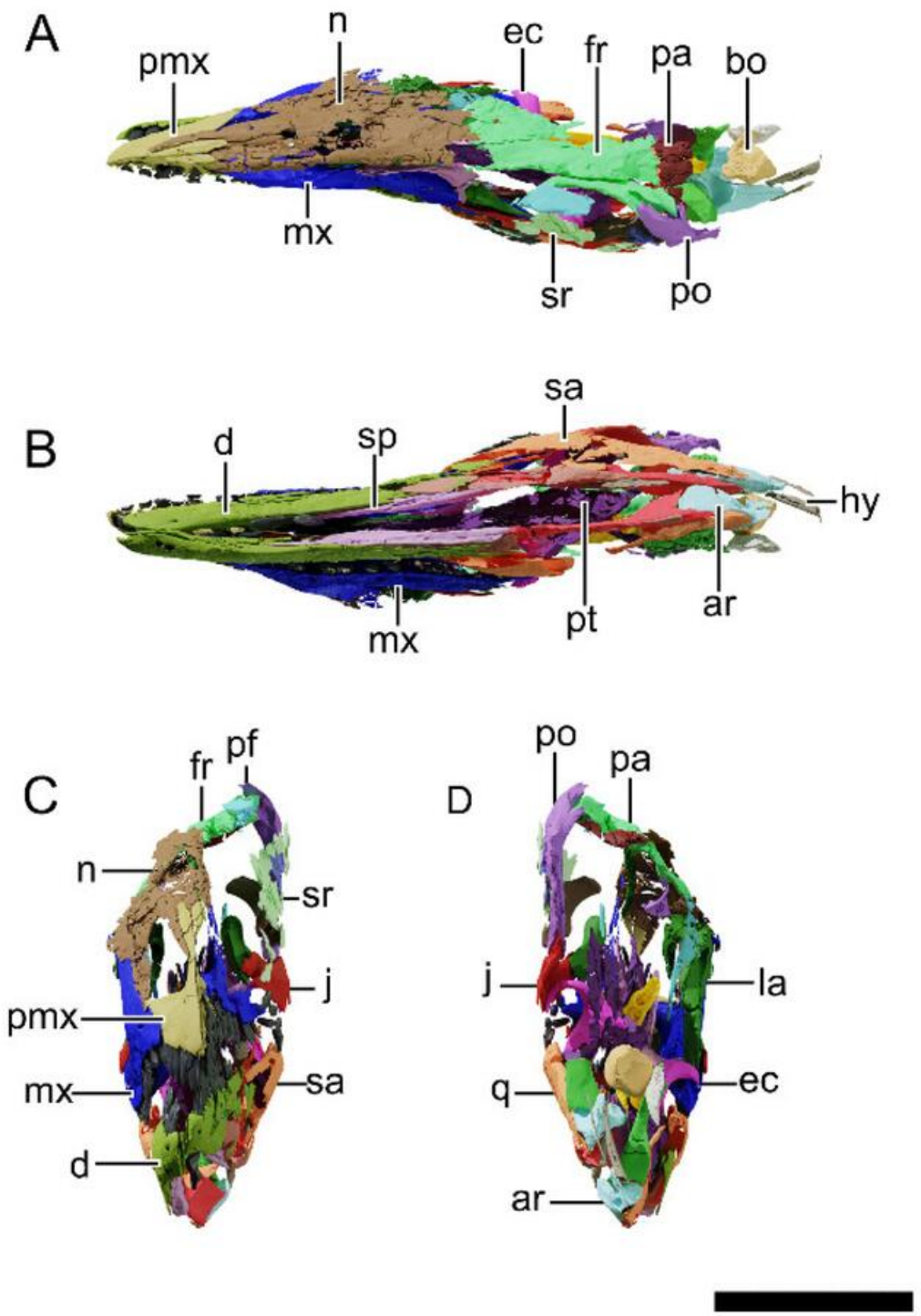

Figure 7. Digital reconstruction of the skull of NHMD 164758. (**A**) Dorsal view. (**B**) Ventral view. (**C**) Anterior view. (**D**) Posterior view. Abbreviations: ar, articular; bo, basioccipital; d, dentary; ec, ectopterygoid; fr, frontal; hy, hyoid; j, jugal; la, lacrimal; mx, maxilla; n, nasal; pa, parietal; pf, prefrontal; pmx, premaxilla; po, postorbital; pra, prearticular; pt, pterygoid; q, quadrate; sa, surangular; sp, splenial; sr, sclerotic ring. Scale bar = 50 mm.

4.5. Locality

NHMD 164741 and NHMD 164758 were collected at Macknight Bjerg site, Jameson Land, central East Greenland, of coordinates 71°23.010′ N, 22°34.114′ W and 71°22.993′ N, 22°33.972′ W, respectively (Figure 1).

4.6. Horizon and Age

NHMD 164741 and NHMD 164758 were collected at Malmros Klint Formation, Fleming Fjord Group, of mid-Norian stage of the Late Triassic [28,29,61].

4.7. Diagnosis

Issi saaneq can be distinguished from other basal sauropodomorphs on the basis of a unique trait combination comprising six phylogenetic synapomorphies (i) and four cranial autapomorphies (ii). (i) weakly developed narial fossa (character 10, state 0); small subnarial foramen (12, 1); anterior margin of the external naris anterior to the mid-length of the premaxilla (17, 0); anteroposterior length of the antorbital fossa less than that of the orbit (28, 1); antorbital fossa ending before the ventral process of the lacrimal (41, 1); strongly curved jugal process of the ectopterygoid (86, 1). (ii) the presence of a small foramen at the medial surface of the premaxilla at the base of the lateral process of the premaxilla; an anteroposteriorly elongated dorsoposterior process of the squamosal; a quadrate relatively tall in comparison to the rostrum height; a well-developed posterodorsal process of the articular, square-shaped in lateral view. *Issi saaneq* possesses features thought to be autapomorphic to other plateosaurids, i.e., five teeth in the premaxilla (as in *Plateosaurus*), a promaxillary fenestra (as in the Brazilian plateosaurids *Mac. itaquii* and *U. tolentinoi*), a lateral sheet of bone in the lacrimal covering the posterodorsal corner of the antorbital fenestra (as in *Pl. trossingensis*), and a secondary fossa ventral to the Meckelian groove (as in *U. tolentinoi*).

4.8. Description and Comparative Anatomy

4.8.1. Generalities

NHMD 164741 consists of a partially complete and almost fully articulated skull. The specimen is almost twice as long as tall (length is measured from the anteriormost preserved region to the end of the squamosal and height is measured from the ventral surface of the left dentary to the apex of the left lacrimal), and due to a lateral crushing, its overall width is around a fifth of its height (see Table 2 for the skull general measurements). The anteriormost region of the snout (anterior part of left premaxilla and whole right premaxilla) and anterior region of both dentaries are missing. Thus, the total length of the skull cannot be precisely measured, although it would not be much longer than preserved. Most elements in the skull of NHMD 164741 are preserved in three dimensions, with little individual deformation, even though the skull is crushed laterally. This lateral compression displaced most bones from the right side of the skull and disarticulated some elements (i.e., left and right frontals, left postorbital, left quadratojugal). The left elements of the skull are mostly present, showing some fractures, but preserving the overall shape of the skull. The orbital region, however, is poorly preserved due to compaction, with the overall orbital shape only tentatively recovered as semi-circular, according to a slight anterodorsal expansion over the caudal margin of the lacrimal. The right jaw joint region of the skull is missing, whereas the left elements of this region are slightly ventrally displaced, but mostly still in association (i.e., quadratojugal, quadrate, articular and the posterior part of the surangular). The braincase and occipital region are mostly disarticulated, its bones missing or too fragmented for precise identification.

Table 2. General skull measurements for the Greenland specimens NHMD 164741 and NHMD 164758. Asterisk (*) indicates maximum preserved measurement.

Measurements (in mm)	NHMD 164741	NHMD 164758
Skull anteroposterior length (from the anterior tip of the premaxilla to posterior margin of occipital condyle)	243.7 *	167.9
Skull maximum dorsoventral height at orbit including the mandible	112.7	93.6
Skull dorsoventral height at orbit excluding mandible	75.2	58.3
Rostrum dorsoventral height (measured at the posterior margin of the external naris level)	57.9	40.9
External naris maximum anteroposterior length	35.1	25.1
Orbit length	52.5 *	49.9
Orbit height	46.5 *	41.0
Premaxilla maximum anteroposterior length	-	36.9
Premaxilla alveolar anteroposterior length	-	24.3
Premaxilla maximum dorsoventral height	40.3	37.8
Narial fossa anteroposterior length	28.7	24.9
Maxilla anteroposterior maximum length	129.9	95.5
Maxilla anteroposterior alveolar length	118.8	85.7
Maxilla dorsoventral height (from the dorsal tip of the dorsal process to ventral margin of maxilla)	57.0	42.0
Antorbital fossa maximum anteroposterior length	46.5	34.8
Nasal anteroposterior length	98.7	80.0
Lacrimal dorsoventral height	64.5	41.9
Lacrimal maximum length of dorsal region	43.1	37.5
Prefrontal dorsoventral maximum height	-	32.3
Frontal maximum anteroposterior length	51.6	42.3
Frontal maximum mediolateral width	49.1	18.7
Postorbital maximum length	48.6	25.5
Postorbital maximum height	40.8	41.6
Squamosal maximum length	49.5	-
Squamosal maximum height	38.9	-
Jugal maximum anteroposterior length	57.8	48.9
Jugal height under the orbit	11.3	10.5
Quadrate dorsoventral height	91.8	-
Quadrate mediolateral width at condylar region	13.9	10.8
Quadrate pterygoid flange anteroposterior length	24.3	17.8
Pterygoid maximum anteroposterior length	92.4	83.8
Pterygoid maximum dorsoventral height	52.4	46.6
Ectopterygoid maximum length of medial flange	29.8	20.5
Ectopterygoid maximum mediolateral width	22.4	21.6
Palatine maximum anteroposterior length	31.3	39.8
Palatine maximum mediolateral width	9.1	13.2
Vomer maximum anteroposterior length	-	42.6
Mandible maximum length	210.1 *	167.1

Table 2. *Cont.*

Measurements (in mm)	NHMD 164741	NHMD 164758
Mandible maximum height	45.6	33.8
Dentary maximum length	118.0 *	100.1
Dentary maximum height	34.4	22.1
Surangular maximum length	118.1	79.8
Surangular maximum height	44.8	25.5

The NHMD 164758 skull is relatively smaller (0.69 in length) than that of NHMD 164741, but its elements show less lateral compaction than NHMD 164741, resulting in a better-preserved palatal region. Similar to NHMD 164741, the skull is relatively dorsoventrally taller than in other plateosaurids (see Table 2). The right elements of the snout are better preserved, as the lateral surface of the left snout elements was eroded. The orbit in NHMD 164758 is subcircular and preserves the left sclerotic ring.

4.8.2. Premaxilla

NHMD 164741 preserves the posterior half of the left premaxilla (Figure 8). NHMD 164758 bears the only complete premaxilla of both specimens (right element, Figure 9). The premaxilla is triangular in lateral profile, encompassing most of the narial fenestra. The main body of the premaxilla is slightly anteroposteriorly longer than dorsoventrally tall and contains five alveoli, the first of which is adjacent to the rostral tip of the bone. A 5-tooth premaxilla is also seen in *Plateosaurus* (except for specimens with 6 premaxillary teeth, i.e., HMN XXIV, SMNS 12949 and SMNS 13200), and the position of the first premaxillary tooth is close to the anterior margin of the premaxilla. An anteriorly located first premaxillary tooth is similar to that of the juvenile *Pl. trossingensis* (MSF 15.8B) and is thought to be related to ontogeny [53], as in mature specimens of *Pl. trossingensis* (i.e., MSF 11.4, MSF 15.8, and 16.1) there is usually a gap between the anterior tip of the premaxilla and the first premaxillary tooth.

The main body is laterally perforated by a small foramen at the base of the dorsal process, at the level of the anterior margin of the second premaxillary tooth. Posterior to this foramen, at the dorsal margin of the premaxilla main body, a shallow recess forms the narial fossa. The narial fossa marginates the posterior margin of the dorsal process of the premaxilla, reaching its deepest point at the lateral mid-length of the premaxillary body, around the level of the third premaxillary tooth. The shallow narial fossa is observed in both NHMD 164741 and NHMD 164758, although the exact anterior extend of this structure on the former is unknown. The narial fossa position, depth and shape differ from that of all *Plateosaurus* skulls described (i.e., AMNH FARB 6810; HMN XXIV; HMN MB.1927.19.1; MSF 11.4; MSF 16.1; MSF 1; SMNS 52968). The narial fossa of these specimens is marked by a ventral rim and is deeply depressed in the premaxilla. The condition observed in NHMD 164758 is closer to that of *U. tolentinoi* (UFSM 11069), *Mac. itaquii* (CAPPA/UFSM 0001a), *Mas. carinatus* (BP/1/4934), and *N. intlokoi* (BP/1/4779), as well as most early sauropodomorphs (such as *Ba. agudoensis* and *Bu. schultzi*).

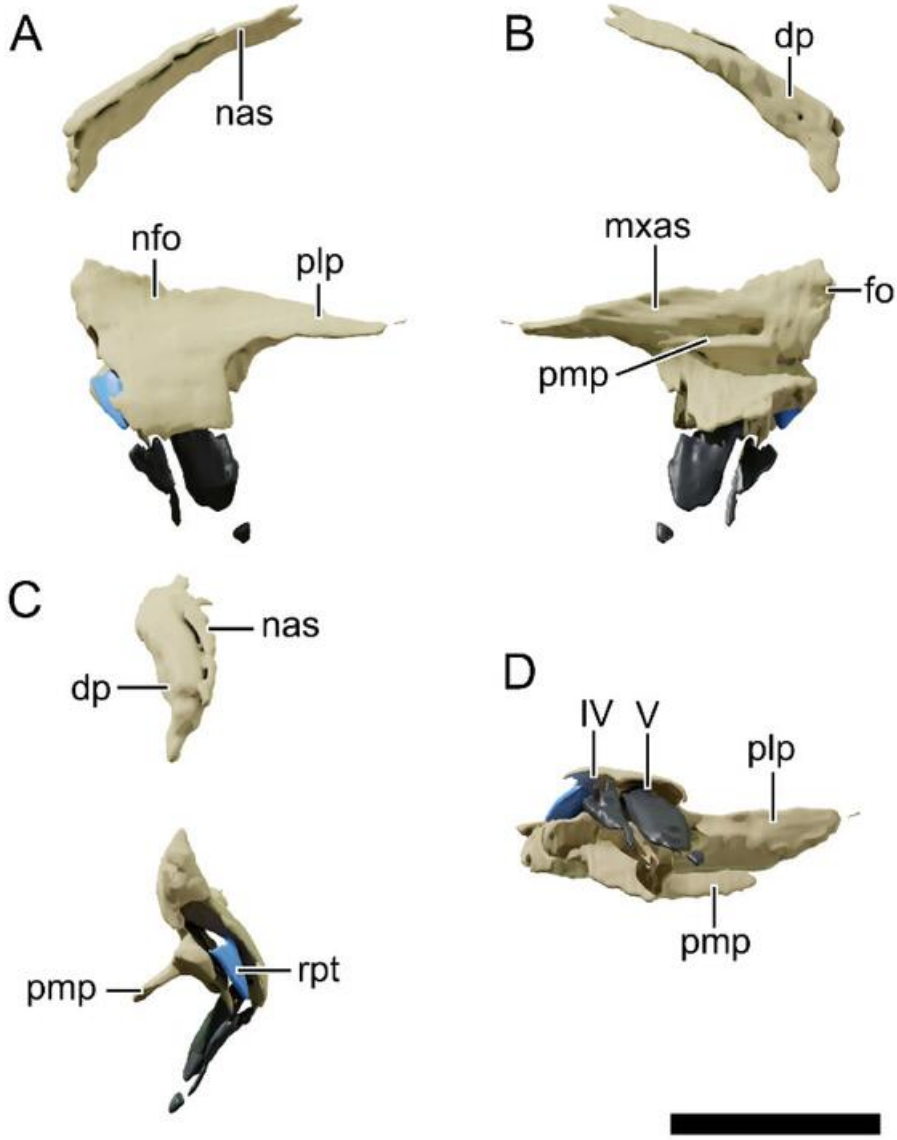

Figure 8. Digital reconstruction of the left premaxilla of NHMD 164741. (**A**) Lateral view. (**B**) Medial view. (**C**) Anterior view. (**D**) Ventral view. Abbreviations: dp, dorsal process; fo, foramen; mxas, articular surface for the maxilla; nas, articular surface for the nasal; nfo, narial fossa; plp, posterolateral process; pmp, posteromedial process; rpt, replacement tooth. IV and V represent the tooth position. Scale bar = 20 mm.

The medial surface of the premaxilla is almost straight at the contact with its counterpart, which occurs in the first half of the premaxillary main body. As in *Pl. trossingensis*, the teeth row forms an angle of 20° with the symphysis, resulting in a V-shaped dorsal and ventral profiles. The maxillary articular facet is delimited by a ventral sharp ridge that constitutes the posteroventral process and a smoother dorsal recess that forms the ventral margin of the posterolateral (=maxillary) process of the premaxilla. This later rests on the anterodorsal margin of the maxillary body and tapers to a point posteriorly until it contacts the rostroventral process of the nasal. Both NHMD 164741 and NHMD 164758 possess a round foramen at the dorsomedial surface of the premaxilla main body, at the base of the dorsal process of the premaxilla (Figures 8 and 9). This foramen is not observed on the disarticulated or exposed medial surface of the premaxillae of the plateosaurids *U. tolentinoi* (UFSM11069) [18] and *Pl. trossingensis* (AMNH FARB 6810 [52], MSF 16.1 [53] and MSF 15.8.935 [53]), nor the derived massospondylid *Mas. carinatus* (BP/1/5241) [16]. However, the saturnaliid sauropodomorph *Pam. berberenai* (ULBRA-PVT016) preserved

a similar foramen at the medial surface of the premaxilla, although more posteriorly and ventrally located in the latter [49]. The dorsal (=nasal) process of the premaxilla slopes posteriorly at an angle of 61° with the main body of the premaxilla. This deflection is lower than in *Mac. itaquii* (45°), *U. tolentinoi* (40°), but similar to some *Plateosaurus* specimens, particularly MB.R.1937. The dorsal process encloses the anterior margin of the narial fenestra and extends posteriorly until the level of the posterior process of the premaxilla. This process contacts its counterpart medially, flattening dorsoventrally at the posterior end. This flattening results in a distal expansion of this process, as in *Plateosaurus*, *Mac. itaquii* and *Coloradisaurus brevis* [43] PVL 3967.

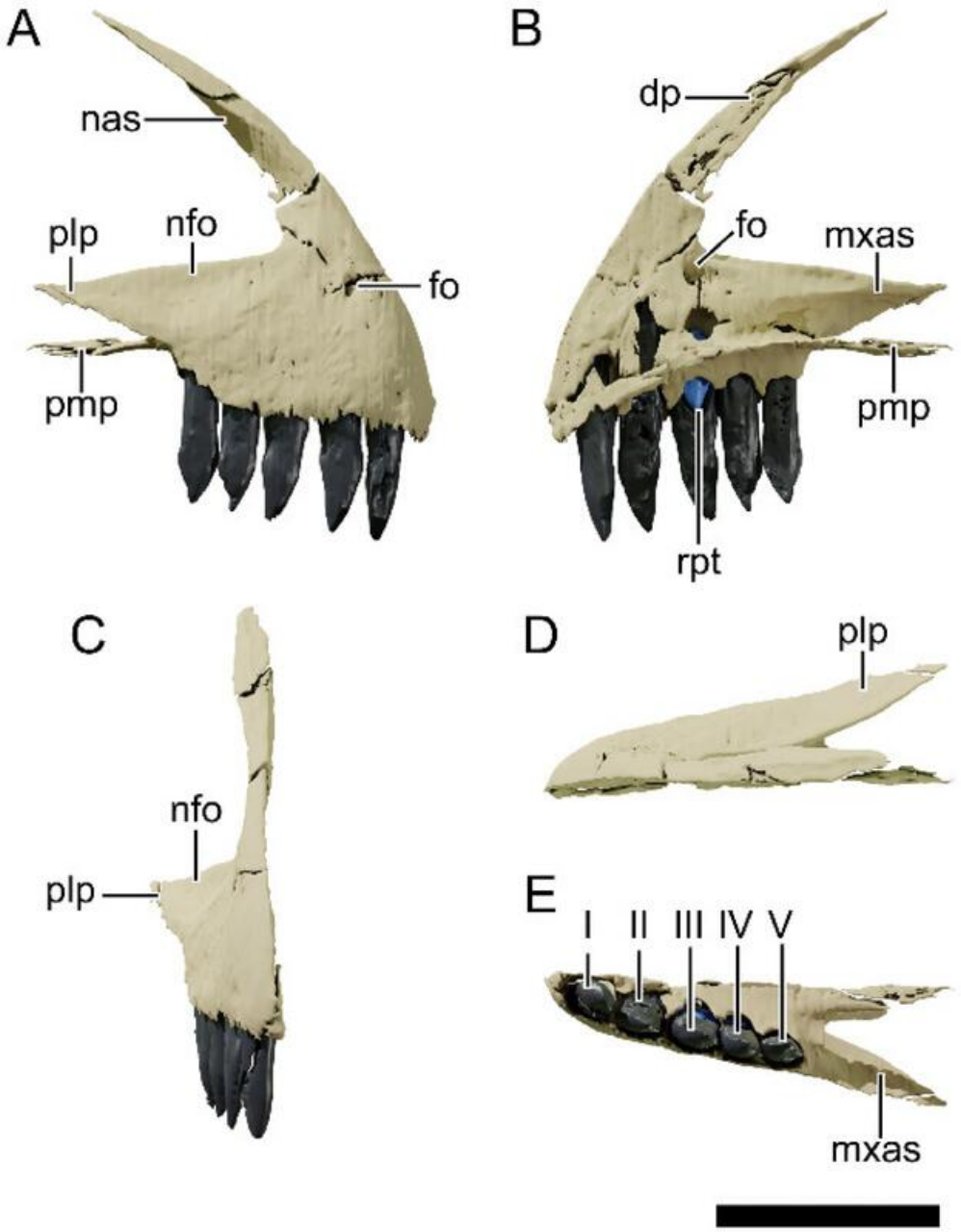

Figure 9. Digital reconstruction of the right premaxilla of NHMD 164758. (**A**) Lateral view. (**B**) Medial view. (**C**) Anterior view. (**D**) Dorsal view. (**E**) Ventral view. Abbreviations: dp, dorsal process; fo, foramen; mxas, articular surface for the maxilla; nas, articular surface for the nasal; nfo, narial fossa; plp, posterolateral process; pmp, posteromedial process; rpt, replacement tooth. I to V represent the tooth position. Scale bar = 20 mm.

4.8.3. Maxilla

The best-preserved maxillae are the left element in NHMD 164741 (Figure 10) and the right element in NHMD 164758 (Figure 11). This bone is triradiate in the lateral profile, with the horizontal main ramus divided by the vertical dorsal process of the maxilla. The main ramus is straight throughout its anteroposterior length, with both dorsal and ventral margins parallel to each other, only tapering at the posteriormost region. The dorsal process deflects slightly posteriorly and marginates the subtriangular antorbital fossa. A maximum of 23 alveoli in NHMD 164758 and 24 alveoli in NHMD 164741 are preserved, both specimens with four alveoli in the anterior segment of the main ramus. In other sauropodomorphs such as *Mac. itaquii*, *U. tolentinoi* (UFSM 11069), *Leyesaurus* (PVSJ 706) and *Mas. carinatus* (BP/1/4934) there are indeed four alveoli in this segment of the maxilla, but in *Plateosaurus* (such as AMNH FARB 6810, MSF 12.3, SMNS 13200) there are five alveoli anterior to the dorsal process of the maxilla.

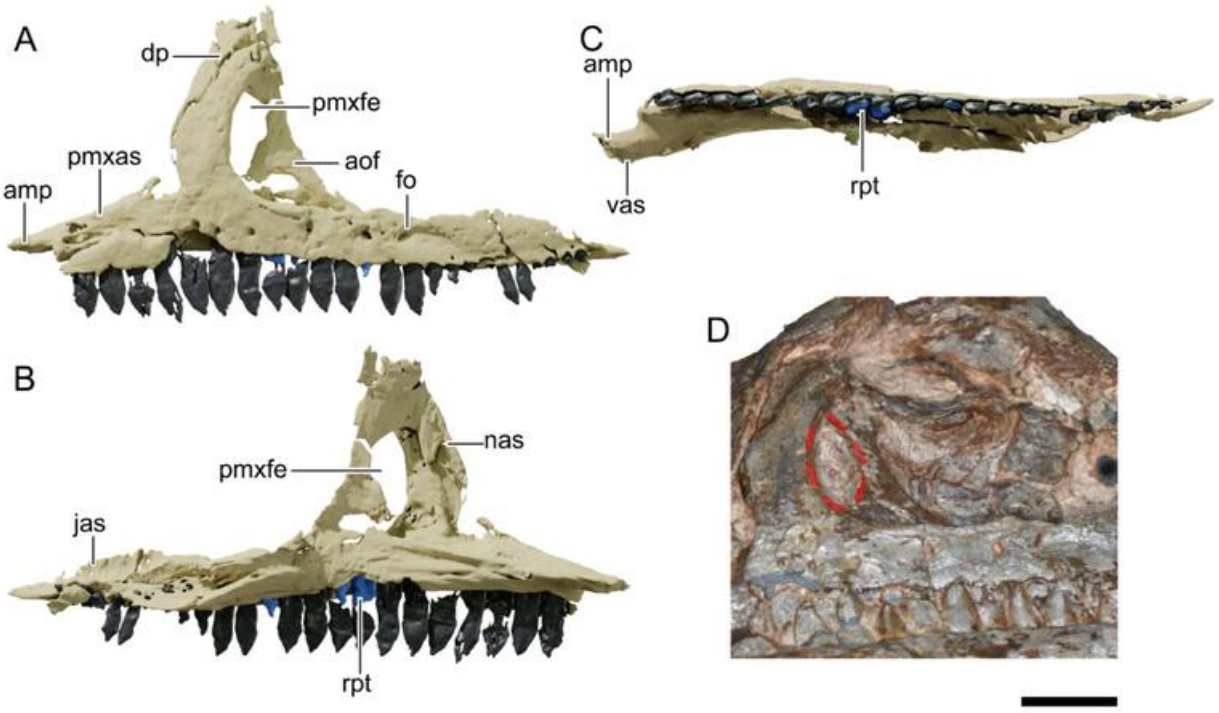

Figure 10. Digital reconstruction of the left maxilla of NHMD 164741. (**A**) Lateral view. (**B**) Medial view. (**C**) Ventral view. (**D**) Photograph of the left maxilla highlighting the promaxillary fenestra. Abbreviations: amp, anteromedial process; aof, antorbital fossa; dp, dorsal process; fo, foramen; jas, articular surface for the jugal; nas, articular surface for the nasal; pmxas, articular surface for the premaxilla; pmxfe, promaxillary fenestra; rpt, replacement tooth; vas, articular surface for the vomer. Scale bar = 20 mm.

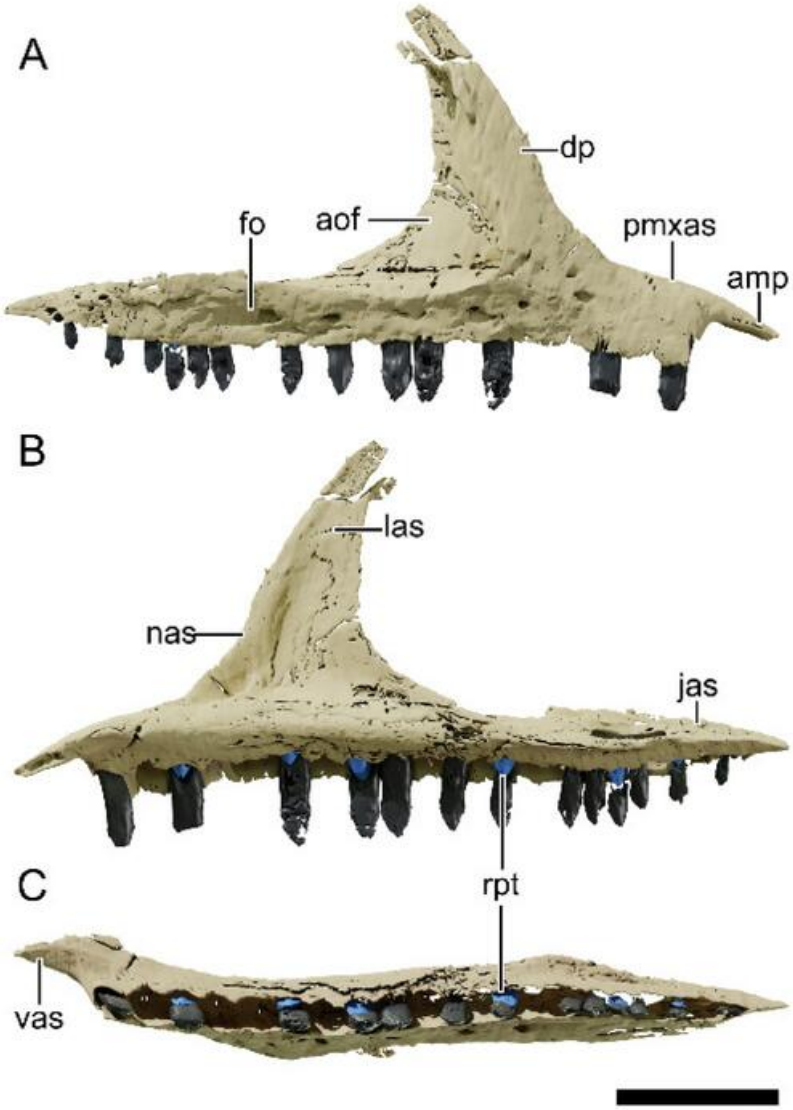

Figure 11. Digital reconstruction of the right maxilla of NHMD 164758. (**A**) Lateral view. (**B**) Medial view. (**C**) Ventral view. Abbreviations: amp, anteromedial process; aof, antorbital fossa; dp, dorsal process; fo, foramen; jas, articular surface for the jugal; las, articular surface for the lacrimal; nas, articular surface for the nasal; pmxas, articular surface for the premaxilla; rpt, replacement tooth; vas, articular surface for the vomer. Scale bar = 20 mm.

The anterior segment of the main ramus of the maxilla is anteroposteriorly shorter than the posterior segment and has no lateral neurovascular foramina. An anterior process of the maxilla extends medial to the premaxilla, tapering to a point anteriorly. This process is gently curved mediolaterally, with a sharp ridge at its dorsal margin, where it contacts laterally the maxillary process of the premaxilla. The anterior process of the maxilla contacts ventrally with the posteroventral process of the premaxilla and medially with the vomer, as in *Plateosaurus*.

The dorsal (=ascending) process of the maxilla tapers dorsally, with a slight dorsoposterior inclination. This process is almost perpendicular to the main ramus of the maxilla, differently from pre-Norian sauropodomorphs, such as non-Bagualosaurian (sensu [49]) and *Ba. agudoensis*. Anteriorly this process bounds the posterior margin of the external naris and laterally contacts the ventral (=maxillary) process of the nasal. The dorsal margin of the antorbital fossa converges to the dorsal tip of the maxillary dorsal process forming an apex, as in *Lufengosaurus huenei* [62] (IVPP V15), but differing from the posteriorly extended antorbital fossae of *Mac. itaquii*. Medially, the dorsal process of the maxilla forms

the anterior margin of the antorbital fossa. In NHMD 164758 the antorbital fossa is fully closed, differing from unaysaurids (i.e., *Mac. itaquii* and *U. tolentinoi*, *sensu* [19,22]), whose antorbital fossae are perforated by a large promaxillary fenestra. In NHMD 164741 this region is fragmented on both left and right maxillae.

However, in the left antorbital fossa, the presence of the promaxillary fenestra (or a blind ridge, as in the right maxilla of *Mac. itaquii* CAPPA/UFSM 0001b, Müller, 2019) is not discarded, as the anteroventral margin of the antorbital fossa possesses an undamaged recess (Figure 10D). The lateral surface of the posterior process of the maxilla is perforated by foramina, the last of which being the largest and opening posteriorly. The dorsal and ventral margins of the posterior process are parallel throughout most of their length, tapering posteriorly with a slight dorsal deflection. Along this deflection, a medial groove is formed on the dorsal margin, where the jugal articulates with the maxilla.

4.8.4. Nasal

The nasals are dorsoventrally thin tetraradiate bones (Figures 3–7), anteroposteriorly longer than lateromedially wide. The nasal is relatively shorter in NHMD 164741 and NHMD 164758 than in *Plateosaurus.* In *Plateosaurus*, the nasal is longer than half the skull roof length, a distinctive feature for the genus [52,53,63]. The main body of the nasal is dorsally convex and overlaps laterally the apex of the maxillary dorsal process. At its posterior region, the nasal contacts the prefrontal laterally and the frontal ventrally. Anteriorly, the nasal radiates in two ventrally oriented processes, separated by a dorsal concavity of the nasal. This area encompasses the posterodorsal region of the narial fenestra. The anteromedial (=premaxillary) process of the nasal contacts the dorsal process of the premaxilla laterally. The lateroventral (=maxillary) process marginates the dorsal process of the maxilla as a ventrally oriented triangular blade. Ventrally, this process tapers to a point that finishes just before contacting the posteriormost tip of the posterolateral process. A point-contact between the distal part of the lateroventral process of the nasal and the posterolateral process of the premaxilla is observed in *Plateosaurus* but not in *Mac. itaquii* and *Mas. carinatus*.

4.8.5. Lacrimal

The best-preserved lacrimals are the left element in NHMD 164741 (Figure 12) and the right element in NHMD 164758 (Figure 13), although in the former the distal part of the maxillary process is broken, and in the latter, the lateral surface is weathered. The lacrimal bounds the posterior margin of the antorbital fenestra and the anterior margin of the orbit. The lacrimal is shaped like an inverted L, with a long anterodorsal (=maxillary) process extending anteriorly. This process is obscured dorsally by the nasal. The anterodorsal process of the lacrimal is hollow and subcircular in cross-section, with the dorsal margin tapering into a ridge. This ridge extends from the dorsomedial margin of the main shaft of the lacrimal until it bisects at the anteriormost region of the process. The ventral projection at the bifid junction is longer than the dorsal projection. The anterodorsal process of the lacrimal bends laterally at its distal part to articulate to the medial margin of the dorsal process of the maxilla. The overall shape of the anterodorsal process of the lacrimal differs from that of *Pl. trossingensis* (AMNH FARB 6810), in which the process is triangular in cross-section at the bifid region, with the dorsal projection of the process being longer than the ventral.

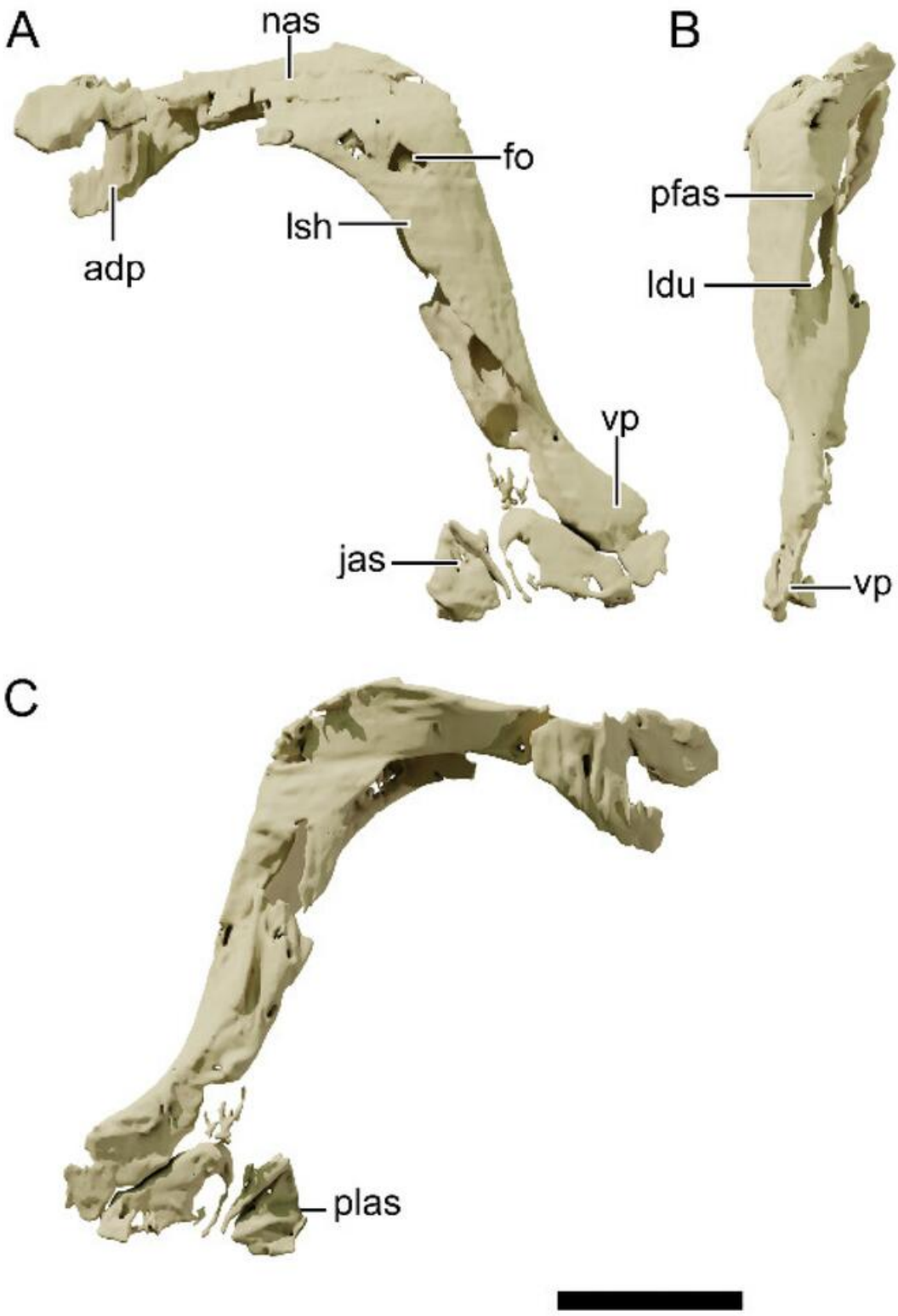

Figure 12. Digital reconstruction of the left lacrimal of NHMD 164741. (**A**) Lateral view. (**B**) Posterior view. (**C**) Medial view. Abbreviations: adp, anterodorsal process; fo, foramen; jas, articular surface for the jugal; ldu, lacrimal duct; lsh, lateral sheet of bone; nas, articular surface for the nasal; pfas, articular surface for the prefrontal; plas, articular surface for the palatine; vp, ventral process. Scale bar = 20 mm.

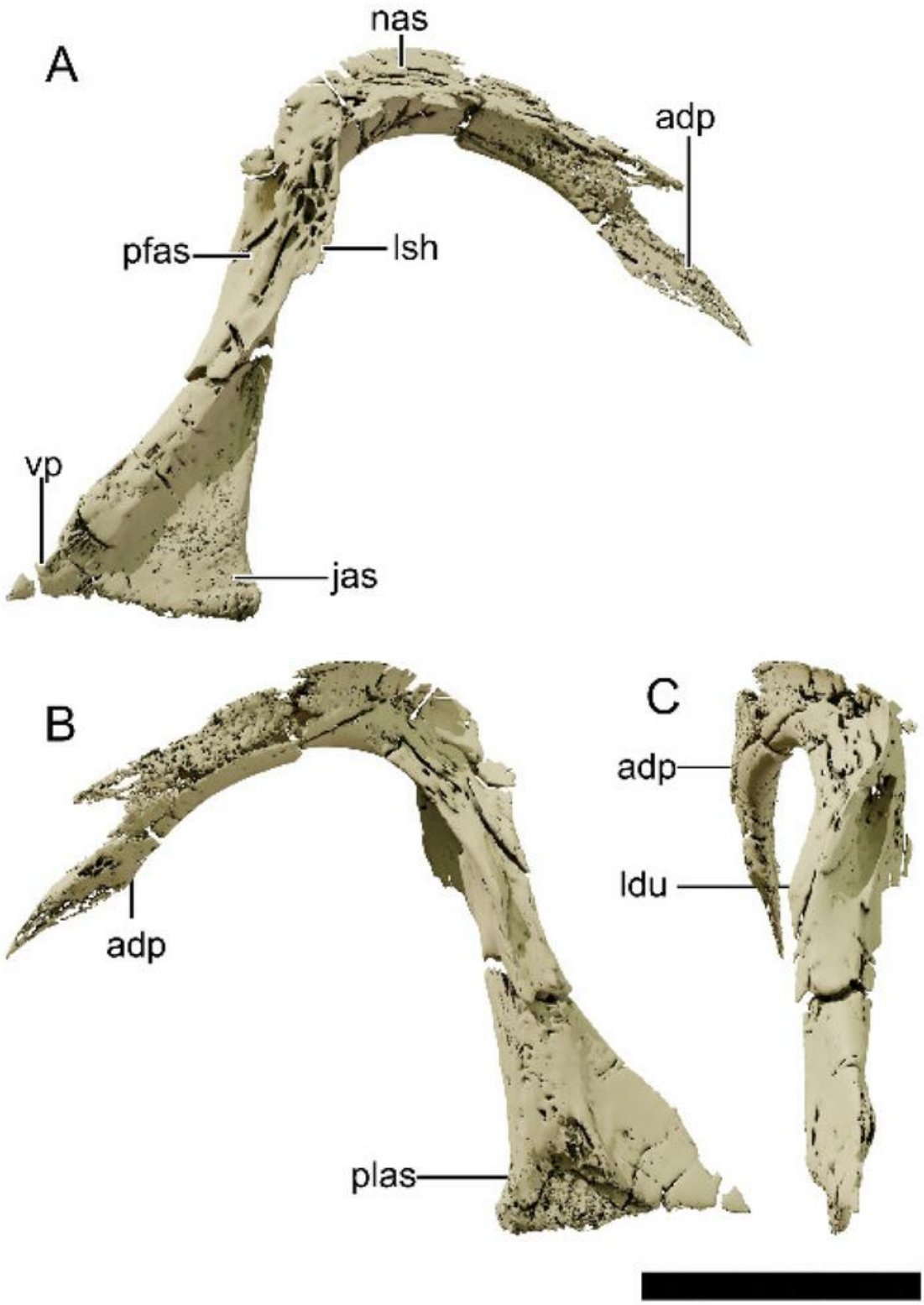

Figure 13. Digital reconstruction of the right lacrimal of NHMD 164758. (**A**) Lateral view. (**B**) Medial view. (**C**) Posterior view. Abbreviations: adp, anterodorsal process; fo, foramen; jas, articular surface for the jugal; ldu, lacrimal duct; lsh, lateral sheet of bone; nas, articular surface for the nasal; pfas, articular surface for the prefrontal; plas, articular surface for the palatine; vp, ventral process. Scale bar = 20 mm.

The main shaft of the lacrimal is inclined anteriorly at an angle of 50° to the long axis of the skull, contrasting with the sub-vertical lacrimal of *Mac. itaquii* and the 30° tilted

lacrimal of *Plateosaurus*. The lateral flange of the shaft is well-developed in NHMD 164741, as in *Pl. trossingensis* and differing from the condition of *E. minor* and *Pl. gracilis*. The dorsal half of the anterior margin of this flange is concave in NHMD 164741. In most specimens of *Pl. trossingensis*, the flange is convex, except for MSF 15.4 and MSF 16.1, in which it is concave. However, this concavity may have been caused by diagenetic deformation in these specimens. Therefore, the condition in NHMD 164741 is similar to that of *N. intlokoi* and *Lu. huenei* but differs from that of *Mas. carinatus* [17].

The lateral surface of the lacrimal is perforated by a laterally opened foramen near the dorsal margin of the main shaft in NHMD 164741, as in *Lu. huenei* (IVPP V15) and *Mac. itaquii*, although on the latter the foramen is reduced in diameter. The posterior margin of the lacrimal is perforated by the ventral-facing lacrimal duct. Ventral to this duct, the lacrimal articulates with the ventral (=lacrimal) process of the prefrontal. The ventral process of the lacrimal projects anteriorly and posteriorly, forming a fin-like shelf, as in *Plateosaurus*. The anterior projection is overlapped laterally by the anterior process of the jugal and medially by the palatine.

4.8.6. Prefrontal

Both NHMD 164741 and NHMD 164758 preserved only fragments of the prefrontals (Figures 3–7). The prefrontal is a dorsoventrally thin bone, anteroposteriorly longer than wide. It forms the anterodorsal margin of the orbit, being slightly concave at its ventral margin, whereas straight at its dorsal margin. In lateral view, the bone is T-shaped, with its posterior process being longer than the anterior, and reaching over half the length of the orbit. This condition is also observed in most post-Carnian sauropodomorphs, but not in *Mac. itaquii*, in which the posterior process does not reach half the orbital length. Medially, the prefrontal is concave, forming a dorsal and a ventral shelf that project medially. An elongated and slender lacrimal process projects ventrally from the medioventral margin of the postorbital. This process marginates the posterior margin of the lacrimal beneath the lacrimal duct opening and participates in the anterior margin of the orbit, although not reaching its anteroventral corner.

The posterior process of the prefrontal is expanded in both NHMD 164741 and NHMD 164758, being anteroposteriorly longer than the anterior process of the prefrontal. However, this elongation does not restrict the participation of the frontal in the orbit, as seen in *Plateosaurus* [2]. In dorsal view, this process tapers distally as in *Plateosaurus* and contacts the anterior region of the frontal medially.

4.8.7. Postorbital

Only the left postorbitals are preserved on both NHMD 164741 (Figure 14) and NHMD 164758 (Figure 15). The postorbital is a triradiate, Y-shaped bone, forming the posterodorsal margin of the orbit, the anterior margin of the infratemporal fenestra and the anterolateral margin of the supratemporal fenestra. The anterodorsal process of the postorbital is oriented anteromedially and dorsally. It is lateromedially broader than dorsoventrally tall. The medial margin of the anterodorsal process is bifurcated to embrace the posterolateral process of the frontal, as in *Mac. itaquii* and *Plateosaurus*. In NHMD 164741, the anteroposterior length of the anterodorsal process of the postorbital is slightly longer than the anteroposterior length of the posterodorsal process of the postorbital. This process is not preserved in NHMD 164758. In *Plateosaurus*, the anteroposterior process of the postorbital is shorter than the other postorbital processes.

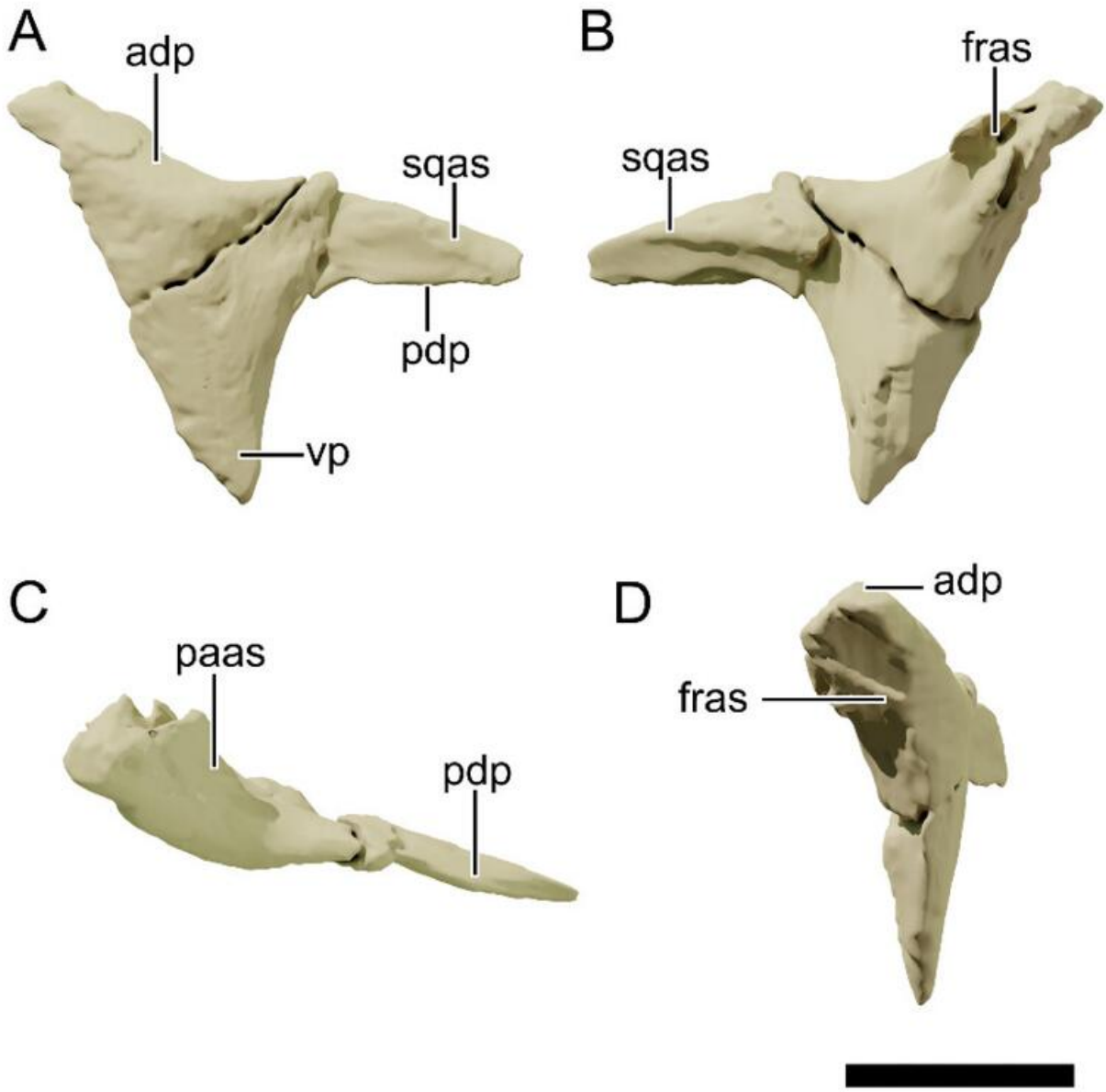

Figure 14. Digital reconstruction of the left postorbital of NHMD 164741. (**A**) Lateral view. (**B**) Medial view. (**C**) Dorsal view. (**D**) Anterior view. Abbreviations: adp, anterodorsal process; fras, articular surface for the frontal; paas, articular surface for the parietal; pdq, posterodorsal process; sqas, articular surface for the squamosal; vp, ventral process. Scale bar = 20 mm.

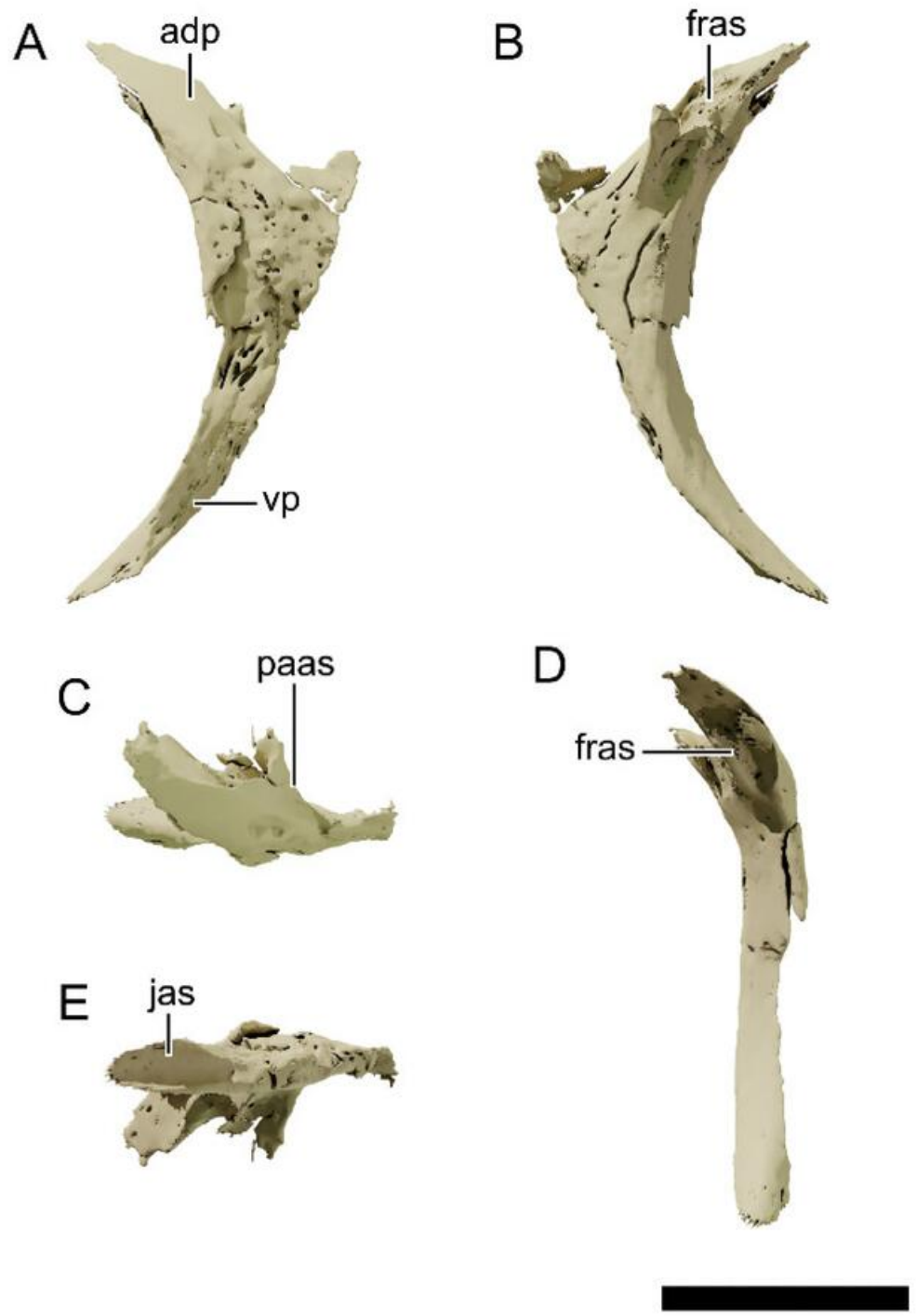

Figure 15. Digital reconstruction of the left postorbital of NHMD 164758. (**A**) Lateral view. (**B**) Medial view. (**C**) Dorsal view. (**D**) Ventral view. (**E**) Anterior view. Abbreviations: adp, anterodorsal process; fras, articular surface for the frontal; jas, articular surface for the jugal; paas, articular surface for the parietal; vp, ventral process. Scale bar = 20 mm.

The posterior process of the postorbital is only preserved in NHMD 164741. This process is lateromedially slender and dorsally convex. It articulates dorsally and medially to the anterior process of the squamosal, with the dorsolateral surface partially covered by the squamosal. The posterior process of the postorbital forms an angle to the anterior process of 149° in NHMD 164741 and 134° in NHMD 164758. In *Plateosaurus* these angles vary between 160° in AMNH FARB 6810 and MSF 11.4, and 110° in MSF 12.3. This latter is thought to be closer to the original condition, as the former were mediolaterally compressed.

The ventral process of the postorbital is broken in NHMD 164741 and best preserved in NHMD 164758 and is the longest process of the postorbital. This process is strongly concave anteriorly bounding the posterior surface of the orbit. It contacts the dorsal process of the jugal posteroventrally and excludes the jugal from the posterior margin of the orbit.

4.8.8. Squamosal

Only the left squamosal of NHMD 164741 is preserved (Figure 16). The squamosal is a tetraradiate bone that bound the dorsoposterior margin of the infratemporal fenestra and the dorsolateral margin of the supratemporal fenestra. The anterolateral (=postorbital) process of the squamosal sheets the posterior process of the postorbital and forms the posteromedial margin of the supratemporal fenestra. The anteromedial (=parietal) process is slightly laterally compressed, diverging from the anterolateral process at an angle of 45°. In *Pl. trossingensis* MSF 12.3 this divergence is 60° and possibly closer to the "in vivo" state [53]. This process marginates the posterior margin of the supratemporal fenestra laterally and contacts the posterior process of the parietal medially. The posterior process of the squamosal is 1.33 times longer than the anterior process, comprising over half the total dorsal length of the squamosal. In *Plateosaurus* and *Mac. itaquii*, the posterior process of the squamosal is shorter than the anterior process in all other described specimens (see Table 3). Ventrally, this process encapsulates the dorsalmost region of the quadrate head. This process is slightly ventrolaterally oriented, with a concave median margin that contacts part of the posterior process of the parietal and the distal surface of the paroccipital process of the otoccipital.

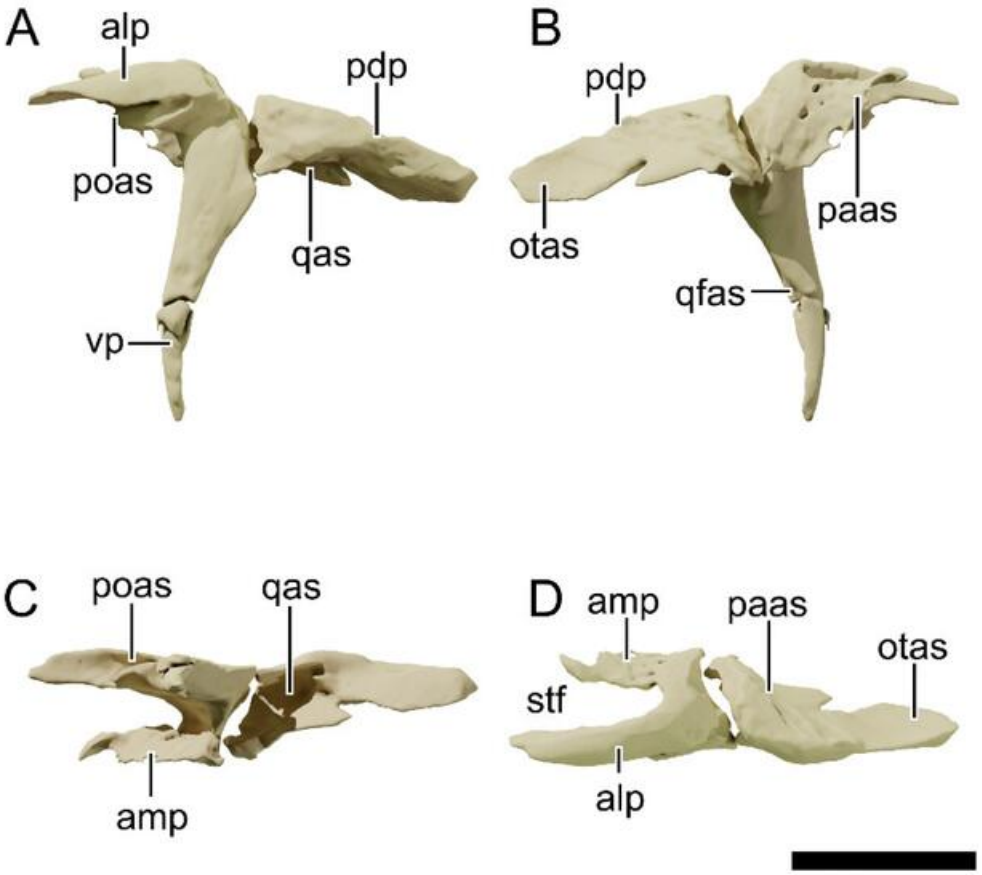

Figure 16. Digital reconstruction of the left squamosal of NHMD 164741. (**A**) Lateral view. (**B**) Medial view. (**C**) Ventral view. (**D**) Dorsal view. Abbreviations: alp, anterolateral process; amp, anteromedial process; otas, articular surface for the otoccipital; paas, articular surface for the parietal; pdt, posterodorsal process; poas, articular surface for the postorbital; qas, articular surface for the quadrate; qfas, articular surface for the quadrate flange; stf, supratemporal fenestra. Scale bar = 20 mm.

Table 3. Relative length of the posterior to the anterolateral processes of the squamosal across basal sauropodomorphs. Measurements were taken on the 3D models when available.

Squamosal—Posterior Process Length to Anterolateral Process Length		
Issi saaneq	NHMD 164741	1.31
Pl. trossingensis	AMNH FARB 6810	0.55
Pl. trossingensis	MSF 16.1	0.41
Pl. trossingensis	NAAG_00011238	0.48
Pl. trossingensis	MSF 12.3	0.53
Pl. trossingensis	MSF 15.4	0.83
Mac. itaquii	CAPPA/UFSM 0001b	0.77
Mas. carinatus	BP/1/5241	0.86
Bu. schultzi	CAPPA/UFSM 0035	0.88

The ventral (=quadrate) process is the longest of the squamosal processes, tapering distally and comprising the dorsoposterior margin of the infratemporal fenestra. It extends ventrally to about 60% of the infratemporal fenestra dorsoventral height. The distal end is deflected posteriorly as in *Plateosaurus*. The articular facet to the squamosal ramus of the quadratojugal is exposed laterally, meaning that it contacts the quadratojugal medially.

4.8.9. Jugal

The left jugal of NHMD 164758 is the best-preserved jugal element from both specimens (Figure 17), only missing the posteroventral process. This bone forms the ventral margin of the orbit and is concave dorsally and straight ventrally.

The anterior process of the jugal is five times anteroposteriorly longer than dorsoventrally tall, as in *Pl. trossingensis*, being relatively taller than in *Mac. itaquii* and *E. minor.* A dorsoventrally high jugal was found to a derived feature of *Pl. trossingensis* [2]. The anterior process of the jugal is laterally concave and divided in the mid-height by a longitudinal ridge. This process articulates to the maxilla beneath this ridge, at its anteroventral half, and medially to the lacrimal anteriorly and the ectopterygoid posterior to it. The posterodorsal (=postorbital) process of the jugal is deflected posteriorly, forming an angle of 137° to the anterior process. It contacts the ventral process of the postorbital anteriorly and bounds the anteroventral margin of the infratemporal fenestra. Medioventrally to this process sits the jugal fossa. The posterior process of the jugal is disarticulated from the main body in NHMD 164741. This process is slender and anteroposteriorly long and articulates with the quadratojugal lateroventrally.

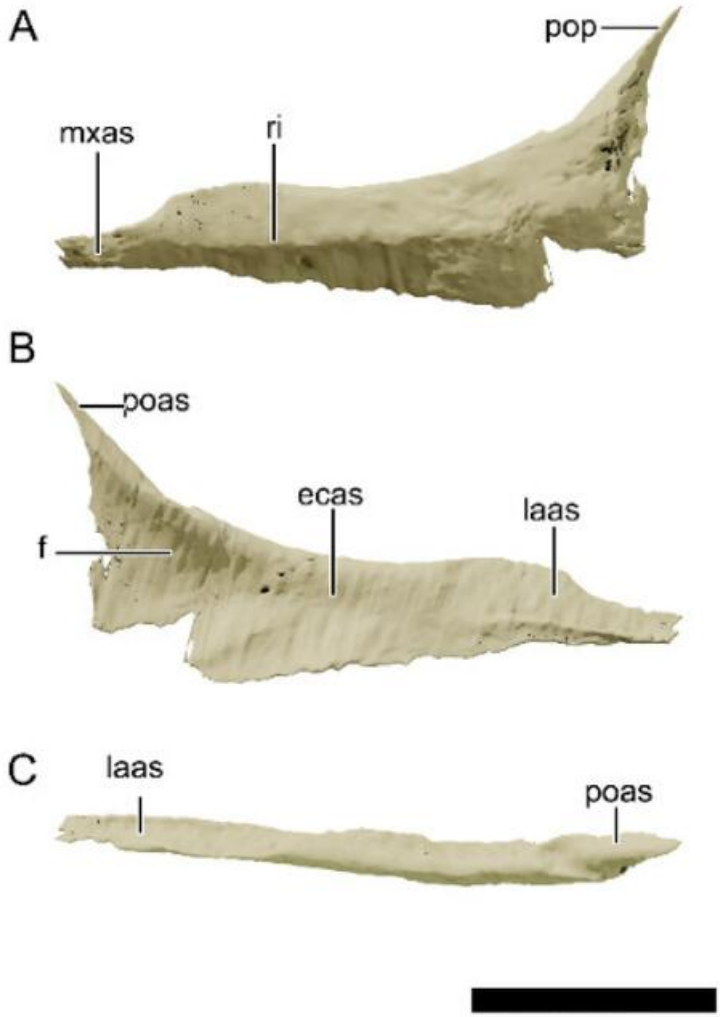

Figure 17. Digital reconstruction of the left jugal of NHMD 164758. (**A**) Lateral view. (**B**) Medial view. (**C**) Dorsal view. Abbreviations: ecas, articular surface for the ectopterygoid; f, fossa; laas, articular surface for the lacrimal; mxas, articular surface for the maxilla; poas, articular surface for the postorbital; pop, postorbital process; ri, ridge. Scale bar = 20 mm.

4.8.10. Quadratojugal

The left quadratojugal of NHMD 164741 is preserved (Figures 4 and 5), however the distal ends of the anteroventral (=jugal) and posterodorsal (=squamosal) processes are missing. The quadratojugal delimits the posteroventral corner of the infratemporal fenestra. The main body of the quadratojugal is posteriorly convex and slightly posteroventrally oriented. The anteroventral and posterodorsal processes are almost perpendicular, being separated by an 84° angle. In some specimens of *Pl. trossingensis*, this angle is less than 45° or subparallel, however, these acute angles are possibly the result of plastic deformation and were originally close to 70° [53,63]. The anteroventral process is laterally convex and articulates to the posteroventral process of the jugal both medially and ventrally, as observed by a ventral fossa in this process. The posterodorsal process is inclined medially to contact the lateral margin of the quadrate.

4.8.11. Quadrate

NHMD 164741 preserves the only complete quadrate (left quadrate, Figure 18), whereas both quadrates of NHMD 164758 have only the distal ends preserved (Figure 19). The main shaft of the quadrate is gently concave posteriorly and forms an angle of 153° to the quadrate head. The anterolateral and dorsal surfaces of the quadrate head are obscured

by the ventral process of the squamosal. The head is anteroposteriorly expanded with a ridge at its lateral surface that continues ventrally to the lateral flange of the quadrate, which is poorly preserved in NHMD 164741. In anterior view, the quadrate is straight for most of its length, but slightly laterally oriented distally. The lateral medial condyle of the quadrate is ventrally positioned in relation to the lateral condyle, and its lateromedially inflated distally. The quadrate in NHMD 164741 is relatively tall when compared to the rostrum height. This ratio is also higher in NHMD 164741 than in other sauropodomorphs (Table 4). The medial (=pterygoid) flange of the quadrate is poorly preserved in NHMD 164741 but is in articulation to the posterolateral process of the pterygoid in the right element of NHMD 164758. This articulation occurs at the medial surface of this flange.

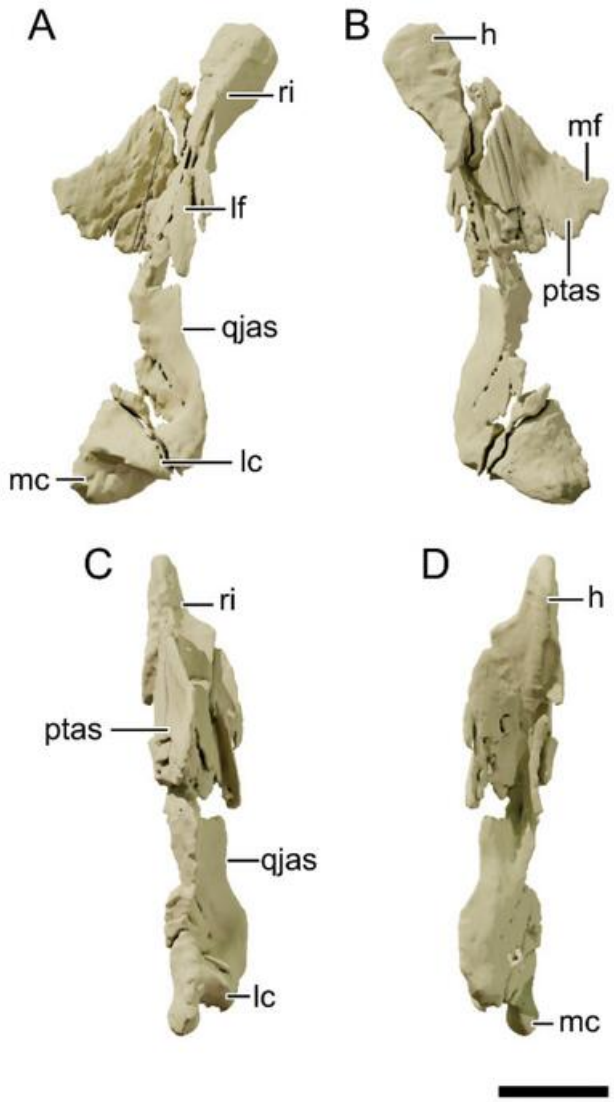

Figure 18. Digital reconstruction of the left quadrate of NHMD 164741. (**A**) Lateral view. (**B**) Medial view. (**C**) Anterior view. (**D**) Posterior view. Abbreviations: h, head; lc, lateral condyle; lf, lateral flange; mc, medial condyle; mf, medial flange; ptas, articular surface for the pterygoid; qjas, articular surface for the quadratojugal; ri, ridge. Scale bar = 20 mm.

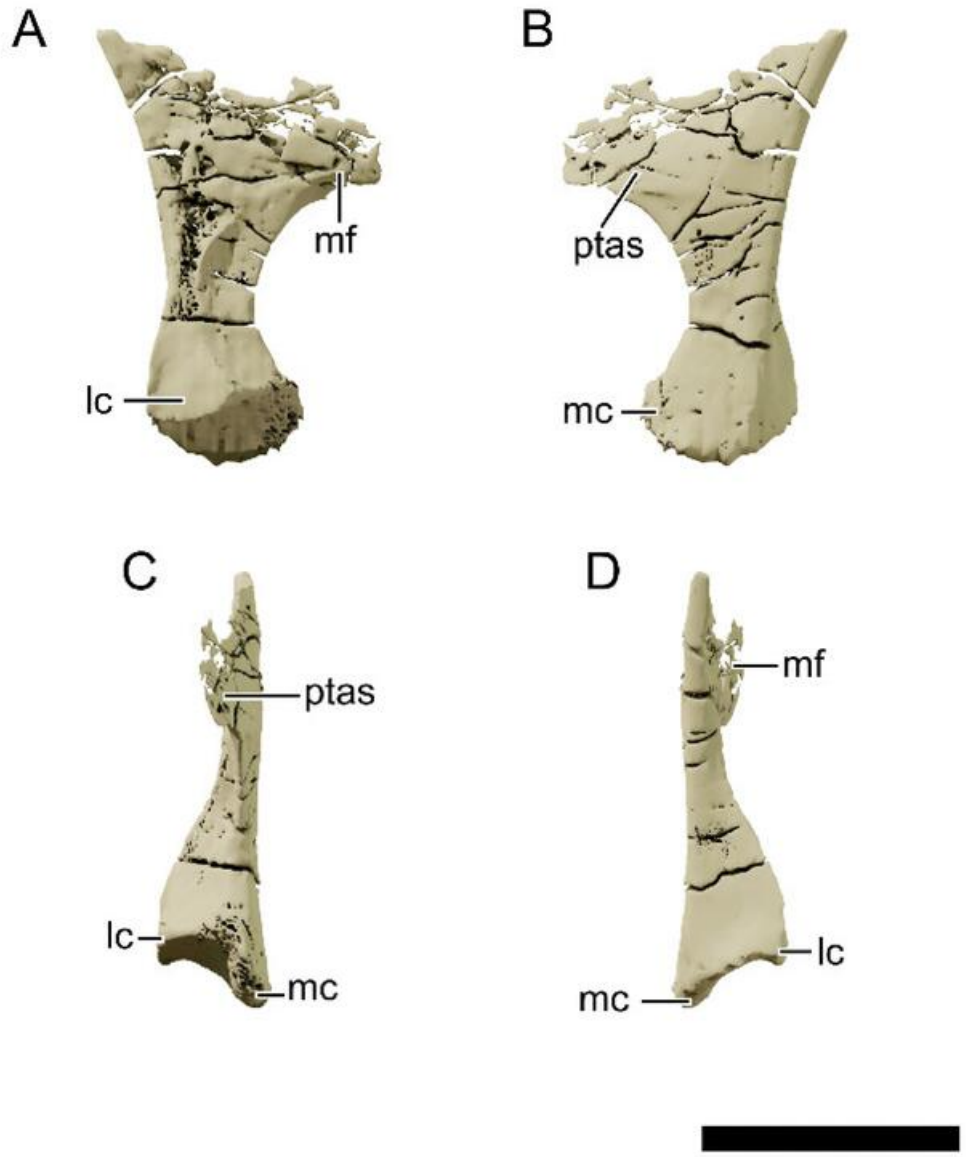

Figure 19. Digital reconstruction of the left quadrate of NHMD 164758. (**A**) Lateral view. (**B**) Medial view. (**C**) Anterior view. (**D**) Posterior view. Abbreviations: lc, lateral condyle; mc, medial condyle; mf, medial flange; ptas, articular surface for the pterygoid. Scale bar = 20 mm.

Table 4. Quadrate dorsoventral height to rostrum dorsoventral height ratio. The rostrum height is measured at the posterior margin of the external naris, from the ventral tip of the maxilla to the dorsal tip of the nasal. Measurements were taken on the 3D models when available.

Quadrate—Dorsoventral Height to Rostrum Dorsoventral Height		
Issi saaneq	NHMD 164741	1.57
Pl. trossingensis	AMNH FARB 6810	1.18
Pl. trossingensis	NAAG_00011238	1.30
Pl. trossingensis	MSF 11.4	1.27
Pl. trossingensis	MSF 15.4	1.13
Mac. itaquii	CAPPA/UFSM 0001a	1.28
Bu. schultzi	CAPPA/UFSM 0035	1.40
Mas. carinatus	BP/1/5241	1.12
N. intlokoi	BP/1/4779	1.11

4.8.12. Frontal

Both frontals of NHMD 164741 are displaced, with the left frontal preserving most of its total length (Figure 20), whereas in NHMD 16758 only the left frontal is preserved (Figure 21). The frontal delimits the orbit lateroventrally but is excluded from the supratemporal fenestra by the parietal. The dorsal margin of the frontal is slightly concave in lateral view. The anterodorsal margin of the frontal forms a depression at its mid-width, raising the lateral and medial margins of the bone. Lateral to this depression, an indentation encapsulates the posterior process of the prefrontal, as in *Plateosaurus*. In dorsal view, directly behind this indentation, the lateral margin of the frontal broadens, forming the posterolateral (=postorbital) process of the frontal. This process is well developed and extends further laterally in NHMD 164741, but not as much in NHMD 164758. The distal end of the process forms a groove for the insertion of the anterodorsal process of the postorbital. The medioventral margin of this process is bound by the parietal in NHMD 164758. The lateral half of the posterior margin of the posterolateral process is excavated forming the anterior margin of the supratemporal fossa, as in *Mac. itaquii* and *Plateosaurus* but absent in *Coloradisaurus* and *Mas. carinatus*.

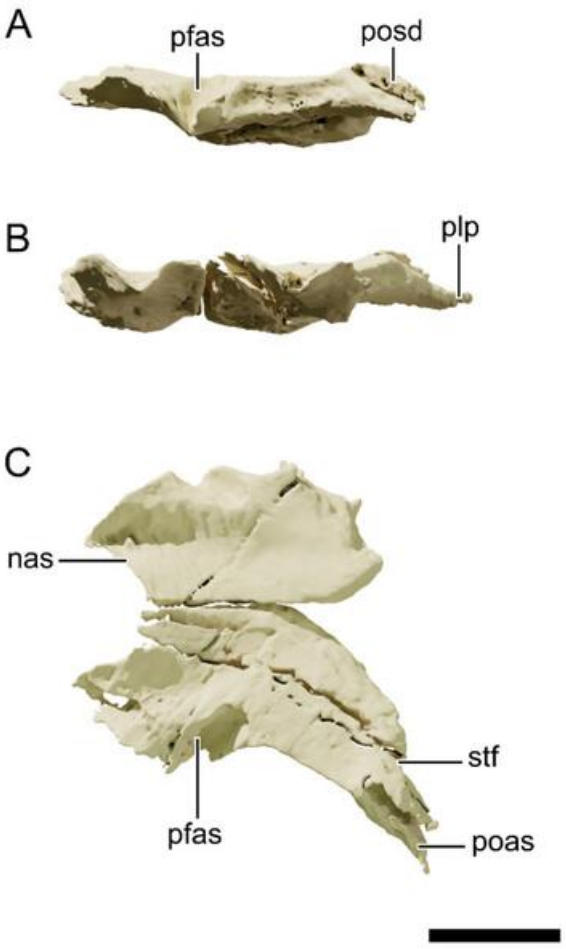

Figure 20. Digital reconstruction of the frontals of NHMD 164741. (**A**) Lateral view. (**B**) Anterior view. (**C**) Dorsal view. The left and right frontals were digitally articulated. Abbreviations: nas, articular surface for the nasal; pfas, articular surface for the prefrontal; poas, articular surface for the postorbital; plp, posterolateral process; stf, supratemporal fossa. Scale bar = 20 mm.

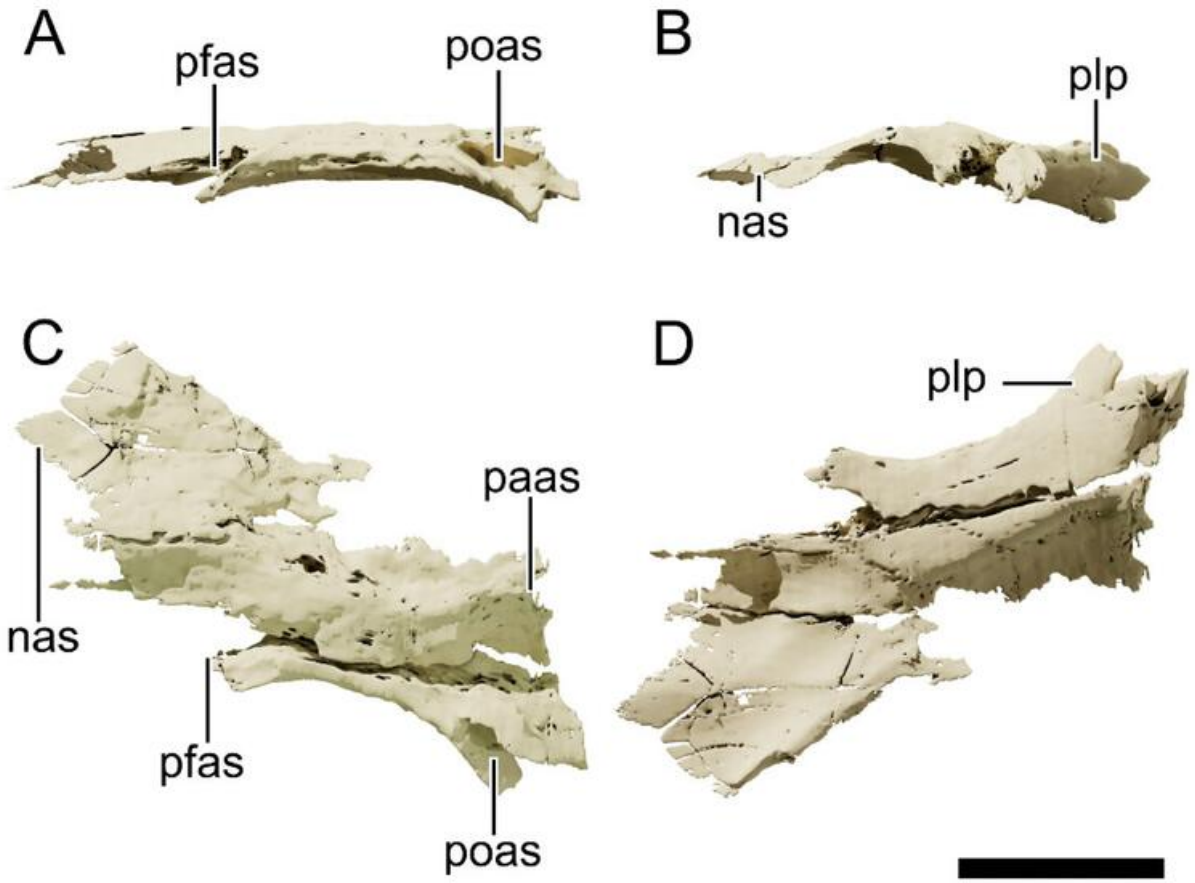

Figure 21. Digital reconstruction of the frontals of NHMD 164758. (**A**) Lateral view. (**B**) Anterior view. (**C**) Dorsal view. (**D**) Posterior view. The left and right frontals were digitally articulated. Abbreviations: nas, articular surface for the nasal; paas, articular surface for the parietal; pfas, articular surface for the prefrontal; poas, articular surface for the postorbital; plp, posterolateral process; stf, supratemporal fossa. Scale bar = 20 mm.

4.8.13. Parietal

Only the anterior part of the left parietal is preserved in NHMD 164758 (Figure 22) and the posterolateral process of the left parietal in NHMD 164741 (Figures 4 and 5). The anterolateral process of the parietal articulates to the mediodorsal process of the postorbital, excluding the frontal from the supratemporal fenestra. This process bounds the anteromedial margin of the supratemporal fenestra. The frontal-parietal suture is rugose and slightly elevated medially, as in *Pl. trossingensis*. The posterolateral process of the parietal is gently convex laterally, anteroposteriorly longer than dorsoventrally tall and mediolaterally flat. Its lateral surface contacts the anteromedial and the proximal half of the posterior processes of the squamosal, and contacts medially the lateral surface of the paroccipital process of the otoccipital. The distal end of this process slopes ventrally.

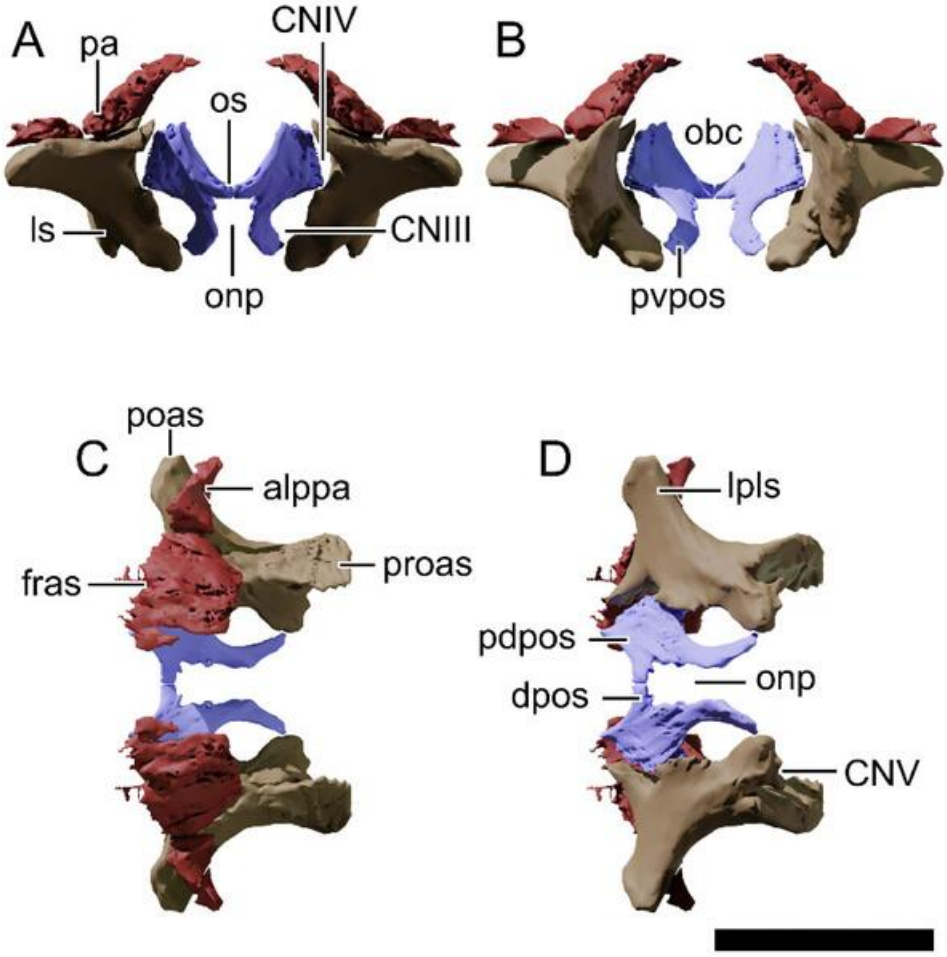

Figure 22. Digital reconstruction of the left upper braincase elements of NHMD 164758. (**A**) Anterior view. (**B**) Posterior view. (**C**) Dorsal view. (**D**) Ventral view. The elements were articulated and mirrored digitally for the reconstruction. Abbreviations: alppa, anterolateral process of the parietal; CN, cranial nerve; dpos, dorsal process of the orbitosphenoid; fras, articular surface for the frontal; lpls, lateral process of the laterosphenoid; ls, laterosphenoid; obc, olfactory bulb canal; onp, optic nerve passage; os, orbitosphenoid; pa, parietal; pdpos, posterodorsal process of the orbitosphenoid; poas, articular surface for the postorbital; proas, articular surface for the prootic; pvpos, posteroventral process of the orbitosphenoid. Scale bar = 20 mm.

4.8.14. Orbitosphenoid

Only the left orbitosphenoid of NHMD 164758 was preserved in the Greenland specimens, corresponding to a thin sheet of bone. When articulated in its original position (Figure 22), the orbitosphenoid forms the anterior wall of the braincase and contacts the laterosphenoid in three points. The orbitosphenoid contains three processes, one on the anterior portion (dorsal process) that contacts its counterpart medially, and two (posterodorsal and posteroventral processes) on the posterior portion, articulating with the laterosphenoid. The dorsal process forms the anteroventral margin of the olfactory bulb. The posteroventral process is the longest. It differs from the condition in *Mas. carinatus* (BP/1/5241) where the posterodorsal process is the longest. The distal half of that process is laterally deflected and its medial surface forms the dorsolateral margins of the optic nerve passage.

The contacts between the laterosphenoid and the orbitosphenoid were digitally reconstructed. These contacts would form two lateral foramina: a dorsal foramen that is smaller in diameter and a larger ventral foramen. This is another feature that distinguishes NHMD 164758 from *Mas. carinatus* (BP/1/5241), as the dorsal foramen is the largest in the latter.

The dorsal foramen would have formed the passage of cranial nerve IV (CNIV), whereas the ventral would have formed the passage of cranial nerve III (CNIII).

4.8.15. Laterosphenoid

The laterosphenoids of both NHMD 164741 and NHMD 164758 are disarticulated and displaced. When articulated in its original position in NHMD 164758 (Figure 22), the laterosphenoid contacts the orbitosphenoid anteriorly, the frontal anterodorsally, the parietal dorsally, and the postorbital laterally. However, it remains unclear if there is a ventral contact to the basisphenoid, as in *Pl. trossingensis*. The anterodorsal ramus of the laterosphenoid is a finger-like anterior projection that contacts the frontal distally and dorsally, and the orbitosphenoid medially. The lateral (=postorbital) process extends laterodorsally and has a distal inflated articular surface for the postorbital. This process is dorsoventrally robust and contacts the medial surface of the anterodorsal process of the postorbital. In *Pl. trossingensis* (AMNH FARB 6810), the postorbital process is proportionally much longer, slender and anterodorsally curving than in NHMD 164758 [52]. In this sense, the laterosphenoid of NHMD 164758 is closer to the condition observed in *Mas. carinatus* and *N. intlokoi*. The posterior region of the laterosphenoid articulates with the prootic and contains a deep notch that forms the anterior margin of the large trigeminal foramen (CNV), as in *Coloradisaurus* and *Plateosaurus*, differing from the gently concave condition in *N. intlokoi* and *Mas. carinatus*.

4.8.16. Otoccipital

The paroccipital process of NHMD 164741 (Figures 4 and 5) is lateromedially flattened and dorsoventrally expanded. Distally it contacts the posterior process of the squamosal. Anteriorly, at its base. the process expands to create the basioccipital articular surface. A deep, oval groove is present at the ventral surface of the proximal part of the paroccipital process, as in *Pl. trossingensis* (AMNH FARB 6810).

4.8.17. Basioccipital

Only a small fragment of the occipital condyle is preserved in NHMD 164741 (Figures 4 and 5), and part of the occipital condyle and the right basal tubera is preserved in NHMD 164758 (Figures 6 and 7). The occipital condyle is convex ventrally and concave dorsally at the foramen magnum exit. The basal tubera is separated from the occipital condyle by a deep lateral fossa. This condition is not as extreme as in *Pl. gracilis* (GPIT 18318a). Due to its disarticulated preservation, it is not possible to discern if the basioccipital is located dorsally to the basisphenoid.

4.8.18. Basisphenoid

The main body of the basisphenoid is missing on NHMD 164758 but preserved disarticulated in NHMD 164741 (Figure 23). Both specimens preserve the right basipterygoid process of the basisphenoid, and the parasphenoid process (Figure 24). As this element is poorly preserved in both specimens, so that the autapomorphic feature of a high interbasipterygoid septum with a median process of *Pl. trossingensis* cannot be assessed. The basipterygoid process is wrapped by the median "hook-like" process of the pterygoid. This feature was considered autapomorphic for *Pl. trossingensis* [10] but was also described for *Mas. carinatus* (BP/1/5241) [16], possibly being a variable trait among early sauropodomorphs [53]. In NHMD 164758, the basipterygoid process extends anteroventrally, as in the juvenile *Mas. carinatus* (BP/1/4376), whereas in NHMD 164741, the process appears to extend ventrally and only slightly anteriorly, as in the adult *Mas. carinatus* (BP/1/5241), *U. tolentinoi* (UFSM11069) and *Thecodontosaurus* (YPM 2192). In *Pl. trossingensis* (MSF 15.8.1043 and MSF 07.M) this process is posteroventrally oriented. The parasphenoid process is a long and slender anteriorly oriented process. In lateral view, it is smooth and does not feature the lateral deep groves observed in *Pl. trossingensis* (MSF 07.M, MSF 08.M, and MSF 15.8.1043). In lateral view, the ventral margin of the

parasphenoid is straight and the dorsal margin is gently convex distally. The dorsal surface of the parasphenoid bears a deep groove, making the cross-section of this bone U-shaped. This condition is similar to that observed in *Mas. carinatus* (BP/1/5241) and appears to be so in *Pl. trossingensis* (MSF 15.8.1043).

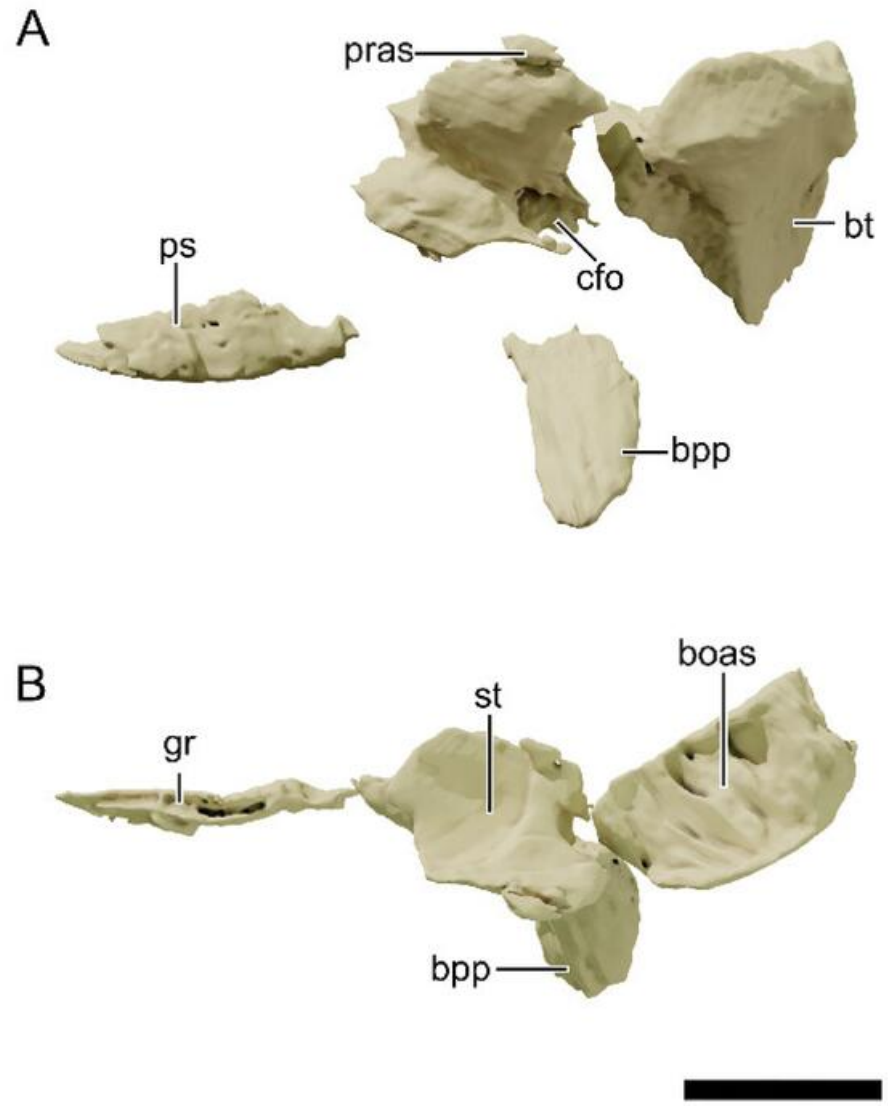

Figure 23. Digital reconstruction of the basisphenoid of NHMD 164741. (**A**) Lateral view. (**B**) Dorsal view. The elements were articulated digitally for the reconstruction. Abbreviations: boas, articular surface for the basioccipital; bpp, basipterygoid process; bt, basal tubera; cfo, carotid foramen; gr, groove; pras, articular surface for the prootic; ps, parasphenoid; st, sella turcica. Scale bar = 20 mm.

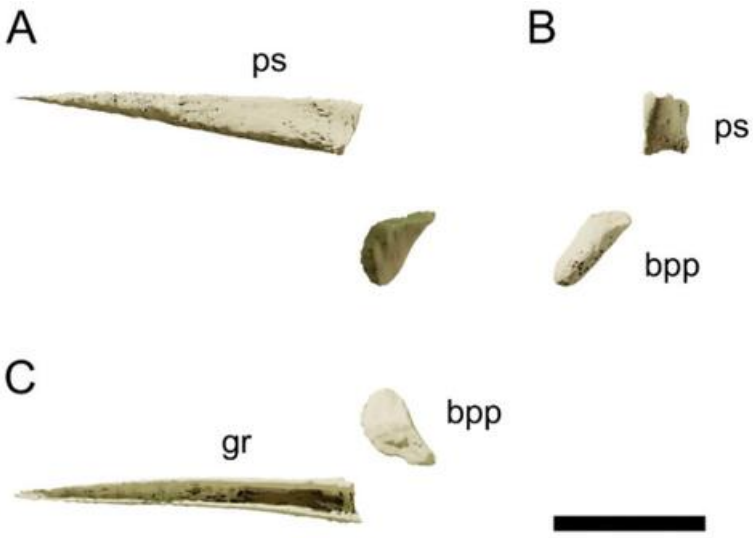

Figure 24. Digital reconstruction of the basisphenoid of NHMD 164758. (**A**) Lateral view. (**B**) Anterior view. (**C**) Dorsal view. The elements were articulated digitally for the reconstruction. Abbreviations: bpp, basipterygoid process; gr, groove; ps, parasphenoid. Scale bar = 20 mm.

4.8.19. Palate

The palate is best preserved in NHMD 164758 (Figures 25 and 26), with all composing elements partially articulated, almost complete and in anatomical position. NHMD 164741 preserves both pterygoids, the left ectopterygoid, fragments of both palatines and fragments of the left vomer. NHMD 164758 preserves both pterygoids, both ectopterygoids, both palatines and both vomers. The postpalatine fenestra is bound anteriorly by the palatine, laterally by the maxillae, medially by the pterygoids and posteriorly by the ectopterygoids. This fenestra is slightly anteroposteriorly longer than lateromedially wide (Figure 25).

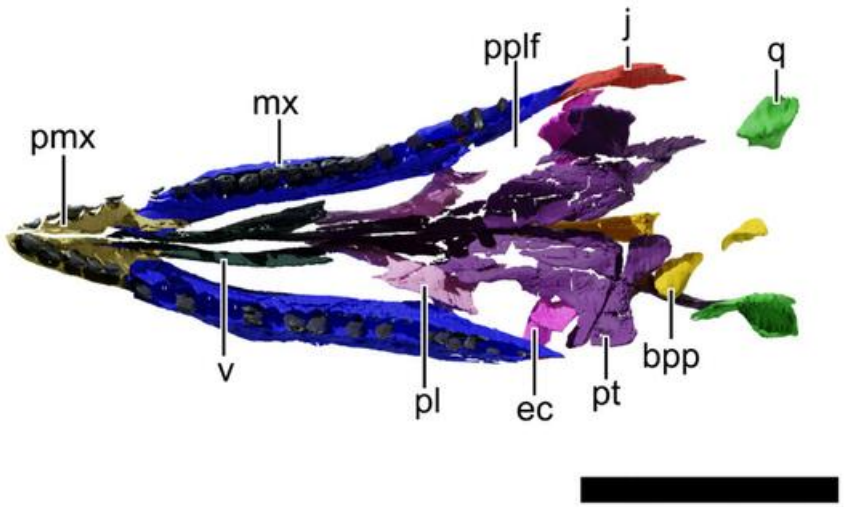

Figure 25. Digital reconstruction of the skull of NHMD 164758 in ventral view. The elements were articulated digitally for the reconstruction. Abbreviations: bpp, basipterygoid process; ec, ectopterygoid; j, jugal; mx, maxilla; pl, palatine; pmx, premaxilla; pplf, postpalatine fenestra; pt, pterygoid; q, quadrate; v, vomer. Scale bar = 50 mm.

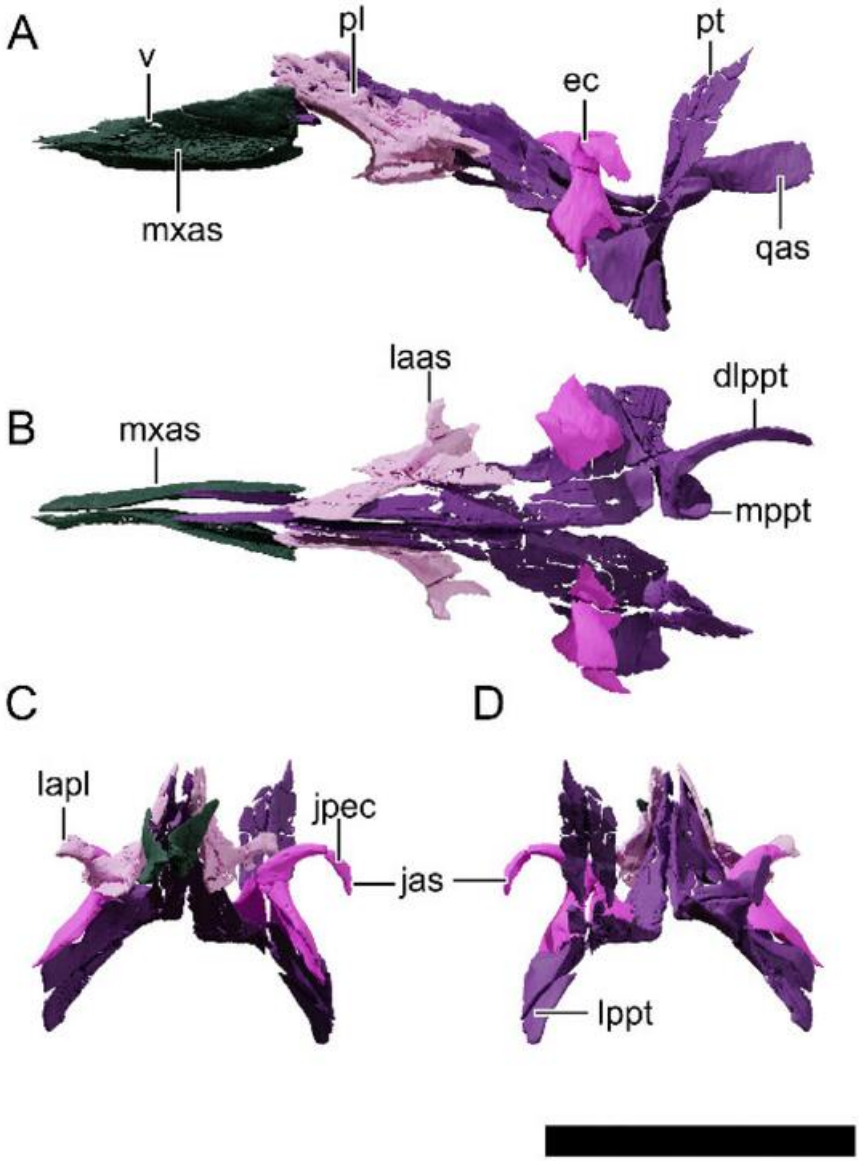

Figure 26. Digital reconstruction of the palate of NHMD 164758. (**A**) Left lateral view. (**B**) Dorsal view. (**C**) Anterior view. (**D**) Posterior view. The elements were articulated digitally for the reconstruction. Abbreviations: dlppt, dorsolateral process of the pterygoid; ec, ectopterygoid; ecf, ectopterygoid fossa; jas, articular surface for the jugal; jpec, jugal process of the ectopterygoid; laas, articular surface for the lacrimal; lapl, lateral process of the palatine; lppt, lateral process of the pterygoid; mppt, posteromedial process of the pterygoid; mxas, articular surface for the maxilla; pl, palatine; pt, pterygoid; qas, articular surface for the quadrate; v, vomer. Scale bar = 20 mm.

4.8.20. Pterygoid

None of the pterygoids are complete, but the best-preserved are the left element in NHMD 164741 (Figure 27) and the right one in NHMD 164758 (Figure 28). The pterygoid is the largest component of the palate. It is a tetraradiate bone that composes the posterolateral area of the palate. The anterior process of the pterygoid is the longest and is subdivided into two areas, a distal half that contacts the vomer laterally, and a proximal half that contacts the palatine dorsally. However, the distalmost part seems to be broken in the latter. The proximal half of the anterior process is lateroventrally expanded forming a dorsoventrally high lamina.

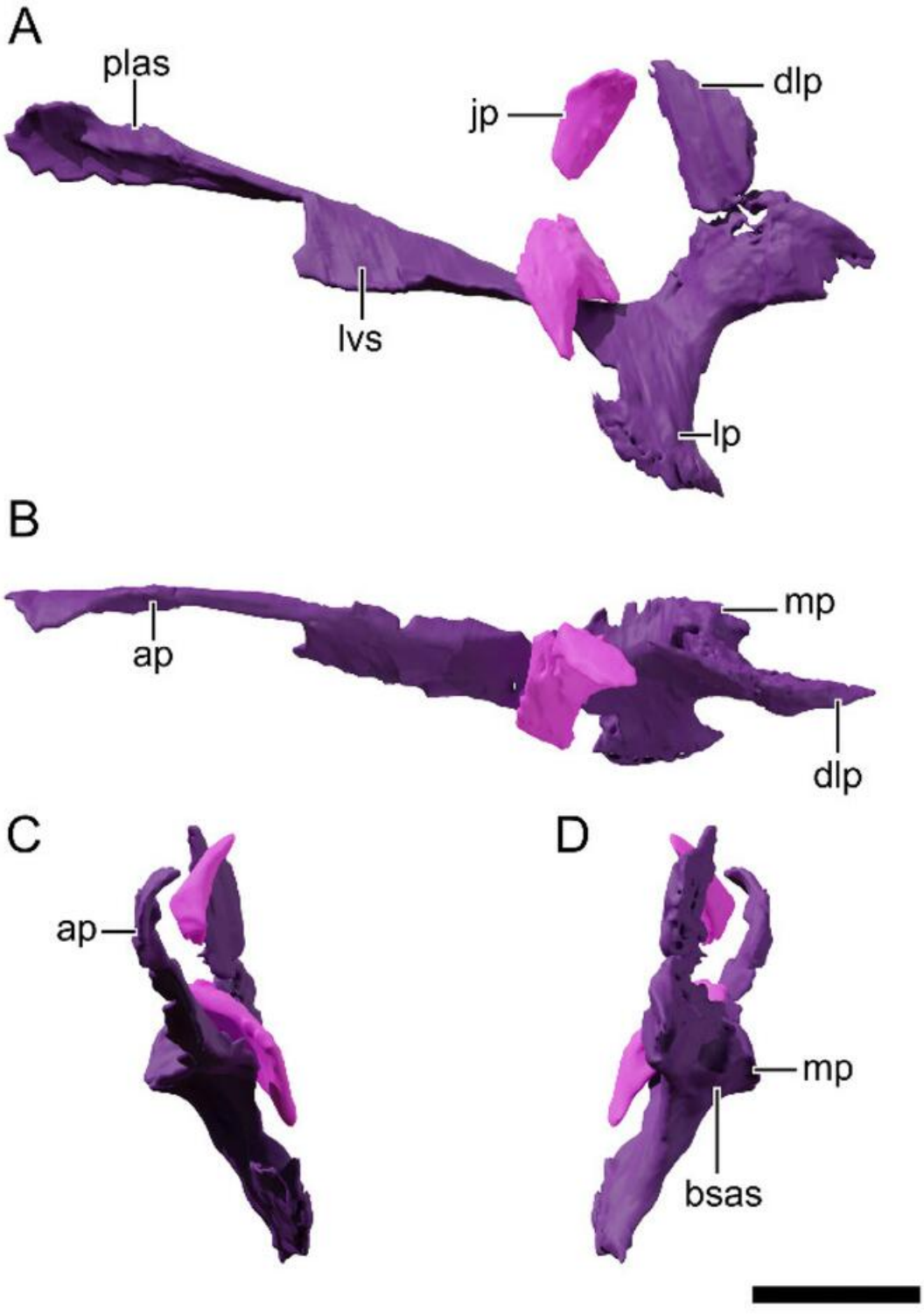

Figure 27. Digital reconstruction of the left pterygoid and ectopterygoid of NHMD 164741. (**A**) Lateral view. (**B**) Dorsal view. (**C**) Anterior view. (**D**) Posterior view. Abbreviations: ap, anterior process; bass, articular surface for the basisphenoid; dlp, dorsolateral process; ecf, ectopterygoid fossa; jp, jugal process; lp, lateral process; lvs, lateroventral sheet of bone; mp, medial process; plas, articular surface for the palatine. Scale bar = 20 mm.

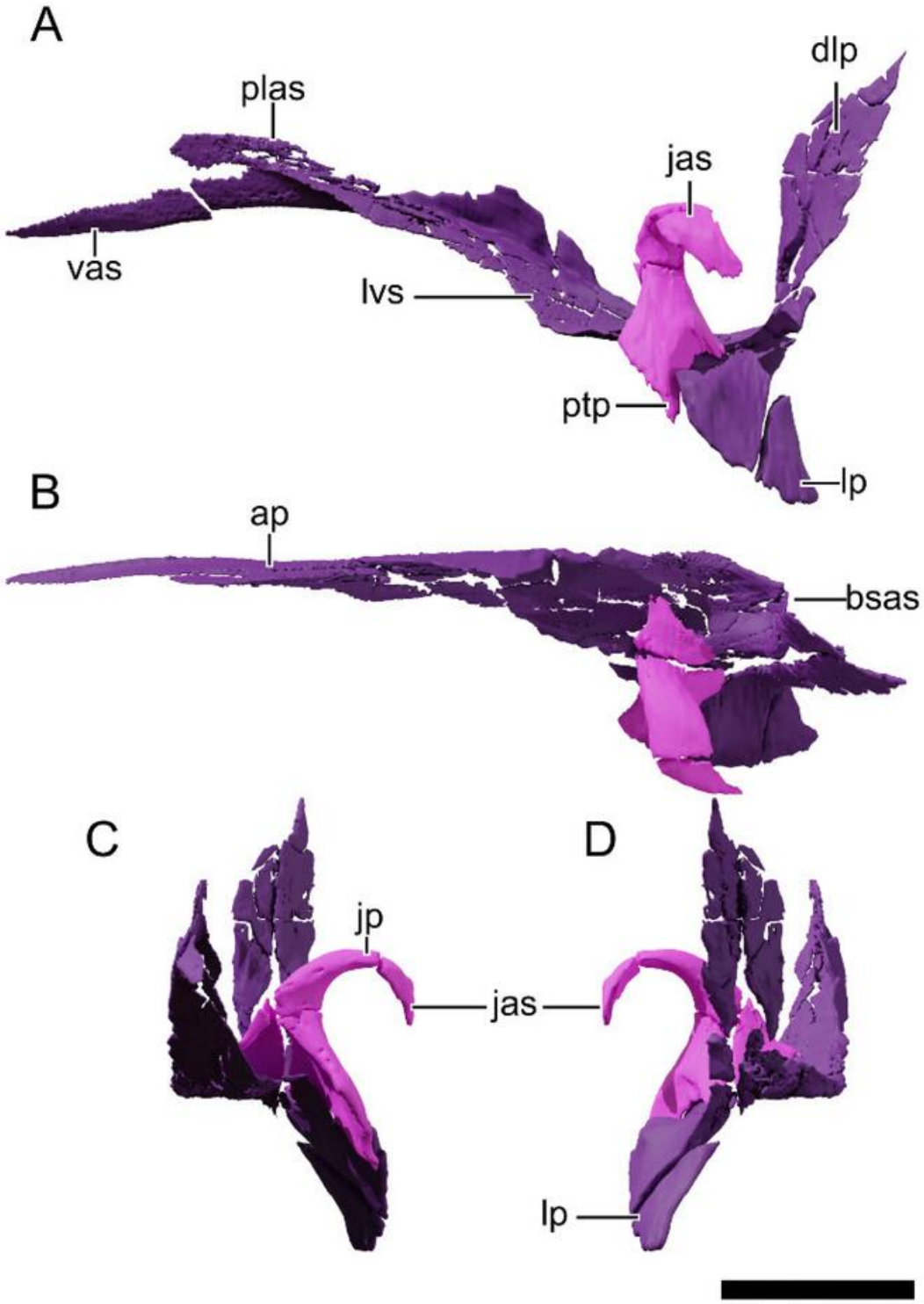

Figure 28. Digital reconstruction of the left pterygoid and ectopterygoid of NHMD 164758. (**A**) Lateral view. (**B**) Dorsal view. (**C**) Anterior view. (**D**) Posterior view. Abbreviations: ap, anterior process; bsas, articular surface for the basisphenoid; dlp, dorsolateral process; ecf, ectopterygoid fossa; jas, articular surface for the jugal; jp, jugal process; lp, lateral process; lvs, lateroventral sheet of bone; mp, medial process; plas, articular surface for the palatine. Scale bar = 20 mm.

The lateral process of the pterygoid is anteroposteriorly expanded and dorsoventrally flattened. This process is separated from the anterior process by an almost 90° angle in lateral view. The medial surface that separates both processes is highly dorsoventrally

concave. The distal area of the lateral process is inflated both anteroposteriorly and dorsoventrally. This process contacts the ectopterygoid laterally and anteriorly.

The dorsolateral (=quadrate) process of the pterygoid is broken in both specimens. This process curves lateroposteriorly and contacts the pterygoid flange of the quadrate laterally. Medially at the proximal surface of this process, it contacts the lateral surface of the basipterygoid process. As mentioned before, the medial process of the pterygoid is hook-shaped and wraps the basipterygoid laterally.

4.8.21. Ectopterygoid

The left ectopterygoid of NHMD 164758 is the best preserved (Figure 28). This bone is divided into dorsal (=jugal) and ventral (=pterygoid) processes. The dorsal process is hook-shaped and expands dorsolaterally in the proximal half and ventrally in the distal half. The distal half contacts laterally the posteroventral half of the jugal. This contact forms the posterior margin of the postpalatine fenestra in dorsal view. The contact margin of the dorsal process of the ectopterygoid is similar to that of *Mac. itaquii*, contrasting with the anteriorly projected, T-shaped tip of *Pl. trossingensis* (AMNH FARB 6810).

The ventral process of the ectopterygoid is dorsoventrally elongated, expanding over the lateral surface of the pterygoid. Its distal tip is dorsally obscured by the distal expansion of the lateral process of the pterygoid.

4.8.22. Palatine

Both palatines are preserved in NHMD 164758 (Figure 29) as well as in NHMD 164741, but are fragmented in the latter. The palatine is anteroposteriorly elongated and lateromedially flattened. Its anterior process expands anterodorsally and slightly laterally. This process contacts the posterior margin of the vomer distally and the anterior process of the pterygoid medially. Ventral to the contact with the pterygoid, the palatine expands medially and posteriorly. This expansion forms a medial ridge and a small tubercle posteriorly. This tubercle, however, does not show the autapomorphic peg-like morphology of *Pl. trossingensis* [52,63]. The lateral process of the palatine forms the anterior and anteromedial margins of the postpalatine fenestra. This process contacts the ventral process of the lacrimal laterally. Ventral to this process, the palatine contacts the maxilla laterally. The posterior process of the palatine contacts the proximal half of the anterior process of the pterygoid dorsomedially.

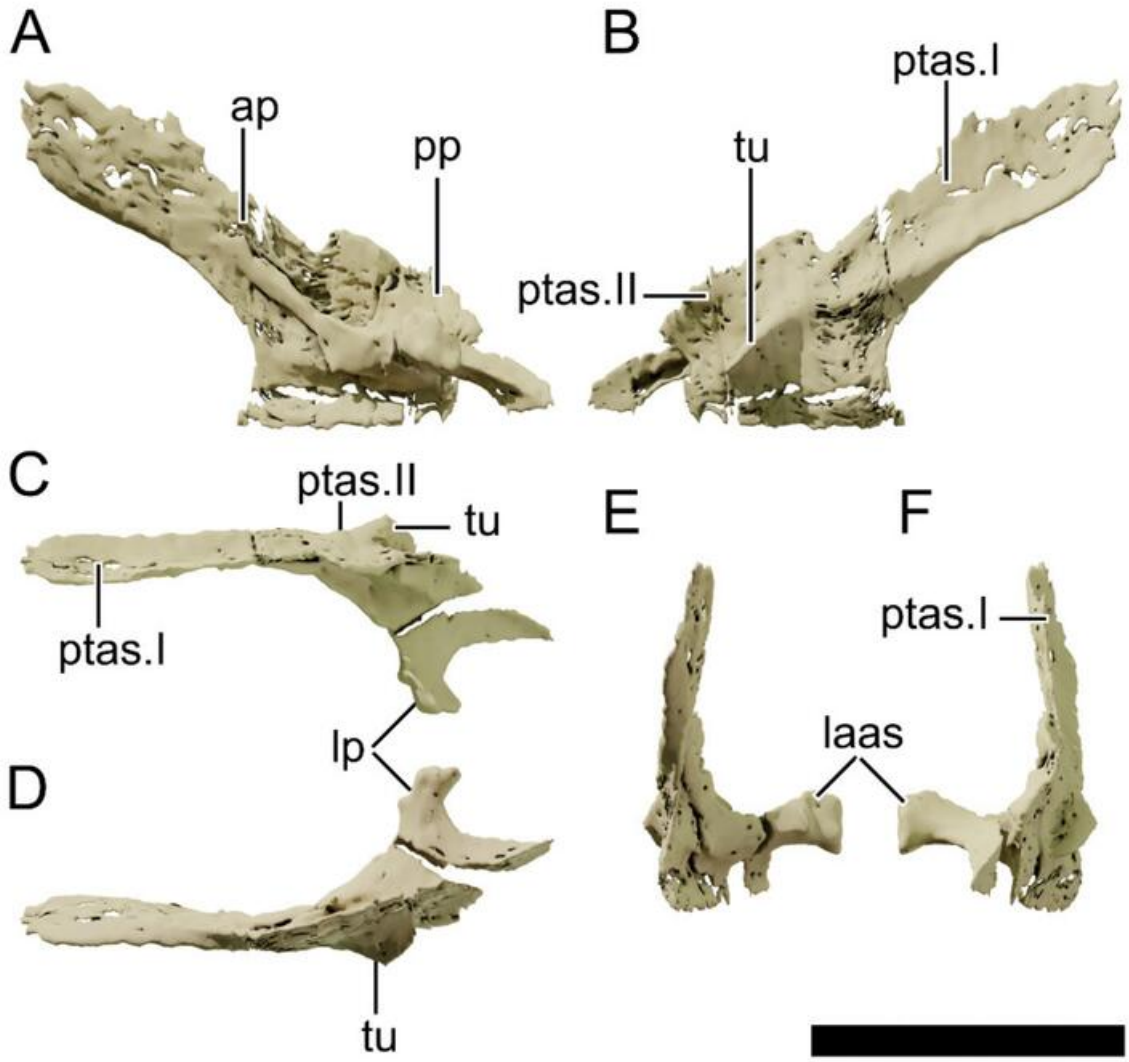

Figure 29. Digital reconstruction of the left palatine of NHMD 164758. (**A**) Lateral view. (**B**) Medial view. (**C**) Dorsal view. (**D**) Ventral view. (**E**) Anterior view. (**F**) Posterior view. Abbreviations: ap, anterior process; laas, articular surface for the lacrimal; lp, lateral process; pp, posterior process; ptas, articular surface for the pterygoid; tu, tubercle.

4.8.23. Vomer

The vomers are better preserved in NHMD 164758 and form the anterior region of the palate (Figures 25 and 26). This bone is anteroposteriorly elongated and triangular in lateral view, with a tapered anterior margin and a dorsoventrally tall posterior margin. The overall shape of the vomer in lateral view and the lack of foramina piecing this bone resemble the anatomy of the vomer in *Pl. trossingensis* (AMNH FARB 6810) and differs from the S-shaped vomer in *Mas. carinatus* (BP/1/5421). The anteroposterior length of the vomer is slightly over 0.25 of the total skull anteroposterior length. This ratio is around 0.18 in *Pl. trossingensis* (AMNH FARB 6810), 0.22 in *N. intlokoi* (BP/1/4779) and 0.31 in *Mas. carinatus* (BP/1/5241). The vomer is laterally convex in anterior view, having a ventral lateral expansion that articulates with the ventromedial surface of the maxilla. The medial surface of the posterior part of the vomer contacts the anterior process of the pterygoid over a shallow medial ridge in the vomer. The posterior surface contacts the anterior process of the palatine in an almost straight margin.

4.8.24. Dentary

NHMD 164741 preserves both dentaries but lacks the anteriormost region of both (Figure 30). NHMD 164758 preserves both complete dentaries partially in articulation (the right mandible is slightly ventrally deflected) (Figure 31). The dentary is the largest bone in the mandible. It articulates posteromedially with the splenial, dorsomedially with the coronoid, posteroventrally with the angular and posterodorsally with the surangular. Posteriorly, the dentary bounds the anterior margin of the mandibular fenestra. The dentary is slender and long, being over six times longer than tall, and over twice taller than wide (see Table 2 for measurements). In lateral view, the dorsal margin of the dentary is straight, and the ventral margin is slightly concave, as in *Pan. protos*, *Ba. agudoensis*, *Bu. Schultzi*, *U. tolentinoi*, *Mac. itaquii* and *Plateosaurus*, and different from the straight margin of early sauropodomorphs such as *Bu. Schultzi* and *Sat. tupiniquim*. The symphysis in NHMD 164758 is straight at the medial contact surface to its counterpart. Posterior to the symphysis, the dentary is laterally deflected. The lateral and medial surfaces are parallel for most of the dentary extent, tapering posteriorly to the last alveolus. The lateral surface of the anteriormost region of the left dentary in NHMD 164741 is missing, exposing three dentary tooth roots. In both NHMD 164741 and 164758, the dentary preserved 18 alveoli, but this number might be underestimated in NHMD 164741 due to the lack of the anteriormost region. However, its anteriormost medial margin includes the posterior part of the symphysis, meaning that it does not miss much of the anterior area. Therefore, NHMD 164741 could have a maximum of 20 dentary teeth, a feature seen in mature individuals [53].

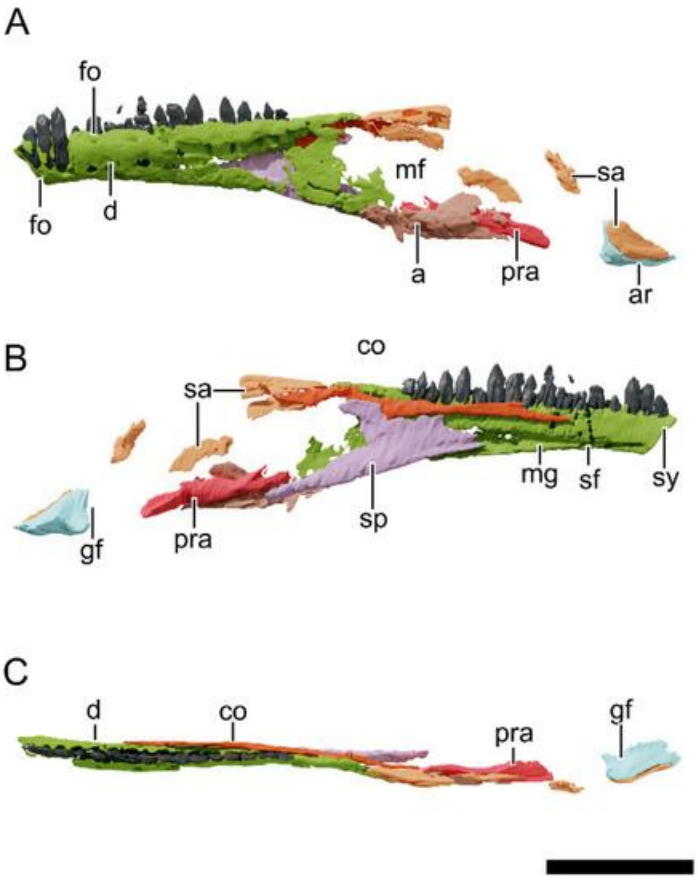

Figure 30. Digital reconstruction of the left mandible of NHMD 164741. (**A**) Lateral view. (**B**) Medial view. (**C**) Dorsal view. Abbreviations: a, angular; ar, articular; co, coronoid; d, dentary; fo, foramen; gf, glenoid fossa; mf, mandibular fenestra; mg, Meckelian groove; pra, prearticular; sa, surangular; sf, secondary fossa; sp, splenial; sy, symphysis. Scale bar = 50 mm.

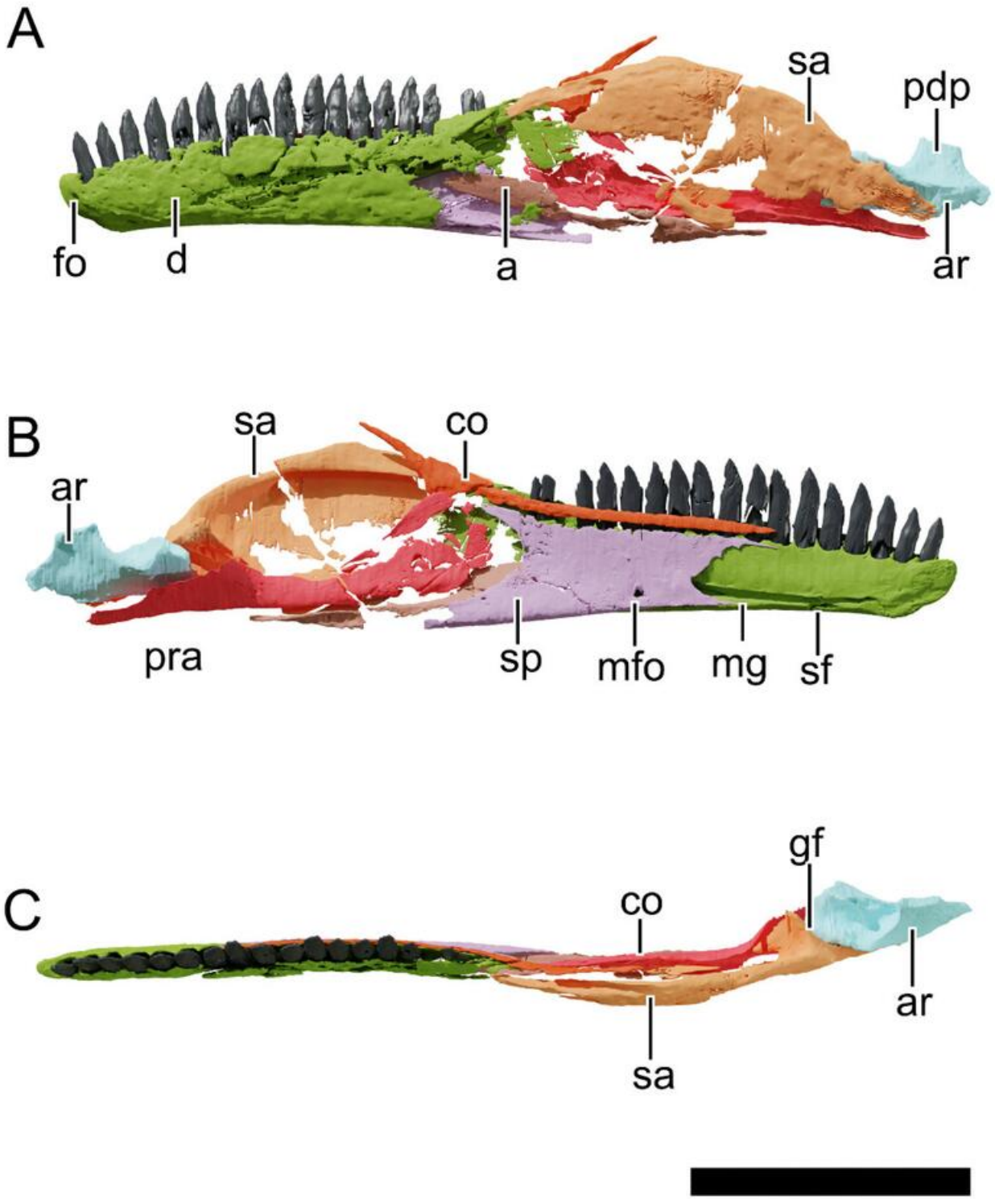

Figure 31. Digital reconstruction of the left mandible of NHMD 164758. (**A**) Lateral view. (**B**) Medial view. (**C**) Dorsal view. Abbreviations: a, angular; ar, articular; co, coronoid; d, dentary; fo, foramen; gf, glenoid fossa; mf, mandibular fenestra; mfo, mylohyoid foramen; mg, Meckelian groove; pdp, posterodorsal process; pra, prearticular; sa, surangular; sf, secondary fossa; sp, splenial; sy, symphysis. Scale bar = 50 mm.

A row of foramina is present at the first half of the dorsolateral surface of the dentary, just below the alveolar margin, as in pre-Norian sauropodomorphs, *U. tolentinoi*, *Mac. itaquii* and *Plateosaurus*. Different from the 9–12 foramina in *Pl. trossingensis* (AMNH FARB 6810, MSF 01 and MSF 16.1), both Greenland specimens only preserve 3–4 foramina.

In NHMD 164741, these foramina are large and open anterodorsally, whereas in NHMD 164758, they are smaller and open dorsally. Both dentaries of NHMD 164758 preserve a small anteroventral foramen at the lateral surface near the ventral corner of the dentary. This foramen was not reported for any other plateosaurid (*Mac. itaquii*, *U. tolentinoi* and *Plateosaurus*), but this might be due to the poorer preservation of this area in most specimens. In NHMD 164741 this feature cannot be assessed with confidence due to damage in this area. In *Pam. berberenai* (ULBRA-PVT016) this foramen is situated more dorsally. *Ba. agudoensis* (UFRGS-PV-1099-T in [39] Figure 2) seems to possess a simitar foramen as NHMD 164758.

The Meckelian groove extends longitudinally along the ventral part of the medial surface of the dentary. Anteriorly, this groove is constricted, but posteriorly it is dorsoventrally expanded and covered by the splenial medially. An anterior sheet of bone expands posteroventrally posterior to the symphysis, covering the anteriormost region of the Meckelian groove. This feature was observed in *Mac. itaquii* and *U. tolentinoi*, but is more developed in the latter. A deep, secondary fossa is present ventral to the anterior region of the Meckelian groove, as in *U. tolentinoi*, and unlike the single fossa of *Mac. itaquii* and *Plateosaurus*.

4.8.25. Splenial

NHMD 164758 preserves both complete splenials (Figure 31), and NHMD 164741 only the left element (Figure 30). The splenial is a rectangular sheet of bone that obscures the posteromedial surface of the dentary. Both the anterior and posterior margins bear two processes, one dorsally and one ventrally, making the anterior and posterior margins of the splenial concave in lateral view. The medial surface of the splenial is gently concave and contains a mylohyoid foramen ventrally at its anterior third. In *Bu. schultzi* (CAPPA/UFSM 0035), this foramen is located at the dorsoventral midpoint. In *Plateosaurus* this foramen is not visible in medial view. The lateral surface of the splenial contains a ventral sheet of bone that lies on the dorsal margin of the ventral region of the dentary. This sheet of bone continues posteriorly, forming the elongated posteroventral process. This process accommodates the anteroventral margin of the prearticular dorsally and the anteroventral margin of the angular ventrally. The dorsal margin of the splenial contacts the coronoid dorsally.

4.8.26. Intercoronoid/Coronoid

The intercoronoid is preserved on both mandibles of NHMD 164758 (Figure 31) and in the left mandible of NHMD 164741 (Figure 30). It is a slender and elongated bone that marginates the lingual surface of the dentary teeth. It extends anteriorly to the first third of the dentary. The coronoid is posterodorsally oriented and contacts the surangular laterally. The ventral margin of the coronoid is anteroposteriorly expanded and ventrally deflected, forming a triangular base as in *Pl. trossingensis* (AMNH FARB 6810). The coronoid is deflected dorsally in *N. intlokoi*.

4.8.27. Surangular

The left surangular in NHMD 164758 is the best-preserved surangular among the Greenland specimens (Figure 31). The bone composes most of the posterolateral surface of the mandible and forms the posterior margin of the mandibular fenestra. The surangular is sigmoid in lateral view, with the anterior half being more dorsoventrally expanded compared to the posterior half. The anterior (=dentary) process of the surangular is dorsally convex. It covers the posterodorsal corner of the dentary and is partially covered anteromedially by the coronoid. The anterior process is medioventrally expanded, forming a ventral groove that covers the dorsal corner of the adductor fossa. The lateral surface of the anterior process is slightly convex in anterior view and extends ventrally to contact the angular at its ventral margin. A medial expansion of the surangular is present posterior to its anterior process. This expansion forms a mediolaterally wide flange that articulates anteroventrally to the prearticular and posterodorsally forms the surangular contribution to the glenoid fossa. This contribution is marked laterally by a deep transverse groove, as in

Pam. berberenai, but is not as deep and marked in *Pl. trossingensis*. Posterior to the glenoid the surangular tapers dorsoventrally, marginating the lateral surface of the articular.

4.8.28. Angular

The left angular of NHMD 164741 is the best-preserved, although broken at its posterior half (Figure 30), whereas in NHMD 164758 both angulars are fragmented (Figure 31). It is a lateromedially flat bone with a medial concavity in anterior view. It contacts the posteroventral process of the dentary medially, the prearticular medially and the surangular dorsally. Anterodorsally it contributes to the posteroventral corner of the mandibular fenestra.

4.8.29. Prearticular

Both prearticulars are present in NHMD 164758 (Figure 31), but only the main shaft of the left prearticular of NHMD 164741 is preserved (Figure 30). Anteriorly, the prearticular is dorsoventrally expanded and lateromedially flat. This anterior region contacts the splenial anteriorly and the surangular dorsally and is sub-circular in lateral view. The main shaft is constricted dorsoventrally and concave laterally. Medially it bounds the ventral corner of the internal mandibular fenestra. The posteromedial process expands dorsally to contact the medial process of the surangular anteriorly and the medial surface of the articular laterally.

4.8.30. Articular

The anterior part of NHMD 164741 left articular is preserved, and both articulars of NHMD 164758 are preserved and in articulation (Figures 31 and 32). The anterior process of the articular forms the posterior half of the glenoid fossa dorsally. It is bound by a dorsolaterally oriented ridge and a well-developed medial pyramidal process, as in *Pl. trossingensis* (AMNH FARB 6810). In *Mac. itaquii*, this medial expansion is less developed. The lateral surface of the articular is concave in anterior view and contacts the posterior process of the surangular, whereas medially the articular is slightly convex and contacts the posterior process of the prearticular. The articular of NHMD 164758 has a peculiar dorsoposterior process, situated posterior to the glenoid fossa (Figure 32). This process is as tall as anteroposteriorly long and squared shaped in lateral view. This morphology differs from the dorsoventrally short, anteroposteriorly elongated and gently dorsally convex dorsoposterior process of the articular in *Mac. itaquii* (CAPPA/UFSM 0001b) [42] and the short (or even absent) and posteriorly convex dorsoposterior process of *Pl. trossingensis* (AMNH FARB 6810) [52]. This process is absent in *Bu. schultzi* (CAPPA/UFSM 0035) [41]. This process tapers lateromedially towards its dorsal end, being triangular in cross-section. The retroarticular process tapers posteriorly and ends posterior to this dorsal process.

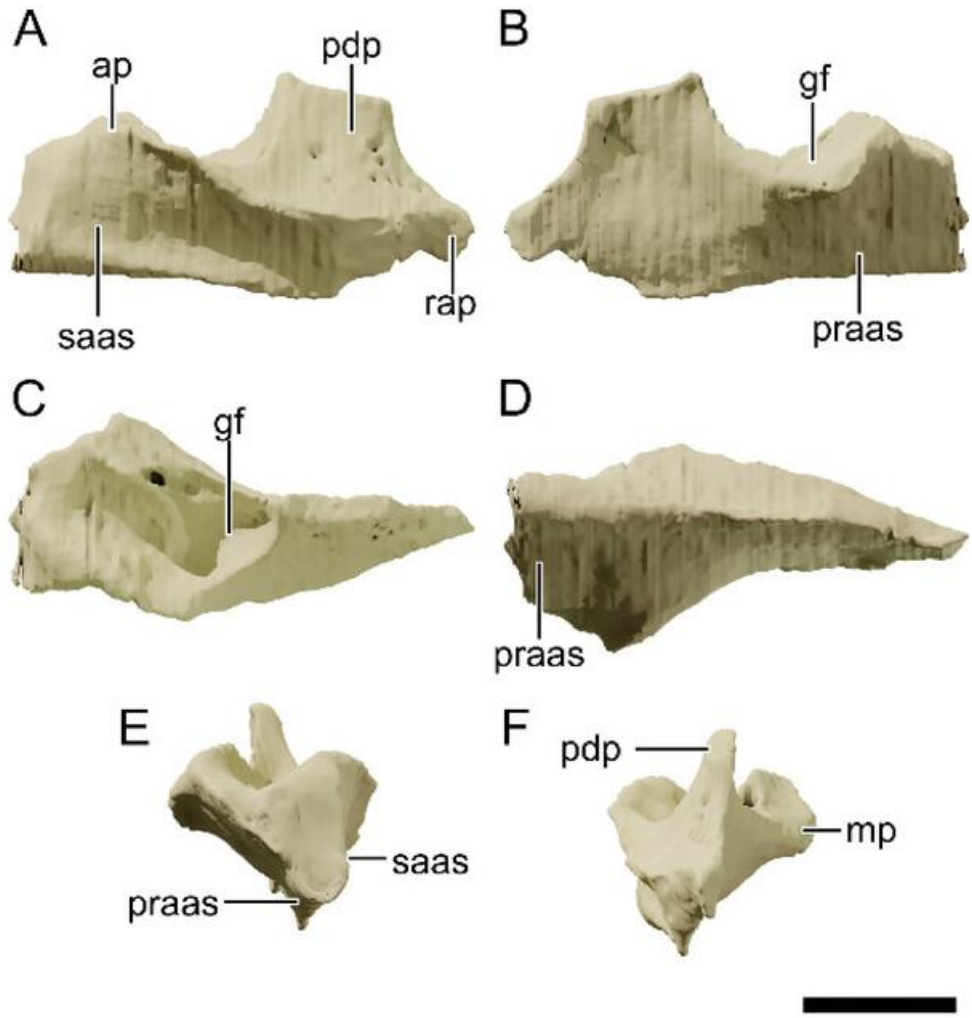

Figure 32. Digital reconstruction of the left articular of NHMD 164758. (**A**) Lateral view. (**B**) Medial view. (**C**) Dorsal view. (**D**) Ventral view. (**E**) Anterior view. (**F**) Posterior view. Abbreviations: ap, anterior process; gf, glenoid fossa; mp, medial process; pdp, posterodorsal process; praas, articular surface for the prearticular; rap, retroarticular process; saas, articular surface for the surangular. Scale bar = 10 mm.

4.8.31. Dentition

The premaxillae of NHMD 164758 preserve a total of five tooth alveoli each. Their roots comprise around two-thirds of the total tooth height on the most complete preserved teeth. The premaxillary tooth crowns are conical and slightly bent distally. In NHMD 164758, the first tooth (mesialmost tooth) of the premaxilla is the tallest in the series, differing from the condition in non-Bagualosaurian sauropodomorphs, and similar to that in *Plateosaurus*, *Ba. agudoensis*, and *Mas. carinatus*. A constriction separates the crown from the root. The mesial carina is convex and lacks denticles, as in most sauropodomorphs. The distal carina is concave and preserves coarse denticles set perpendicular to the tooth margin. These denticles are set apical to the basal third of the crown height and end just before reaching the apex. Both premaxillae contain replacement teeth erupting from the lingual side of the descended teeth. By the time the root of the replacement tooth starts to form, the crown and its denticles are fully developed, as observed in NHMD 164758 (Figure 33).

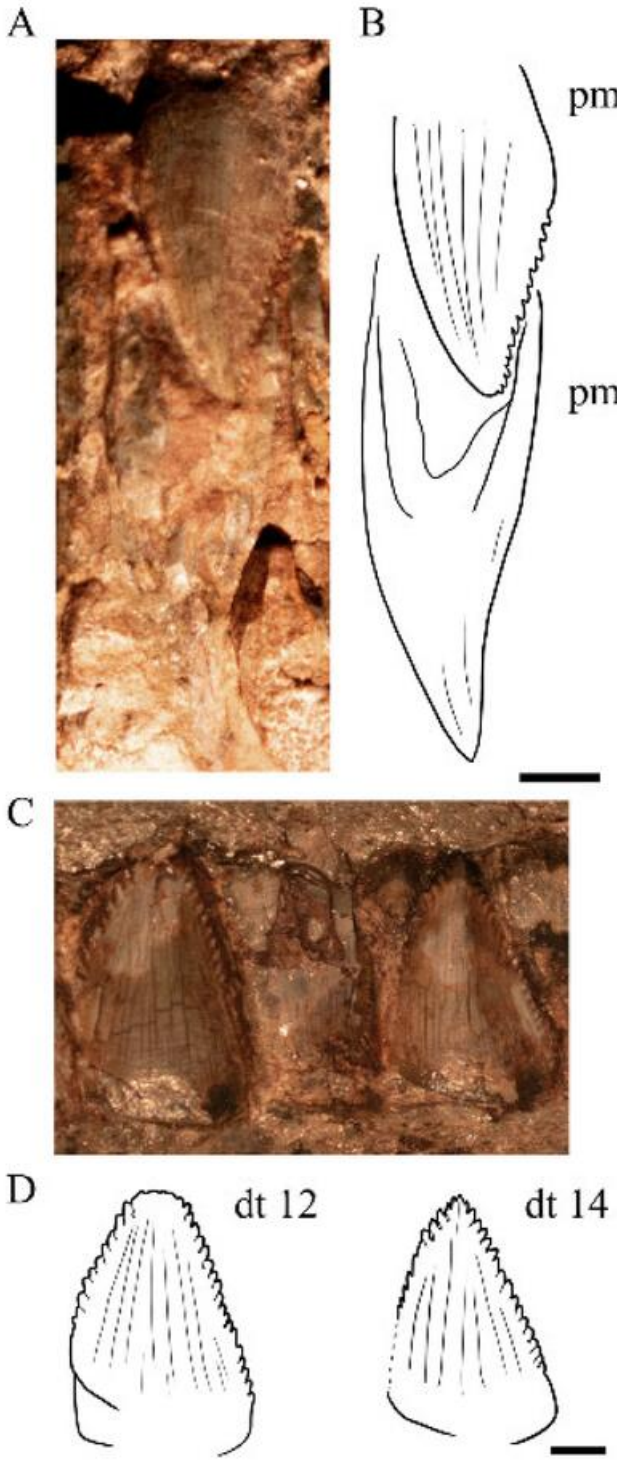

Figure 33. Photograph and schematic drawing of the teeth of NHMD 164741 and NHMD 164758. (**A**) Photograph of the left premaxillary teeth of NHMD 164758 in labial view. (**B**) Schematic drawing of the left premaxillary teeth of NHMD 164758 in labial view. (**C**) Photograph of the left dentary teeth 12 to 14 of NHMD 164741 in labial view. (**D**) Schematic drawing of the left dentary teeth 12 to 14 of NHMD 164741 in labial view. Abbreviations: dt, dentary tooth; pmt, premaxillary tooth. The numbers indicate the tooth position. Scale bar = 2 mm.

The mesialmost teeth (i.e., anterior left premaxilla, anterior right maxilla, anterior left and right dentaries) are missing in NHMD 164741. The left premaxilla preserves the two distalmost teeth in NHMD 164741. Both teeth are descended teeth with the replacement

teeth already contained inside the alveoli. NHMD 164741 and NHMD 164758 preserve 24 and 23 maxillary alveoli on the left maxilla, respectively, and 18 dentary alveoli on the left dentary. Both on the maxilla and dentary, the tooth size decreases at the caudal-most part of the series.

The maxillary and dentary tooth crowns are leaf-shaped, with both labial and lingual surfaces slightly convex and the mesial and distal carinas covered with coarse denticles. The denticles are deflected apically and are occupy more area on the distal carina. As in the premaxillary teeth, the denticles start apical to the basal third of the crown (Figure 33C,D). The apex of the teeth lacks denticles. The tooth roots are slender and comprises most of the tooth height (average root height = 14.2 mm; average crown height = 8.6 mm in NHMD 164741). The labial surface of the root is slightly convex, whereas the lingual surface of the root is marked by a shallow groove, making the root overall B-shaped in cross-section (Figure 34).

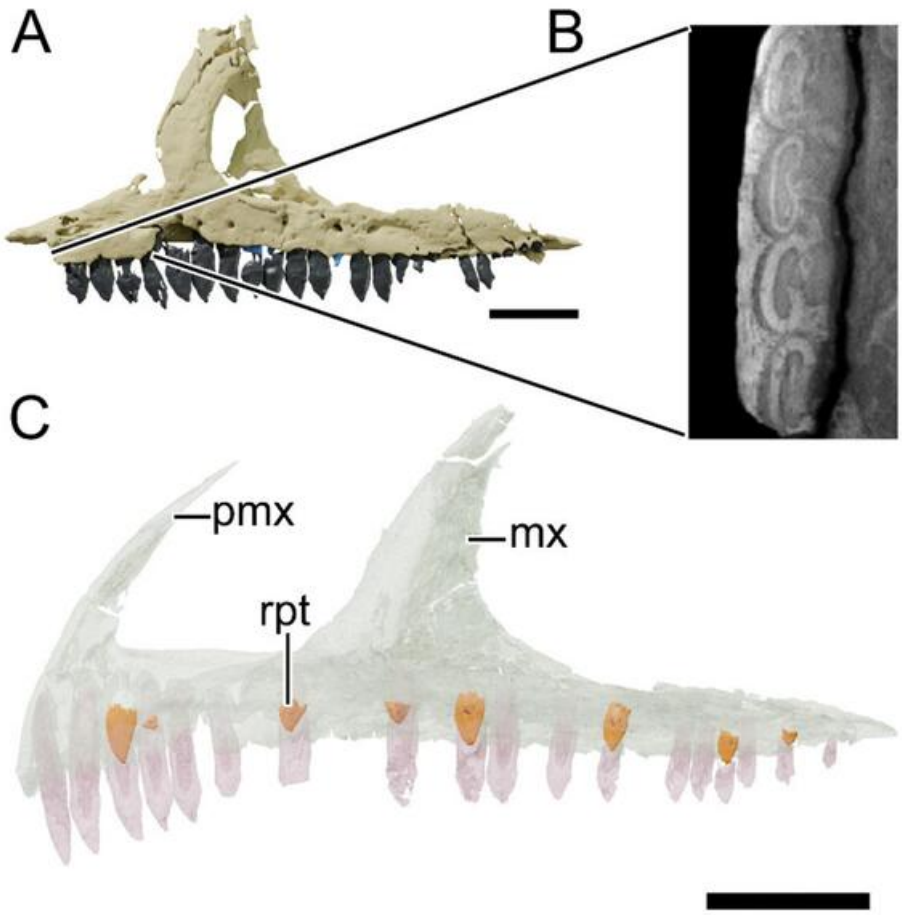

Figure 34. Digital reconstruction and CT-scan slide of the maxilla of NHMD 164741 and digital reconstruction of the right premaxilla and maxilla of NHMD 164758 in transparent display. (**A**) Digital reconstruction of the left maxilla of NHMD 164741 in lateral view. (**B**) Slice of the anterior teeth of the maxilla of NHMD 164741 showing the teeth roots in cross-section. (**C**) Mirrored reconstruction of the upper jaw of NHMD 164758. Abbreviations: mx, maxilla; pmx, premaxilla; rpt, replacement tooth. Scale bar = 50 mm.

4.8.32. Hyoid

Four long and slender bone fragments pertaining to the hyoid apparatus are preserved in NHMD 164758. All fragments pertain to the left ceratobranchial, with different diameters pertaining possibly to the position of these fragments when the bone was complete. One of these rod-like fragments is thicker and longer than the other three fragments (Figures 6 and 7). It is sigmoid in lateral view, with a convex dorsal margin at its anterior

half and a concave dorsal margin at its posterior half. This bone has an anterior rounded and blunt edge and ends posteriorly in an expanded and lateromedially flattened process. The posterior process is laterally depressed. The three slender fragments are located behind the left articular and are equal in diameter. These elements are arched anteroposteriorly but only preserved in the mid-shaft region.

4.8.33. Sclerotic Ring

A total of 18 lateromedially thin and square-shaped plates are partially in articulation in NHMD 164758 left orbit (Figure 35). These plates form a circular arrangement, but the identification of positive and negative plates is not clear, nor is it possible to determine if the 18 plates constitute the whole sclerotic ring.

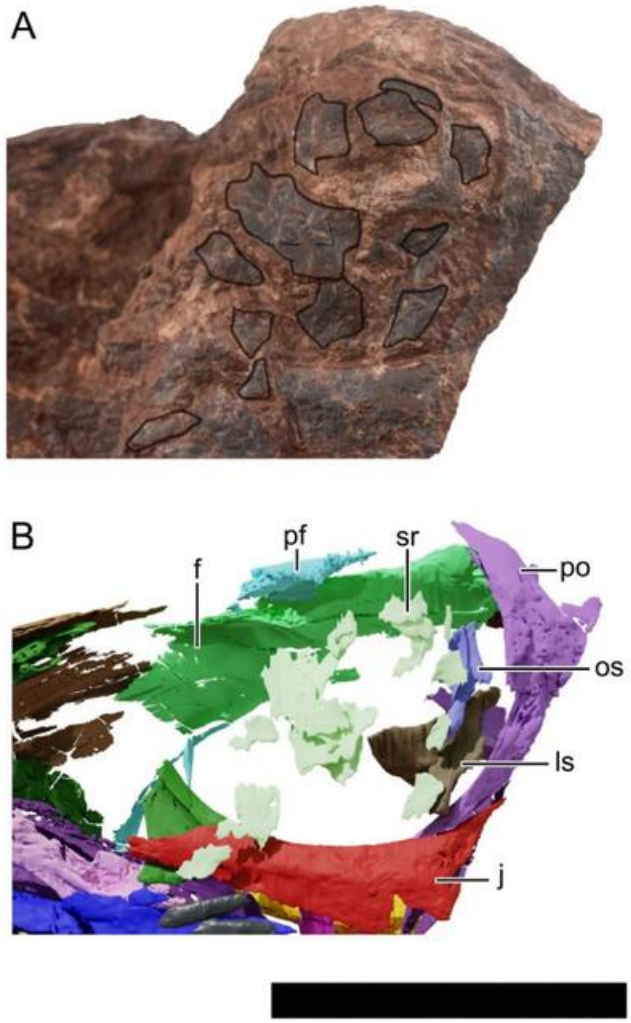

Figure 35. Photograph and digital reconstruction of the left orbital region of NHMD 164758. (**A**) Photograph of the left orbital region of NHMD 164758. (**B**) Digital reconstruction of the left orbital region of NHMD 164758. Scale bar = 50 mm.

4.9. Phylogenetic Analysis

The phylogenetic analysis (see Section 3.4) recovered a total of 400 MPTs of 1582 steps, with consistency index (CI) of 0.286 and retention index of 0.657. Their strict consensus tree with Bremer Support values is found below (Figure 36). The Greenland sauropodomorphs were nested together in our analysis as a sister clade of *Pl. trossingensis* plus *Pl. gracilis*. This clade is characterized by four unambiguous cranial synapomorphies: the postorbital rim of the orbit raised and projecting laterally (54, 1), shared with Massospondylidae; a central

tubercle on the ventral surface of the palatine (90, 1), also shared with Massospondylidae; vomer anteroposterior length over 0.25 of the skull total length [92, (1)], shared with *Melanorosaurus*; and five or more premaxillary teeth (106, 1).

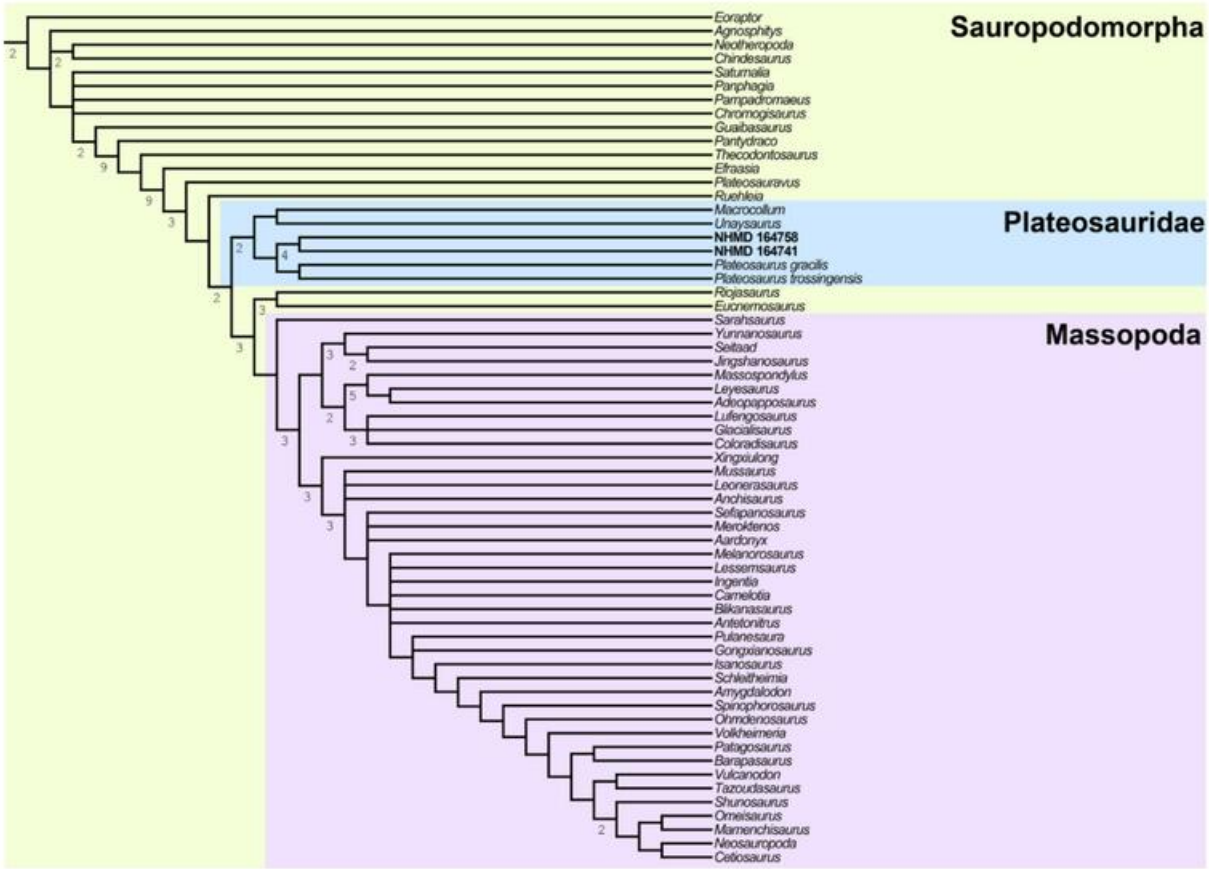

Figure 36. Strict consensus tree of the Greenland specimens. Strict consensus tree of Sauropodomorpha including the Greenland specimens as separate OTUs. Bremer support number (>1) are found under the nodes.

The specimens NHMD 164741 and NHMD 164758 form a clade supported by six unambiguous synapomorphies: weakly developed narial fossa (character 10, state 0), shared with *Mac. Itaquii*, and other more derived sauropodomorphs; small subnarial foramen (12, 1), shared with *Sarahsaurus* and early sauropodomorphs; anterior margin of the external naris anterior to the mid-length of the premaxilla [17, (0)], reversal of a plesiomorphic feature for Sauropodomorpha; anteroposterior length of the antorbital fossa less than the orbit (28, 1), shared with Massopoda (*sensu* [15]); antorbital fossa ending before the ventral process of the lacrimal (41, 1), shared with *Yunnanosaurus*; strongly curved jugal process of the ectopterygoid (86, 1), shared with *Pantydraco*, *Leyesaurus* and *Sarahsaurus*.

The genus *Plateosaurus* (i.e., *Pl. trossingensis* and *Pl. gracilis*) bears three unambiguous cranial synapomorphies: point contact of the posterolateral process of the premaxilla and the anteroventral process of the nasal (7, 1), shared with *E. minor* and *U. tolentinoi*; a depression behind the naris at the dorsal profile of the skull (19, 1), shared with Massospondylidae (*sensu* [15]); length of the posterior process of the prefrontal equal to that of the orbit (42, 1), shared with Massopoda.

The clade Plateosauridae is supported by two cranial and two post-cranial synapomorphies: basipterygoid processes and the parasphenoid rostrum below the level of the basioccipital condyle and the basal tuberae (80, 1), not visible in the Greenland sauropodomorphs and *Mac. itaquii*; strongly ventrally curved dentary symphyseal end (98, 1), also shared with Massospondylidae; ventrolateral twisting of the transverse axis of the distal end of the first phalanx of manual digit one relative to its proximal end of 60° (244, 2), not preserved

on NHMD 164741, NHMD 164758 and *Pl. gracilis*; transverse width of the conjoined distal ischial expansions less than their sagittal depth (292, 1), only observed in *Mac. itaquii* and *Pl. trossingensis*.

In contrast to the analysis of Müller [19], *Mac. itaquii* forms a clade with *U. tolentinoi* at the base of Plateosauridae. This clade is supported by four ambiguous post-cranial synapomorphies: absence of ventral keels on the cervical vertebrae (132, 0); transverse width of the distal end of the humerus over 0.33 of the total length of the bone (217, 1); the first phalanx of manual digit one shorter than the first metacarpal (245, 1); femoral length between 200 and 399 mm (379, 1).

5. Discussion

5.1. Arguments for a New Taxon and Comparisons

The taxonomy of early sauropodomorphs, and plateosaurids specifically, is still not fully resolved and any attempt to erect a new taxon should be done carefully and be well-grounded. The Greenland sauropodomorphs were recovered from rocks of similar age to the central European *Plateosaurus* [28], therefore age separation provides no additional argument for the validity of a separate taxon. Both described skulls suffered some degree of taphonomic deformation, but this degree is not sufficient to explain the differences observed between the Greenland specimens and other sauropodomorphs.

As mentioned above, there are six unambiguous synapomorphies shared between NHMD 164741 and NHMD 164758 and three unambiguous apomorphies supporting *Plateosaurus* as the sister clade for the Greenland specimens. Although these features cannot be caused by taphonomic deformation alone, some of the apomorphies of *Issi saaneq* could indeed be attributed to intraspecific variation. The developmental plasticity of the closely related *Plateosaurus* was noted for specimens from Trossingen [64] and Frick [53]. This plasticity ranges from the total size and proportions of individuals to skull characters usually employed in phylogenetic studies. Phylogenetic characters such as the shape and size of the narial and antorbital fossae or the position of the external naris in the premaxilla found as apomorphic for *Issi saaneq* are highly variable among *Pl. trossingensis* specimens [53]. Therefore, these characters should be revised in future phylogenetic analyses. Nevertheless, some apomorphies of *Issi saaneq*, such as the weak development of the narial fossa and the strongly curved jugal ramus of the ectopterygoid, differ clearly from the condition observed in the described specimens of *Plateosaurus* [2,45,52,53,65]. Furthermore, the three above mentioned synapomorphies supporting the clade *Plateosaurus* are clearly different from the conditions observed in the Greenland specimens.

Issi saaneq possess a unique combination of traits that is not observed in other early sauropodomorphs. NHMD 164741 and NHMD 164758 share a foramen in the medial surface of the premaxilla, absent in *U. tolentinoi*, *Plateosaurus* and *Mas. carinatus*, and different from the more posteriorly located foramen in *Pam. berberenai*. The squamosal of NHMD 164741 preserves a uniquely elongated posterior process. This process is relatively longer anteroposteriorly than in other early sauropodomorphs (Figure 16 and see Table 3). NHMD 164741 also preserved a dorsoventrally elongated and mediolaterally slender quadrate that differs from this condition in all other closely related sauropodomorphs (Figure 18 and see Table 4). This makes the skull of NHMD 164741 dorsoventrally taller at its posterior half than that of other sauropodomorphs such as *Pl. trossingensis*, *Mac. itaquii*, *Bu. schultzi*, *N. intlokoi* and *Mas. carinatus*. NHMD 164758 preserves a unique morphology of the articular among early sauropodomorphs (Figure 32), not preserved in NHMD 164741. The dorsoposterior process of the articular is well-developed and dorsally tall, forming a squared blade in lateral view.

A combination of additional features further differentiates *Issi saaneq* gen. et sp. nov. from *Plateosaurus.* The nasals of NHMD 164741 and NHMD 164758 occupy 0.41 and 0.48, respectively, of the total skull roof length, whereas in *Plateosaurus* the nasal occupies over 0.5 of that length [52,53,63]. The lateral process of the laterosphenoid is elongated and arches laterally in *Pl. trossingensis* (AMNH FARB 6810) [52], whereas in NHMD 164758 this

process is short and straight, as is the condition in other sauropodomorphs such as *Mac. itaquii*, *N. intlokoi* and *Mas. carinatus*. The autapomorphic feature of a ventrally located, central peg-like process of the palatine of *Pl. trossingensis* is absent in both NHMD 164741 and NHMD 164758. Only two of the autapomorphic features for *Pl. trossingensis* are present in *Issi saaneq*. The lateral sheet of bone in the lacrimal is present in NHMD 164741, although differing from that of *Pl. trossingensis* in having a foramen in the dorsolateral surface of this flange, similar to the lateral foramen of *Mac. itaquii*. In *Issi saaneq*, this flange is concave in its anterior margin, whereas it is convex in *Pl. trossingensis*. The dorsoventrally high jugal of *Pl. trossingensis* is visible in NHMD 164758 left jugal. This bone is morphologically similar to that of most *Pl. trossingensis* specimens. *Issi saaneq* also shares features with the Brazilian plateosaurids *Mac. itaquii* and *U. tolentinoi*, that are lacking in *Plateosaurus.* These features include a weakly developed narial fossa (observed on *Issi saaneq* and the Brazilian plateosaurids), a promaxillary fenestra (observed only in NHMD 164741 and the Brazilian plateosaurids), a foramen in the lateral surface of the lacrimal (observed in NHMD 164741 and *Mac. itaquii*) and a secondary fossa ventral to the Meckelian groove (observed in both *Issi saaneq* specimens and *U. tolentinoi*).

5.2. Arguments for a Single New Species

The specimens NHMD 164741 and NHMD 164758 are almost complete skulls of different sizes, varying only slightly in their morphology. Both were recovered from the same locality, meaning that both specimens existed coevally. Both specimens received the same scores for every coded character in the phylogenetic analysis, forming together the sister clade of *Plateosaurus*. However, due to incomplete preservation only one autapomorphy is preserved in both NHMD 164741 and NHMD 164758, the medial foramen of the premaxilla. The squamosal and dorsal half of the quadrates are missing in NHMD 164758 and the posterior half of the articular is missing in NHMD 164741, hampering the assessment of these autapomorphies. NHMD 164741 differs from NHMD 164758 in having a promaxillary fenestra in the antorbital fossa (Figures 10 and 11), the shape of the anterodorsal process of the lacrimal (which is distally broken in NHMD 164741, Figures 12 and 13) and in bulkier postorbitals (Figures 14 and 15) and frontals (Figures 20 and 21). The presence of a promaxillary fenestra was recovered as a synapomorphy for the Brazilian "unaysaurids" *Mac. itaquii* and *U. tolentinoi* [18,19,22]. Because this feature is plastic and can even be present in one element and absent in the other for the same individual [19], the presence of a promaxillary fenestra does not support a separation of the Greenland specimens in different species. The difference in the anterodorsal process of the lacrimal and the bulkier postorbital in NHMD 164741 could be attributed to ontogeny or even intraspecific variation, as is the case of the main body of the postorbital in *Pl. trossingensis* [53]. Due to the lack of features distinguishing both Greenland specimens, NHMD 164741 and NHMD 164758 are here regarded as belonging to the same new genus and species, *Issi saaneq* (Figures 37 and 38).

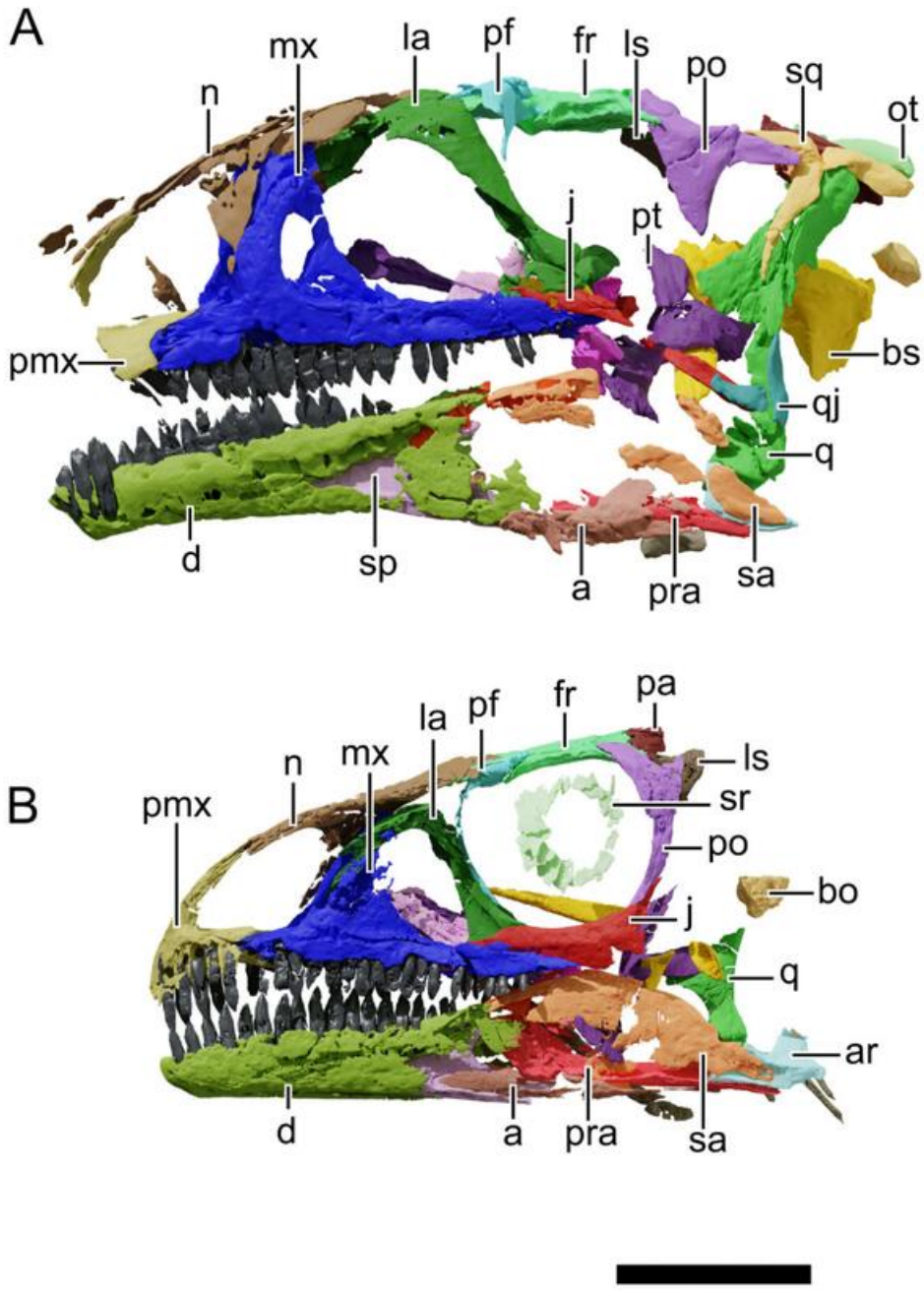

Figure 37. Digital reconstruction of the skulls NHMD 164741 and NHMD 164758 in articulation. Digital arrangement of preserved bone elements of NHMD 164741 (**A**) and NHMD 164758 (**B**) in left lateral view. Abbreviations: ar, articular; bo, basioccipital; bs, basisphenoid; d, dentary; fr, frontal; j, jugal; la, lacrimal; ls, laterosphenoid; mx, maxilla; n, nasal; ot, otoccipital; pf, prefrontal; pmx, premaxilla; po, postorbital; pra, prearticular; pt, pterygoid; q, quadrate; qj, quadratojugal; sa, surangular; sp, splenial; sq, squamosal; sr, sclerotic ring. Scale bar = 50 mm.

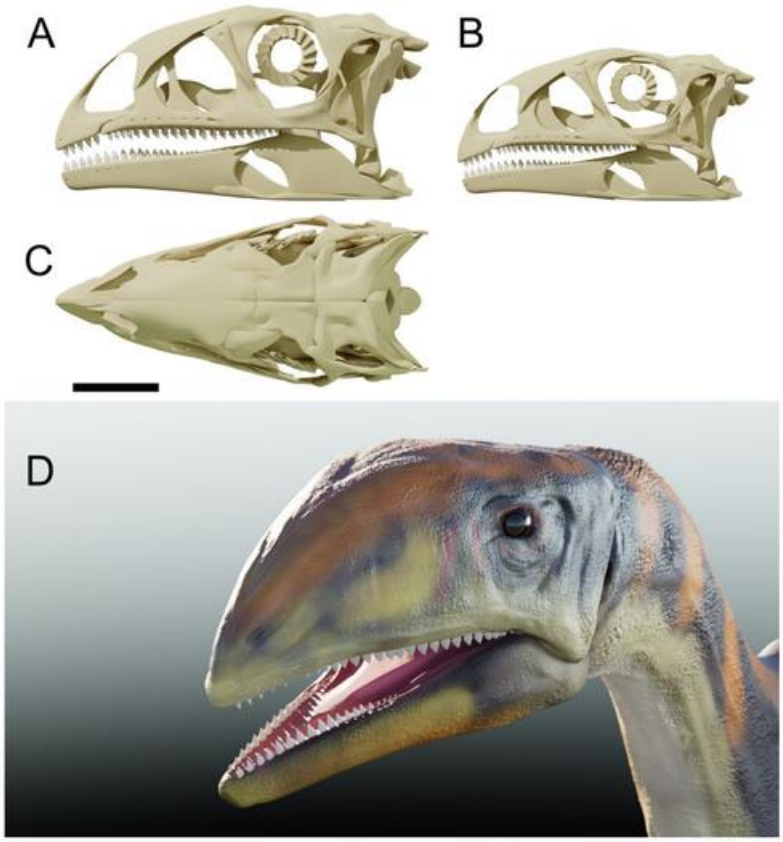

Figure 38. Digital interpretative reconstruction of the skulls NHMD 164741 and NHMD 164758 and living representation of *Issi saaneq*. (**A**) Digital interpretative reconstruction of the skull NHMD 164741 in left lateral view. (**B**) Digital interpretative reconstruction of the skull NHMD 164758 in left lateral view. (**C**) Digital interpretative reconstruction of skull NHMD 164741 in dorsal view. (**D**) Living representation of *Issi saaneq*. Scale bar = 50 mm.

5.3. Ontogeny

Although representing the same taxon, NHMD 164741 and NHMD 164758 differ in size and the skull proportions. Because size is not a good proxy for the ontogenetic stage in the closely related *Pl. trossingensis* [64,66], this may be also the case for the Greenland specimens. NHMD 164741 measures 1.45 times the anteroposterior length of that of NHMD 164758, even with the former lacking the anteriormost region of the skull (which would account for half the premaxilla main body length, possibly making the skull 15 to 20 mm longer). The orbit length in NHMD 164741 can only be estimated with the digital articulation of the preserved bones. This estimation ranges from 41 to 45.5 mm in length, meaning that the orbit length to skull length of NHMD 164741 would range from 0.17 to 0.20 (Figure 37A). NHMD 164758 preserved the orbit region still in articulation, with minor deformation (Figure 33). The orbit length measures 47.2 mm in this specimen, so that the orbit to skull length ratio (approximately 0.28) is higher than in NHMD 164741. A larger orbit is supposed to be a juvenile feature, as shown by the late-stage juvenile of *Pl. trossingensis* (MSF 12.3) [53]. The reduced dentary teeth count (<20 tooth position) is also a feature related to ontogeny in plateosaurids [53]. NHMD 164758 shows only 18 tooth positions in its dentaries, and NHMD 164741 preserves a minimum of 18 tooth positions. In the latter this number might be underestimated, as the anterior region of the dentary is missing, so that it could have reached at least 20 teeth when complete. The reduced gap between the first premaxillary tooth and the anterior tip of the premaxilla is observed in NHMD 164758, representing another juvenile feature for this specimen [53]. The orientation of the basipterygoid process of the basisphenoid can also be an indicative of ontogenetic stage in some sauropodomorphs, such as in *Mas. carinatus* [16]. The differences

between the slightly anteriorly deflected basipterygoid process of NHMD 164758 and the sub-perpendicular basipterygoid process of NHMD 164741 may be related to their ontogenetic stages. All these discussed features position NHMD 164758 in an earlier stage of development than NHMD 164741, the former being interpreted as an early-stage juvenile and the latter as a possible late-stage juvenile or young adult.

5.4. Paleobiogeographic and Chronological Implications

Plateosaurid sauropodomorphs were found in Upper Triassic (Norian) strata of Brazil, Germany, France, Switzerland and Norway [19,22,52,53,63,67–71] and are now confidently reported for Greenland. *Issi saaneq* is the first sauropodomorph to reach paleolatitudes of over 40° N and is the first known non-*Plateosaurus* plateosaurid for Laurasia. The shared features of *Issi saaneq* and *Plateosaurus* were expected due to their contemporaneity during the mid-Norian (around 218-214 Mya, but possibly constrained to 217 Mya according to [28]) and paleogeographic proximity (the distance between localities is roughly estimated at 1000-2000 km). However, *Issi saaneq* shares additional features with *Mac. itaquii* and *U. tolentinoi*. The plateosaurid sauropodomorphs from Brazil were recovered in the Candelária Sequence at an estimated absolute age of 225.4 Mya (mid-Norian according to [72]). Due to their older age, the Brazilian plateosaurids may represent a key moment in the early evolution and dispersal of plateosaurids. However, the possible timing and evolution of plateosaurid sauropodomorphs can only be addressed with additional findings for this clade, either in North America or Africa. As of now, mid-Norian outcrops which could yield sauropodomorphs are rare in Africa, whereas Late Triassic dinosaurs are relatively well-known from North America [73]. The latter, however, lacks Triassic sauropodomorph dinosaurs until now [73]. The first basal sauropodomorphs from North America include *Anchisaurus polyzelus* [74] from the Portland Formation, USA and *Sarahsaurus aurifontanalis* [75] from the Kayenta Formation, USA; both Early Jurassic (Sinemurian-Pliensbachian) in age.

6. Conclusions

Two skulls of the new basal sauropodomorph (plateosaurid) dinosaur taxon *Issi saaneq* gen. nov. sp. nov. from the Late Triassic (Norian) of Jameson Land, central East Greenland are described based on data retrieved with μCT-scan image segmentation and photogrammetry. Both specimens, NHMD 164741 and NHMD 164758, were recovered from the uppermost Malmros Klint Formation in Greenland, and due to strong morphological similarities and no robust distinguishing features between them, are here regarded as a single taxon. The smaller NHMD 164758 represents an early-stage juvenile, due to the reduced gap between the first premaxillary teeth and the anterior margin of the premaxilla, large orbit, low number of teeth positions in the dentary and an anteriorly deflected basipterygoid process of the basisphenoid. The specimen NHMD 164741 represents either a late-stage juvenile or a young adult, due to a proportionally shorter orbit than NHMD 164758 and having a possible maximum of 20 dentary teeth positions. *Issi saaneq* differs from all other basal sauropodomorphs in four observed autapomorphies: (1) the presence of a small foramen at the medial surface of the premaxilla at the base of the lateral process of the premaxilla; (2) an anteroposteriorly elongated dorsoposterior process of the squamosal; (3) a quadrate relatively tall in comparison to the rostrum height; and (4) a well-developed, square-shaped in lateral view posterodorsal process of the articular.

Six ambiguous synapomorphies position *Issi saaneq* as the sister clade to *Plateosaurus* (*Pl. trossingensis* and *Pl. gracilis*). The Brazilian sauropodomorphs were recovered at the base of Plateosauridae and forming the sister clade to the clade containing *Issi saaneq* and *Plateosaurus*. *Issi saaneq* possesses a set of features thought to be exclusive of the Brazilian plateosaurids. *Issi saaneq* is the first sauropodomorph to reach the Northernmost parts of Laurasia and increases our understanding of the diversity of plateosaurids.

Supplementary Materials: The following is available online at https://www.mdpi.com/article/10.3390/d13110561/s1, Data S1: Data matrix 01.

Author Contributions: Conceptualization, V.B., O.M., O.W., J.M., L.B.C.; methodology, V.B., O.M., O.W.; software, V.B.; formal analysis, V.B., O.M., O.W., J.M., L.B.C.; investigation, V.B., O.M., O.W., J.M., L.B.C.; data curation, V.B.; writing—original draft preparation, V.B., O.M., O.W., J.M., L.B.C.; writing—review and editing, V.B., O.M., O.W., J.M., L.B.C.; visualization, V.B.; figures and 3D models, V.B.; supervision, O.M. and L.B.C. All authors have read and agreed to the published version of the manuscript.

Funding: This research benefited from the grant GeoBioTec-GeoBioSciences, GeoTechnologies and GeoEngineering NOVA [GeoBioCiências, GeoTecnologias e GeoEngenharias], grant UIDB/04035/2020 by the Fundação para a Ciência e Tecnologia. The geological work of LBC was supported by the Carlsberg Foundation, the Independent Research Fund Denmark, and Geocenter Møns Klint.

Institutional Review Board Statement: Not applicable.

Informed Consent Statement: Not applicable.

Data Availability Statement: All specimens in this study are housed at the Natural History Museum of Denmark (NHMD). All CT-scan data and 3D models of both specimens will be available in MorphoSource at: (ark:/87602/m4/393344).

Acknowledgments: We would like to thank the team that uncovered both specimens here described, William W. Amaral, William R. Downs, Stephen M. Gatesy, Neil H. Shubin and Niels Bonde and Farish Jenkins. We also would like to thank Marco Marzola, Filippo Rotatori and Alexandra Fernandes for the CT-scan of the specimens.

Conflicts of Interest: The authors declare no conflict of interest.

References

1. Meyer, H. Briefliche mitteilung an Prof. Bronn über *Plateosaurus engelhardti*. *Neues Jahrb. Mineral. Geogn. Geol. Petrefakten-Kunde* **1837**, *24*, 314–316.
2. Yates, A.M. The species taxonomy of the sauropodomorph dinosaurs from the Lowenstein Formation (Norian, Late Triassic) of Germany. *Palaeontology* **2003**, *46*, 317–337. [CrossRef]
3. Galton, P.M. Prosauropod Dinosaur *Plateosaurus* (=*Gresslyosaurus*) (*Saurischia: Sauropodomorpha*) from the Upper Triassic of Switzerland. *Geol. Palaeontol.* **1986**, *20*, 167–183.
4. Rütimeyer, L. Reptilien knochen aus dem Keuper von Liestal. *Verh. Schweiz. Nat. Ges.* **1856**, *41*, 62–64.
5. Huene, F.F. Über die Trias-Dinosaurier Europas. *Z. Dtsch. Geol. Ges.* **1905**, *57*, 345–349.
6. Huene, F.F. *Die Dinosaurier der Europäischen Triasformation mit Berücksichtigung der Aussereuropäischen Vorkommnisse*; G. Fischer: Jena, Germany, 1908; Volume 1.
7. Fraas, E. Die neuesten Dinosaurierfunde in der Schwäbischen Trias. *Naturwissenschaften* **1913**, *1*, 1097–1100. [CrossRef]
8. Yates, A.M. Solving a dinosaurian puzzle: The identity of *Aliwalia Rex* Galton. *Hist. Biol.* **2007**, *19*, 93–123. [CrossRef]
9. Yates, A.M. A revision of the problematic sauropodomorph dinosaurs from Manchester, Connecticut and the Status of *Anchisaurus* Marsh: The taxonomic status of Anchisaurus. *Palaeontology* **2010**, *53*, 739–752. [CrossRef]
10. Galton, P.M.; Kermack, D. The anatomy of *Pantydraco Caducus*, a very basal Sauropodomorph Dinosaur from the Rhaetian (Upper Triassic) of South Wales, UK. *Rev. Palóbiologie* **2010**, *29*, 341–404.
11. Apaldetti, C.; Martinez, R.N.; Alcober, O.A.; Pol, D. A new basal Sauropodomorph (*Dinosauria: Saurischia*) from Quebrada Del Barro formation (Marayes-El Carrizal Basin), Northwestern Argentina. *PLoS ONE* **2011**, *6*, e26964. [CrossRef]
12. Rauhut, O.W.M.; Holwerda, F.M.; Furrer, H. A derived Sauropodiform Dinosaur and other sauropodomorph material from the Late Triassic of Canton Schaffhausen, Switzerland. *Swiss J. Geosci.* **2020**, *113*, 8. [CrossRef]
13. Galton, P.M. Case 3560 *Plateosaurus Engelhardti* Meyer, 1837 (*Dinosauria, Sauropodomorpha*): Proposed replacement of unidentifiable name-bearing type by a neotype. *Bull. Zool. Nomencl.* **2012**, *69*, 203–212. [CrossRef]
14. ICZN. Opinion 2435 (Case 3560) *Plateosaurus* Meyer, 1837 (*Dinosauria, Sauropodomorpha*): New type species designated. *Bull. Zool. Nomencl.* **2019**, *76*, 144–145. [CrossRef]
15. Yates, A.M. The first complete skull of the triassic dinosaur *Melanorosaurus Haughton* (*Sauropodomorpha: Anchisauria*). *Spec. Pap. Palaeontol.* **2007**, *77*, 9–55.
16. Chapelle, K.E.J.; Choiniere, J.N. A revised cranial description of *Massospondylus Carinatus* owen (*Dinosauria: Sauropodomorpha*) based on computed tomographic scans and a review of cranial characters for basal Sauropodomorpha. *PeerJ* **2018**, *6*, e4224. [CrossRef] [PubMed]
17. Chapelle, K.E.J.; Barrett, P.M.; Botha, J.; Choiniere, J.N. *Ngwevu Intloko*: A new early sauropodomorph dinosaur from the lower jurassic elliot formation of South Africa and comments on cranial ontogeny in *Massospondylus carinatus*. *PeerJ* **2019**, *7*, e7240. [CrossRef]

18. McPhee, B.W.; Bittencourt, J.S.; Langer, M.C.; Apaldetti, C.; Da Rosa, Á.A.S. Reassessment of *Unaysaurus Tolentinoi* (Dinosauria: Sauropodomorpha) from the Late Triassic (Early Norian) of Brazil, with a consideration of the evidence for monophyly within non-sauropodan sauropodomorphs. *J. Syst. Palaeontol.* **2020**, *18*, 259–293. [CrossRef]
19. Müller, R.T. Craniomandibular osteology of *Macrocollum Itaquii* (*Dinosauria: Sauropodomorpha*) from the Late Triassic of Southern Brazil. *J. Syst. Palaeontol.* **2020**, *18*, 805–841. [CrossRef]
20. Leal, L.A.; Azevedo, S.A.K.; Kellner, A.W.A.; Rosa, Á.A.S. A new early dinosaur (Sauropodomorpha) from the Caturrita Formation (Late Triassic), Paraná Basin, Brazil. *Zootaxa* **2004**, *690*, 1–24. [CrossRef]
21. McPhee, B.W.; Choiniere, J.N.; Yates, A.M.; Viglietti, P.A. A second species of *Eucnemesaurus* Van Hoepen, 1920 (*Dinosauria, Sauropodomorpha*): New information on the diversity and evolution of the sauropodomorph fauna of South Africa's Lower Elliot Formation (Latest Triassic). *J. Vertebr. Paleontol.* **2015**, *35*, e980504. [CrossRef]
22. Müller, R.T.; Langer, M.C.; Dias-da-Silva, S. An exceptionally preserved association of complete dinosaur skeletons reveals the oldest long-necked sauropodomorphs. *Biol. Lett.* **2018**, *14*, 20180633. [CrossRef] [PubMed]
23. Novas, F.E.; Ezcurra, M.D.; Chatterjee, S.; Kutty, T.S. New dinosaur species from the upper Triassic upper Maleri and lower Dharmaram formations of Central India. *Earth Environ. Sci. Trans. R. Soc. Edinb.* **2011**, *101*, 333–349. [CrossRef]
24. Novas, F.E.; Ezcurra, M.D.; Chatterjee, S.; Kutty, T.S. *Late Triassic Continental Vertebrates and Depositional Environments of the Fleming Fjord Formation, Jameson Land, East. Greenland*; Jenkins, F.A., Shubin, N.H., Amaral, W.W., Gatesy, S.M., Schaff, C.R., Clemmensen, L.B., Downs, W.R., Davidson, A.R., Bonde, N., Osbaeck, F., Eds.; Meddelelser om Grønland Geoscience: Brenderup, Denmark, 1994; ISBN 978-87-601-4573-5.
25. Clemmensen, L.B.; Kent, D.W.; Mau, M.; Mateus, O.; Milàn, J. Triassic lithostratigraphy of the Jameson land basin (Central East Greenland), with emphasis on the New Fleming Fjord Group. *Bull. Geol. Soc. Den.* **2020**, *68*, 95–132. [CrossRef]
26. Marzola, M.; Mateus, O.; Milàn, J.; Clemmensen, L.B. A review of Palaeozoic and Mesozoic Tetrapods from Greenland. *Bull. Geol. Soc. Den.* **2018**, *66*, 21–46. [CrossRef]
27. Guarnieri, P.; Brethes, A.; Rasmussen, T.M. Geometry and kinematics of the Triassic rift basin in Jameson Land (East Greenland): Triassic rift basin East Greenland. *Tectonics* **2017**, *36*, 602–614. [CrossRef]
28. Kent, D.V.; Clemmensen, L.B. Northward dispersal of dinosaurs from Gondwana to Greenland at the Mid-Norian (215–212 Ma, Late Triassic) dip in atmospheric pCO_2. *Proc. Natl. Acad. Sci. USA* **2021**, *118*, e2020778118. [CrossRef] [PubMed]
29. Clemmensen, L.B.; Kent, D.V.; Jenkins, F.A. A late triassic lake system in East Greenland: Facies, depositional cycles and palaeoclimate. *Palaeogeogr. Palaeoclimatol. Palaeoecol.* **1998**, *140*, 135–159. [CrossRef]
30. Sellwood, B.W.; Valdes, P.J. Mesozoic climates: General circulation models and the rock record. *Sediment. Geol.* **2006**, *190*, 269–287. [CrossRef]
31. Agnolin, F.L.; Mateus, O.; Milàn, J.; Marzola, M.; Wings, O.; Adolfssen, J.S.; Clemmensen, L.B. *Ceratodus Tunuensis*, Sp. Nov., a new lungfish (Sarcopterygii, Dipnoi) from the Upper Triassic of Central East Greenland. *J. Vertebr. Paleontol.* **2018**, *38*, e1439834. [CrossRef]
32. Sulej, T.; Wolniewicz, A.; Bonde, N.; Błażejowski, B.; Niedźwiedzki, G.; Tałanda, M. New perspectives on the Late Triassic vertebrates of East Greenland: Preliminary results of a Polish−Danish palaeontological expedition. *Pol. Polar Res.* **2014**, *35*, 541–552. [CrossRef]
33. Clemmensen, L.B.; Milàn, J.; Adolfssen, J.S.; Estrup, E.J.; Frobøse, N.; Klein, N.; Mateus, O.; Wings, O. The vertebrate-bearing Late Triassic Fleming Fjord Formation of Central East Greenland revisited: Stratigraphy, palaeoclimate and new palaeontological data. *Geol. Soc. Lond. Spec. Publ.* **2016**, *434*, 31–47. [CrossRef]
34. Marzola, M.; Mateus, O.; Shubin, N.H.; Clemmensen, L.B. *Cyclotosaurus Naraserluki* Sp. Nov., a new Late Triassic Cyclotosaurid (*Amphibia, Temnospondyli*) from the Fleming Fjord Formation of the Jameson Land Basin (East Greenland). *J. Vertebr. Paleontol.* **2017**, *37*, e1303501. [CrossRef]
35. Niedźwiedzki, G.; Sulej, T. Theropod dinosaur fossils from the Gipsdalen and Fleming fjord formations (Carnian-Norian, Upper Triassic), East Greenland. In Proceedings of the 34th Nordic Geological Winter Meeting, Oslo, Norway, 8–10 January 2020; Nakrem, H.A., Hus, A.M., Eds.; Geological Society of Norway: Oslo, Norway, 2020; Volume 2020, p. 151.
36. Milàn, J.; Octávio, M.; Mau, M.; Rudra, A.; Sanei, H.; Clemmensen, L.B. A possible phytosaurian (*Archosauria, Pseudosuchia*) coprolite from the Late Triassic Fleming Fjord Group of Jameson Land, Central East Greenland. *Bull. Geol. Soc. Den.* **2021**, *69*, 71–80. [CrossRef]
37. Jenkins, F.A.; Gatesy, S.M.; Shubin, N.H.; Amaral, W.W. Haramiyids and Triassic mammalian evolution. *Nature* **1997**, *385*, 715–718. [CrossRef]
38. Sulej, T.; Krzesiński, G.; Tałanda, M.; Wolniewicz, A.S.; Błażejowski, B.; Bonde, N.; Gutowski, P.; Sienkiewicz, M.; Niedźwiedzki, G. The earliest-known mammaliaform fossil from Greenland sheds light on origin of mammals. *Proc. Natl. Acad. Sci. USA* **2020**, *117*, 26861–26867. [CrossRef] [PubMed]
39. Pretto, F.A.; Langer, M.C.; Schultz, C.L. A new dinosaur (*Saurischia: Sauropodomorpha*) from the Late Triassic of Brazil provides insights on the evolution of Sauropodomorph body plan. *Zool. J. Linn. Soc.* **2019**, *185*, 388–416. [CrossRef]
40. Cabreira, S.F.; Kellner, A.W.A.; Dias-da-Silva, S.; Roberto da Silva, L.; Bronzati, M.; de Almeida Marsola, J.C.; Müller, R.T.; de Souza Bittencourt, J.; Batista, B.J.; Raugust, T.; et al. A unique Late Triassic Dinosauromorph assemblage reveals dinosaur ancestral anatomy and Diet. *Curr. Biol.* **2016**, *26*, 3090–3095. [CrossRef] [PubMed]

41. Müller, R.T.; Langer, M.C.; Bronzati, M.; Pacheco, C.P.; Cabreira, S.F.; Dias-da-Silva, S. Early evolution of Sauropodomorphs: Anatomy and phylogenetic relationships of a remarkably well-preserved dinosaur from the Upper Triassic of Southern Brazil. *Zool. J. Linn. Soc.* **2018**, *184*, 1187–1248. [CrossRef]
42. Müller, R.T.; Ferreira, J.D.; Pretto, F.A.; Bronzati, M.; Kerber, L. The endocranial anatomy of *Buriolestes Schultzi* (*Dinosauria: Saurischia*) and the early evolution of brain tissues in sauropodomorph dinosaurs. *J. Anat.* **2021**, *238*, 809–827. [CrossRef]
43. Bonaparte, J.F. *Coloradia Brevis* n. g. et n. Sp. (*Saurischia, Prosauropoda*), a Plateosaurid dinosaur from the Los Colorados Formation, Upper Triassic of La Rioja, Argentina. *Ameghiniana* **1978**, *15*, 7.
44. Apaldetti, C.; Martinez, R.N.; Pol, D.; Souter, T. Redescription of the skull of *Coloradisaurus Brevis* (*Dinosauria, Sauropodomorpha*) from the Late Triassic Los Colorados Formation of the Ischigualasto-Villa Union Basin, Northwestern Argentina. *J. Vertebr. Paleontol.* **2014**, *34*, 1113–1132. [CrossRef]
45. Galton, P.M. Cranial anatomy of the prosauropod dinosaur *Plateosaurus* from the Knollenmergel (Middle Keuper, Upper Triassic) of Germany. II. All the cranial material and details of soft-part anatomy. *Geol. Palaeontol.* **1985**, *19*, 119–159.
46. Bronzati, M.; Rauhut, O.W.M. Braincase redescription of *Efraasia Minor*. Huene, 1908 (*Dinosauria: Sauropodomorpha*) from the Late Triassic of Germany, with comments on the evolution of the sauropodomorph braincase. *Zool. J. Linn. Soc.* **2018**, *182*, 173–224. [CrossRef]
47. Barrett, P.M.; Upchurch, P.; Xiao-Lin, W. Cranial osteology of *Lufengosaurus Huenei* young (*Dinosauria: Prosauropoda*) from the lower jurassic of Yunnan, People's Republic of China. *J. Vertebr. Paleontol.* **2005**, *25*, 806–822. [CrossRef]
48. Barrett, P.M. A new basal sauropodomorph dinosaur from the Upper Elliot Formation (Lower Jurassic) of South Africa. *J. Vertebr. Paleontol.* **2009**, *29*, 1032–1045. [CrossRef]
49. Langer, M.C.; McPhee, B.W.; Marsola, J.C.D.A.; Roberto-Da-Silva, L.; Cabreira, S.F. Anatomy of the dinosaur *Pampadromaeus Barberenai* (*Saurischia—Sauropodomorpha*) from the Late Triassic Santa Maria Formation of Southern Brazil. *PLoS ONE* **2019**, *14*, e0212543. [CrossRef]
50. Martinez, R.N.; Alcober, O.A. A Basal Sauropodomorph (Dinosauria: Saurischia) from the Ischigualasto Formation (Triassic, Carnian) and the early evolution of Sauropodomorpha. *PLoS ONE* **2009**, *4*, e4397. [CrossRef] [PubMed]
51. Galton, P.M. The Prosauropod Dinosaur Plateosaurus Meyer, 1837 (*Saurischia: Sauropodomorpha*; Upper Triassic). II. Notes on the referred species. *Rev. Paléobiologie* **2001**, *20*, 435–502.
52. Prieto-Márquez, A.; Norell, M.A. Redescription of a Nearly complete skull of *Plateosaurus* (*Dinosauria: Sauropodomorpha*) from the Late Triassic of Trossingen (Germany). *Am. Mus. Novit.* **2011**, *3727*, 1–58. [CrossRef]
53. Lallensack, J.N.; Teschner, E.; Pabst, B.; Sander, P.M. New skulls of the Basal Sauropodomorph *Plateosaurus Trossingensis* from Frick, Switzerland: Is there more than one species? *Acta Palaeontol. Pol.* **2021**, *66*, 1–28. [CrossRef]
54. Langer, M.C.; Abdala, F.; Richter, M.; Benton, M.J. A Sauropodomorph dinosaur from the Upper Triassic (Carnian) of Southern Brazil. *Académie Sci.* **1999**, *329*, 511–517.
55. Mallison, H.; Wings, O. Photogrammetry in paleontology—A practical guide. *J. Paleontol. Tech.* **2014**, *12*, 1–31.
56. Goloboff, P.A.; Catalano, S.A. TNT version 1.5, including a full implementation of phylogenetic morphometrics. *Cladistics* **2016**, *32*, 221–238. [CrossRef]
57. Owen, R. *Report on British Fossil Reptiles. Part. II*; Report of the British Association for the Advancement of Science; British Association for the Advancement of Science: London, UK, 1842.
58. Seeley, H.G. I. On the classification of the fossil animals commonly named Dinosauria. *Proc. R. Soc. Lond.* **1887**, *43*, 165–171. [CrossRef]
59. Huene, F.F. *Die Fossile Reptil-Ordnung Saurischia, ihre Entwicklung und Geschichte*; Verlag von Gebrüder Borntraeger: Leipzic, Germany, 1932.
60. Marsh, O.C. On the affinities and classification of the dinosaurian reptiles. *Am. J. Sci.* **1895**, *3*, 483–498. [CrossRef]
61. Clemmensen, L.B. Triassic lithostratigraphy of East Greenland between Scoresby Sund and Kejser Franz Josephs Fjord. *Grønlands Geol. Undersøgelse Bull.* **1980**, *139*, 56.
62. Young, C.-C. A Complete Osteology of Lufengosaurus Heunei Young (Gen. et Sp. Nov.) from Lufeng, Yunnan, China. *Geol. Surv. China* **1941**, *7*, 53.
63. Galton, P.M.; Upchurch, P. 12. Prosauropoda. In *The Dinosauria*, 2nd ed.; University of California Press: Berkeley, CA, USA, 2004; pp. 232–258.
64. Sander, P.M.; Klein, N. Developmental plasticity in the life history of a prosauropod dinosaur. *Science* **2005**, *310*, 1800–1802. [CrossRef] [PubMed]
65. Galton, P.M. Cranial anatomy of the prosauropod dinosaur *Plateosaurus* from the Knollenmergel (Middle Keuper, Upper Triassic) of Germany. I. Two complete skulls from Trossingen/Württ. with comments on the diet. *Geol. Palaeontol.* **1984**, *18*, 139–171.
66. Klein, N.; Sander, P.M. Bone histology and growth of the prosauropod dinosaur *Plateosaurus Engelhardti* von Meyer, 1837 from the Norian Bonebeds of Trossingen (Germany) and Frick (Switzerland). *Spec. Pap. Palaeontol.* **2007**, *77*, 169–206.
67. Sander, P.M. The norian *Plateosaurus* Bonebeds of Central Europe and Their yaphonomy. *Palaeogeogr. Palaeoclimatol. Palaeoecol.* **1992**, *93*, 255–299. [CrossRef]
68. Moser, M. *Plateosaurus engelhardti* Meyer, 1837 (*Dinosauria: Sauropodomorpha*) aus dem Feuerletten (Mittelkeuper; Obertrias) von Bayern. *Zitteliana* **2003**, *24*, 3–186.

69. Hurum, J.H.; Bergan, M.; Müller, R.; Nystuen, J.P.; Klein, N. A Late Triassic dinosaur bone, Offshore Norway. *Norwigian J. Geol.* **2006**, *86*, 117–123.
70. Mallison, H. The digital *Plateosaurus* I: Body mass, mass distribution and posture assessed using Cad and Cae on a digitally mounted complete skeleton. *Palaeontol. Electron.* **2010**, *13*, 26.
71. Nau, D.; Lallensack, J.N.; Bachmann, U.; Sander, P.M. Postcranial osteology of the first early-stage juvenile skeleton of *Plateosaurus Trossingensis* (Norian, Frick, Switzerland). *Acta Palaeontol. Pol.* **2020**, *65*, 679–708. [CrossRef]
72. Langer, M.C.; Ramezani, J.; Da Rosa, Á.A.S. U-Pb age constraints on dinosaur rise from South Brazil. *Gondwana Res.* **2018**, *57*, 133–140. [CrossRef]
73. Nesbitt, S.J.; Irmis, R.B.; Parker, W.G. A Critical re-evaluation of the Late Triassic dinosaur taxa of North America. *J. Syst. Palaeontol.* **2007**, *5*, 209–243. [CrossRef]
74. Marsh, O.C. Names of extinct reptiles. *Am. J. Sci.* **1885**, *29*, 169.
75. Rowe, T.B.; Sues, H.-D.; Reisz, R.R. Dispersal and diversity in the earliest North American Sauropodomorph dinosaurs, with a description of a New Taxon. *Proc. R. Soc. B* **2011**, *278*, 1044–1053. [CrossRef]